[American Journal of Science, Vol. 304, June, 2004, P. 477–532]

American Journal of Science

JUNE 2004

THRUSTING AND EXTENSION IN THE SCANDIAN HINTERLAND, NORWAY: NEW U-Pb AGES AND TECTONOSTRATIGRAPHIC EVIDENCE

ROBERT D. TUCKER*, PETER ROBINSON**,***, ARNE SOLLI**, DAVID G. GEE****, TERJE THORSNES**, THOMAS E. KROGH*****, ØYSTEIN NORDGULEN**, and M. E. BICKFORD******

ABSTRACT. A new regional compilation map and U-Pb ages on a suite of variably deformed, Ordovician, calc-alkaline intrusive igneous rocks requires a reinterpretation of the nature of continental collision and extensional exhumation of deep-seated rocks of the Western Gneiss Region west and northwest of Trondheim. A suite of calc-alkaline plutonic rocks, in the age range 482 to 438 Ma, previously known from the region of Smøla-Hitra-Ørlandet-Froan above the Høybakken extensional detachment fault associated with the Devonian 'Old Red Sandstone' basins, is shown to extend over wide areas below the fault, commonly as strongly foliated and lineated gneisses that had been previously mistaken for parts of the Proterozoic Western Gneiss Region. At Follafoss, a member of this intrusive suite is unconformably overlain by weakly metamorphosed conglomerate and volcanogenic sedimentary rocks of probable Late Ordovician age, suggesting that both the sedimentary rocks and the underlying intrusions correlate with the Støren Nappe in the upper part of the local sequence of Caledonide nappes.

U-Pb evidence of metamorphic ages from deep-seated rocks of the Western Gneiss Region include: 1) zircon reaction rims on Proterozoic igneous baddeleyite in the Selnes Gabbro at 401 ± 2 Ma; 2) widespread development of zircon overgrowth and metamorphic zircon with omphacite and coesite inclusions from the Hareidlandet eclogite at 402 ± 2 Ma; and 3) extreme Devonian thermal resetting and neocrystallization of titanite over a wide area of the Proterozoic basement gneisses ending at 395 ± 3 Ma, here fully documented for the first time. At Kjørsvika, west of Trondheimsfjord, a ductilely deformed gneiss of the Ordovician intrusive suite contains igneous titanite dated at 455 Ma that shows little evidence for Devonian thermal resetting. This gneiss lies only 1 to 2 km northwest from a large area of Proterozoic gneisses with 100 percent Devonian reset titanite across a ductilely deformed contact that must represent a phase of extensional detachment (Agdenes detachment) much older than the more brittle detachments (compare Høybakken detachment) associated with some of the present outcrops of the Devonian clastic basins.

These and other relationships suggest the following broad sequence of Siluro-Devonian events in the region: A) Early Scandian (430 - 410 Ma) thrusting with emplacement of the composite Støren Nappe onto the relatively cool Baltoscandian margin of Baltica during contemporaneous subduction of its distal part, locally

*Department of Earth and Planetary Sciences, Washington University, St. Louis, Missouri 63130 U. S. A.; tucker@levee.wustl.edu

**Norges geologiske undersøkelse, N-7491, Trondheim, Norway; Peter.Robinson@ngu.no; Arne.Solli@ngu.no; Terje.Thorsnes@ngu.no; Oystein.Nordgulen@ngu.no

***Department of Geosciences, University of Massachusetts, Amherst, Massachusetts 01003, U. S. A.

****Department of Earth Sciences, Uppsala University, Villavägen 16, S-752 36 Uppsala, Sweden; David.Gee@geo.uu.se

*****Department of Mineralogy, Royal Ontario Museum, Toronto, Ontario, Canada; Heronisl@istar.ca

******Department of Geology, Syracuse University, Syracuse, New York 13244-1070, U.S.A.; mebickfo@mailbox

producing eclogites, possibly representing the earliest initiation of high-level 'post-orogenic' clastic basins. B) Early mid-Scandian (410 - 406 Ma) continued subduction and imbrication of a more proximal part of the Baltoscandian margin, with its heating and high-pressure metamorphism. Continued deep-level thickening by imbrication providing the gravitational potential for foreland- and hinterland-directed extension at high levels, while deposition in Devonian clastic basins probably continued. C) Late mid-Scandian (406 - 396 Ma) continued subduction of more proximal Baltican continental basement with common production of HP and UHP eclogites. Imbricate thrusting of a subducted and heated proximal continental slab provided the gravitational potential to initate hinterland backsliding and extensional emplacement of the cool high-level Støren Nappe against the cooling basement. Deposition in high-level Devonian clastic basins was active. D) Early late-Scandian (396 - 390 Ma). The extension and cooling initiated in C) brought an enormous volume of Proterozoic basement from high amphibolite facies to low amphibolite facies and through about 600°C, terminating Pb loss and neocrystallization of titanite at 395 ± 3 Ma. During this phase, ductile extensional deformation progressed into a sinistral shear field, producing folds and subhorizontal stretching lineations within the previously thrust and extensionally juxtaposed, deep and high-level packages. E) Late Scandian (390 - 375 Ma) extension in a sinistral shear field bringing the ductilely deformed package into contact with brittle, highest-level rocks along detachments associated with outcrop areas of the Devonian clastic basins. In this sequence, the brittle detachments (E) played a relatively minor role, whereas the mid-Scandian deep-crustal imbrication and related high-level collapse (B, C and early D) were the main events that brought deep metamorphic rocks relatively close to the surface.

INTRODUCTION

Within the Scandinavian Caledonides (or Scandes), major allochthons, derived from both the Baltoscandian margin of Baltica and outboard terranes, have been thrust several hundreds of kilometers eastwards onto the Baltoscandian platform. Some of the main thrust sheets (for example, the Seve Nappes) can be traced nearly two hundred kilometers across the orogen from the mountain front far into the hinterland, where they are found deeply infolded together with the basement along the Norwegian west coast. In relation to their vast areal development, the thrust sheets are thin - a few kilometers thick in the east, reduced to a few hundreds of meters or less in the west - and their mode of emplacement onto the Baltoscandian platform is clearly the result of both collisional contraction and extensional collapse. The interplay of compression and extension in the Scandes, and the relative importance of syn- and post-contractional extension are the much-debated subject of this paper.

The crystalline basement of the Paleozoic Baltican plate is part of the Fennoscandian Shield. It is mainly Paleoproterozoic, but partly Archean in the north and Mesoproterozoic in the south, and can be followed from the mountain front, beneath the thin platform Cambro-Ordovician (locally Silurian) successions, via the many antiformal windows across the orogen into the hinterland (fig. 1). The character of this basement and the overlying platform successions allows correlation across the orogen (Gee, 1980; Stephens, 1988) despite increasing metamorphic grade from subgreenschist facies in the mountain front to greenschist facies in the border zone between Norway and Sweden, and amphibolite facies in the hinterland (Bryhni and Andréasson, 1985). In western parts of the hinterland the occurrence of eclogites in the basement (Eskola, 1921; Griffin and others, 1985) has been shown (Krogh and others, 1974; Griffin and Brueckner, 1980; Lutro and others, 1997; Terry and others, 2000a) to be Caledonian in age (ca. 430 - 400 Ma), apparently the result of Scandian collisional thickening of the crust during underthrusting of the Baltoscandian margin beneath Laurentia. Other interpretations are possible (for example, Gilotti and Hull, 1993), if widely accepted lithological and stratigraphical correlations are neglected or rejected.

Uplift of the basement in the hinterland was rapid during the early Devonian with widespread isotopic evidence (Ar/Ar hornblende and muscovite; and U/Pb titanite)

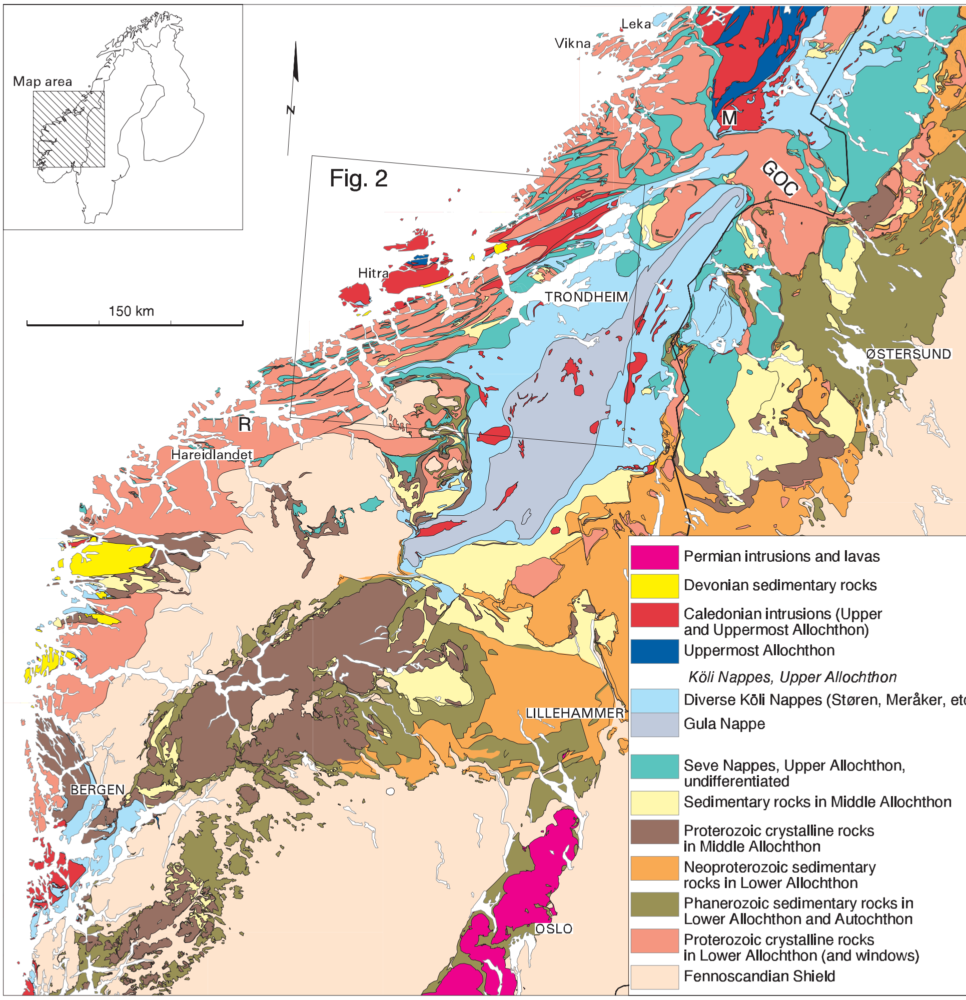

Fig. 1. Generalized geologic map of the southern part of the Scandinavian Caledonides showing the setting of the Trondheimsfjord region (modified from Koistinen and others, 2001). Outline indicates the area of figure 2. GOC indicates Grong-Olden Culmination, R indicates Reksdalshesten (Robinson, 1997), M indicates Møklevatnet.

of ca. 400 to 395 Ma cooling ages. In Norway, near the classical eclogite terranes, extensional collapse is well documented (Anderson and Jamtveit, 1990) in kilometer-thick west-vergent extensional shear zones, beneath the late Early Devonian 'Old Red Sandstone' graben (Hossack, 1984; Norton, 1987). The final phases of extensional collapse of the orogen may have continued into the last (Famennian) stage of the late Devonian (Terry and others, 2000a).

Of particular importance, for the understanding of Scandian orogeny, however, is the evidence in the central part of the mountain hinterland of syn-contractional extension that occurred during the development of the Devonian basins and prior to their final extensional emplacement on brittle faults. This paper concentrates on new evidence relevant to this early extension.

An understanding of the hinterland regions of the Scandinavian Caledonides requires the recognition and characterization of the following:

1) Tectonostratigraphy, with Baltican basement and its sedimentary cover in the deeper structural levels overlain by thrust sheets including rocks of Baltoscandian, oceanic (Iapetus), and Laurentian affinities.
2) Structures related to initial thrust nappe emplacement of the allochthons, as well as features characteristic of the nappes before emplacement. Also structural features such as recumbent folds superimposed on parts of the nappe pile after emplacement.
3) Structural features and metamorphic contrasts produced during early phases of extensional collapse, juxtaposing, for example, Baltica basement in Scandian eclogite facies against greenschist-facies or low-amphibolite-facies high-level nappes.
4) Later major structural features including superimposed recumbent folds, upright anticlines and synclines, and longitudinal extensional and shear fabrics produced during later phases of extensional collapse, and features related to development and deformation of Devonian basins.

The essential tectonostratigraphy of the nappes as developed in the frontal regions of the orogen, the Grong-Olden Culmination, and the Trondheim Region, has been extended into the hinterland (Gee, 1975), including the areas of Tømmerås (Gee, 1974), Trollheimen (Gee, 1980; Krill, 1980, 1985), the Surnadal syncline (Krill and Roshoff, 1981; Krill, 1985; Rickard, 1985), and the region west of Orkanger (Tucker, 1986). More recently, a characteristic sequence of nappes has been mapped along Moldefjord as far west as Brattvåg adjacent to basement in the highest eclogite facies (Robinson and Krill, 1991, 1994; Robinson, 1995; Terry and others, 2000b), and tectonostratigraphic concepts have been extended into a broad part of the Western Gneiss Region northwest of Trondheim (Thorsnes, 1988; Solli, 1995; Solli and others, 1997; Roberts, 1997).

The present paper results from 1) completion of a major compilation map of Nord-Trøndelag and Fosen (1/275,000) by Solli (1995), including the Namsos and Grong 1/250,000 sheets (Solli and others, 1997; Roberts, 1997); 2) new U-Pb ages on igneous zircon and metamorphic zircon and titanite by Tucker (1988; Tucker and Krogh, 1988; Tucker and others, 1987, 1990, and this paper) and by Bickford; 3) recognition of the nature of an unconformity at Follafoss in inner Fosen by Thorsnes (personal communication, 1995), and 4) examinations of critical field relationships by Gee, Robinson and Solli in June 1995, and Robinson and Solli in August 1996 and July 1997 (Robinson and others, 1996, 1997; Tucker and others, 1997a). We concur with previous authors (Gilotti and Hull, 1993) that there is widespread evidence of W-vergent displacement on contacts between basement and overlying allochthons. Evidence is presented here that this W-directed movement occurred during vertical shortening of the nappe stack, whereas major juxtaposition of low-grade on high-grade rocks occurred prior to complex refolding of the entire tectonostratigraphy.

GEOLOGIC FRAMEWORK OF THE TRONDHEIMSFJORD REGION

The area discussed in this paper is covered in figure 2. The Caledonide geology of the area is composed of Baltica continental basement and a series of far-traveled thrust sheets believed to have been rooted to the northwest. Together these produce a layer-cake tectono-stratigraphy, of highly variable thickness, listed in the explanation of figure 2 and described briefly below.

The southeastern part of figure 2 is occupied by a part of the Trondheim basin containing large areas of exposure of the Upper Allochthon (Seve, Støren, Gula, and Meråker Nappes) of low-amphibolite-facies to greenschist-facies rocks. Southeast of Surnadalsøra lies the NE-plunging anticlinal hinge of Trollheimen in an eastern promontory of the Western Gneiss Region of exposed Proterozoic basement. The NE-plunging Surnadal Syncline separates Trollheimen from the more highly deformed and metamorphosed region centered on Kristiansund, where mafic rocks in

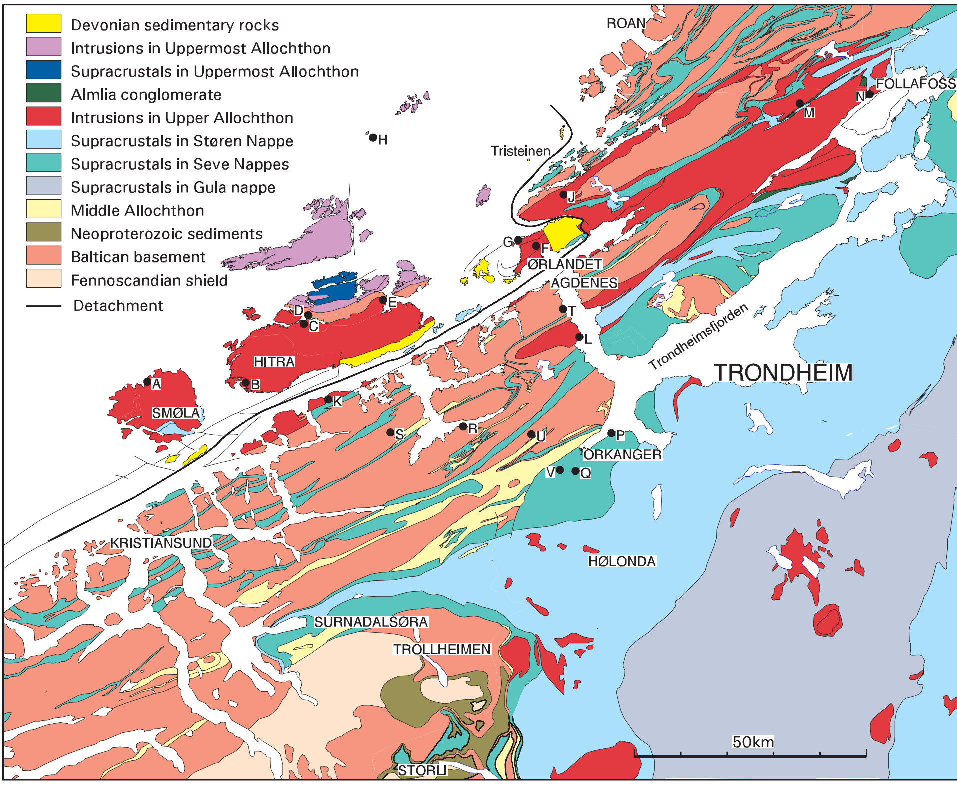

Fig. 2. Generalized map showing distribution of tectonostratigraphic units in the Trondheimsfjord region. Compiled by Solli with contributions by Tucker. Heavy line is the Høybakken detachment fault associated with Devonian basins on Ørlandet as shown by Séranne (1992), and its southwestern prolongation as the Hitra-Snåsa Fault. For simplicity, other major faults of the Møre-Trøndelag Fault Complex are omitted. Lettered dots are sample localities for U-Pb analyses of igneous zircon and titanite and metamorphic zircon given in table 1 and in Concordia diagrams.

the Proterozoic basement are consistently in the eclogite or high-amphibolite facies. This highly deformed region, containing rocks at most tectonostratigraphic levels, extends continuously in a NE-SW-trending band from Kristiansund to the coast northwest of Follafoss. The map pattern is dominated by prominent anticlinal and synclinal hinges, mostly plunging NE, that are merely the latest in a sequence of fold deformations that deformed the pre-existing thrust nappe stack (see more detailed discussion near the end of the paper). Eclogite-facies metamorphism dies out along a vaguely defined line about 30 km west of Orkanger, but relict eclogites are also reported in the Roan Window on the coast northwest of Follafoss (Möller, 1988).

The northwestern part of figure 2 is occupied by rocks of the Støren Nappe of the upper allochthon, unconformably overlain by Devonian clastics and the Helgeland Nappe Complex of the uppermost allochthon. Together these form part of an extensional allochthon transported west-southwestward many tens of kilometers during late Scandian sinistral transtension (Krabbendam and Dewey, 1997) along a major ductile-to-brittle detachment fault (Seranne, 1992), the Høybakken detachment, highlighted in figure 2. Movement on the fault was essentially parallel to regional strike. Where the fault is curved near Ørlandet it outlines a paired SW-plunging syncline and a SW-plunging anticline. The Devonian strata within the syncline dip east, contrary to the dip of the detachment, and form an E-plunging fold. In the ductilely deformed terrane east and southeast of the Høybakken detachment, evidence given below indicates the presence of another major detachment, named Agdenes detachment (Robinson and others, 2004). Other late- or post-metamorphic faults are not emphasized in figure 2. These include the Hitra-Snåsa Fault, which extends continuously from the detachment at Ørlandet northeast through Locality M and off the map, and the Verran Fault, which runs parallel to the narrow branch fjord 20 km southwest of Follafoss. These and other faults in the region have commonly been assigned to the Møre-Trøndelag Fault Complex (Gabrielsen and Ramberg, 1979). The youngest bedrock geologic features are small fault-bounded submarine basins of Jurassic sedimentary rocks, one outlined in the fjord south of Follafoss, one in the open area northwest of Ørlandet and one south of Smøla (Bøe and Bjerkli, 1988; Bøe, 1991; Sommaruga and Bøe, 2002).

TECTONOSTRATIGRAPHY

Introduction

Understanding of the Scandinavian Caledonides is based on 1) the identification and mapping of a complex sequence of tectonostratigraphic units; and 2) the recognition that these represent rocks generated in a wide variety of settings that were later assembled in continent-arc accretionary events, and then in a major, terminal continental-continent collision, during which shortening and thrust translation over distances of 100's of kilometers was characteristic. For the non-specialist, the array of units and unit names is challenging (Gee and Sturt, 1985), and the details of correlation, even for the area of interest in west-central Trøndelag (fig. 2), is beyond the scope of this paper. Here we have adopted a general and very simplified sequence of units most easily understood both in local terms and in terms of orogen-wide correlations. The correlation of the units used here and those used in other papers on west-central Trøndelag and adjacent areas is shown in figure 3, and is the basis for the map in figure 2.

Baltican Basement

The lowest tectonostratigraphic unit exposed in the map area of figure 2 is the Baltican crystalline basement, a segment of the former craton of Baltica or the Fennoscandian Shield dominated by Late Paleoproterozoic granitoid intrusive rocks, in the age range 1686 to 1650 Ma (Tucker and others, 1990) that were locally intruded by rapakivi granites dated in one location near Molde at 1508 Ma (Tucker and others, 1990; Austreim and others, 2003) and by gabbros dated at 1657 +5-3 Ma and 1462 ± 2 Ma (Tucker and others, 1990). The oldest dated rock in the region of figure 1 is the 1.84 Ga tonalitic gneiss south of Leka (Schouenborg and others, 1991). The Paleoproterozoic granitoids are similar in age to part of the Transcandinavian Igneous Belt, but are geochemically unlike it (Roland Gorbatschev, personal communication, 1997). Approximately 1650 Ma U-Pb ages on zircon from partial melt leucosomes in some of the gneisses (Tucker and others, 1990) suggest there may have been a widespread high-grade regional metamorphism at this time. Generally there is evidence of an early-Scandian overprint ranging in intensity from low-amphibolite facies to eclogite facies, followed by a general late-Scandian amphibolite-facies overprint (Terry and Robinson, 2003). The best recent understanding is that the Baltica basement in the map area, although providing the basement for emplacement of the sequence of far-traveled thrust nappes, is not truly autochthonous with respect to the Fennoscandian Shield exposed in front of the Scandian orogen in Sweden and southern Norway. Evidence for this fact comes in two main forms. In the part of the Western Gneiss Region exposed in Trollheimen, in the south-central part of figure 2, maps clearly delineate two levels of basement, each capped by a quasi-continuous layer of variably deformed Neoproterozoic quartzite and pebble conglomerate. The upper level of

Tectonic Units	Northwestern Areas		Southwestern Areas			Central Areas		Eastern Areas
		Hemne	Molde	Trollheimen	Oppdal	West-central	East Jämtland	Central and southern
	This Paper	*Tucker (1986)*	*Robinson (1995)*	*Gee (1980)*	*Krill (1980)*	*Roberts and Wolff (1981)*		*Gee (1975)*
Late-orogenic sediments	Devonian					Late Silurian/ Mid-Devonian	Early Devonian	
Upper	Støren Nappe		Støren Nappe		Tronget Unit	Støren Nappe / Gula Nappe	Meråker Nappe	Köli Nappes
Allochthon	Seve Nappe	Gagnåsvatn Nappe Unit	Blåhø-Surna Nappe	Blåhø Unit	Surna Unit Blåhø Unit	Levanger/ Skjøtingen Nappes	Øyfjell/ Essandsjø Nappes	Seve Nappes
Middle	Särv Nappe	Songa Nappe Unit	Sætra Nappe	Sætra Nappe	Sætra Unit	Leksdalvatn Nappe	Remsklepp Nappe	Särv Nappe
Allochthon	Risberget Nappe	Rønningen Augen Gneiss	Risberget Nappe	Augen Gneiss	Risberget Unit	Hærvola Nappe		Tännäs Augen Gneiss Nappe
Lower Allochthon And Parauthochthon	Absent or too thin to show	Øyangen Formation	Åmotsdal Quartzite	Gjevilvatnet Group	Åmotsdal Unit	Quartzite, rhyolite, granitic gneiss Bjørndalen Formation *Gee (1977)*	Quartzites, Black phyllites	Jämtland Nappes
Autochthon	Baltican Basement	Våvatn Migmatite Gneiss	Baltica Basement		Lønset Unit	Precambrian crystalline basement		Precambrian granite and gneisses

Fig. 3. Tectonostratigraphic correlation chart for the Trøndelag-Jämtland-Trollheimen-Molde region, central Norway and Sweden, illustrating the simplified nomenclature used in this paper.

basement forms a vast and highly folded thrust sheet emplaced above the lower level of basement and its autochthonous cover (Nilsen and Wolff, 1989). Robinson (1997) has deduced a similar situation within the anticlinal culmination centered on Rekdalshesten (R in fig. 1), and there are various other indications of probable segmentation of Baltica basement within the northern part of the Western Gneiss Region. The second form of evidence is in the deep-seismic profile from Trøndelag across the orogen to the autochthonous basement in Sweden (Hurich and others, 1988; Palm and others, 1991; Juhojunttii and others, 2001) clearly showing that the Baltican basement exposed in various tectonic windows near the Norwegian-Swedish border lies above a major shallowly dipping reflector that appears to correspond to the top of the autochthon exposed at the front of the orogen.

Authochthonous Cover and Lower Allochthon

Above the Paleo- to Mesoproterozoic Baltica basement in various parts of the map area are vestiges of a very thin, autochthonous sedimentary cover sequence (Gee, 1980), usually consisting of probable Neoproterozoic quartzites and conglomerates, overlying pelites representing metamorphosed Cambrian alum shale, and discontinuous limestones. Within the map area of figure 2, at the scale used, these units of the Autochthon and Lower Allochthon are too thin to show. In many parts of the map area they are entirely absent or recognized with difficulty, and usually not distinguishable from each other. They are, however, reported locally, for example in the previously mentioned quartzites of Trollheimen, and in the Øyangen Formation (Tucker, 1986) of quartzite and overlying mica schist in an area west of Orkanger. In the unmetamorphosed lowest thrust allochthon in Sweden, these are overlain by a thicker sequence, which includes Baltica basement, Neoproterozoic sandstones, a limestone-shale sequence of Cambrian-Ordovician age, and a thin Silurian sequence of sandstone and limestone grading upward into turbidites that may range into lowest Devonian (Gee, 1975).

Middle Allochthon

Above the autochthonous cover and Lower Allochthon, and commonly in direct contact with Baltica basement, are the rocks of the Middle Allochthon. In the area of figure 2 the lowest recognized unit, again too thin to show, is the Risberget Augen Gneiss Nappe correlated with the Tännäs Augen Gneiss Nappe, a division of the Offerdal Nappe in Sweden. The unit is dominated by variously deformed Mesoproterozoic rapakivi granites with various associated gabbros, anorthosites, and other granitoid rocks. Earlier assigned an age of 1500 Ma (Krill, 1983), new concordant zircon ages (Handke and others, 1995) indicate that these distinctive rapakivi granites fall into two age groups, 1659 to 1642 Ma and 1190 to 1180 Ma. The other key part of the Middle Allochthon, finally extensive enough to show on figure 2, consists of feldspathic quartzites derived from Neoproterozoic feldspathic sandstones, interlayered with amphibolites derived from Late Neoproterozoic diabase dikes. This unit variously known in Norway as the Sætra, Songa, and Leksdalsvatn Nappes, is here assigned the Swedish term Särv Nappe, to emphasize the importance of orogen-wide correlation. Furthermore, a few areas of very feldspathic rocks, intricately interlayered with amphibolites, might not be the Särv itself, but Baltica basement to the Särv Nappe heavily intruded by the same Neoproterozoic dike swarm. In the front of the Caledonides in Sweden, the Neoproterozoic sandstones of the Särv Nappe are as much as 2 km thick. By contrast, in parts of the Western Gneiss Region mapping has shown that the equivalent quartzite-amphibolite sequence ranges from 10 m (Robinson, 1995) to as thin as 1 m (Terry and Robinson, 1996; Robinson and others, 2003).

Upper Allochthon

In Sweden, the Upper Allochthon has traditionally been mapped as two major units, the lower Seve Nappes, characteristically containing medium- to high-grade metamorphic rocks, and the upper Köli Nappes containing medium- to low-grade metamorphic rocks, locally with Ordovician fossils. In Norway, in the area covered by figure 1, traditional equivalent names for the Seve are the Skjøtingen and Blåhø Nappes, whereas the Köli Nappes have a variety of names. In the Trondheim Region (southeastern part of fig. 2), the Köli Nappes are represented by the Trondheim Nappe Complex, comprising the Støren, Meråker and Gula Nappes (see, Roberts and Stephens, 2000). Geotectonically, the rocks of the Seve and Gula Nappes have been considered as the extreme outboard assemblage of the Baltica continental margin, and to have been subjected to high-grade, even locally high-P metamorphism in pre-Scandian and/or early Scandian time. The Støren and Meråker Nappes are considered to have a largely exotic origin from the Iapetus Ocean as Late Cambrian - Earliest Ordovician deformed ophiolitic and volcanic-arc sequences overlain unconformably by Late Arenig to possibly early Silurian basinal successions. Ordovician fossil affinities in the Støren Nappe at Hølonda and at Smøla suggest deposition proximal to Laurentia, and possibly even that the strata were thrust or obducted onto Laurentia in the Ordovician Taconian orogeny, and then later transferred onto the Baltic margin in the Scandian collision (see below).

In detailed subdivision of the Seve equivalents in the Trollheimen region of Norway, Krill (1987) identified a lower Surna Nappe characterized by higher grade metamorphism and abundant intrusions of trondhjemite and pegmatite, and an upper Blåhø Nappe, usually slightly less metamorphosed and lacking such intrusions. Robinson (1995) did not attempt to use this distinction in his correlation within the Moldefjord region and adopted the composite term Blåhø-Surna Nappe, but for the Ålesund and Ulsteinvik 1/250,000 sheets Tveten and others (1998) simplified this term to Blåhø Nappe.

Within the area of figure 2, excluding the Gula to the southeast, it has been most practical to distinguish two principal nappes in the Upper Allochthon, Seve below and Støren above. The 'lower nappe' is characterized by medium- to high-grade mica schists, commonly with garnet, kyanite, sillimanite, and with variably distributed granitoid intrusions and pegmatites, by abundant coarse amphibolites, commonly with garnet and pyroxenes, and by fairly common layers of coarse-grained marble. The 'upper nappe' is dominated by low- to medium-grade metamorphosed volcanic and related intrusive rocks including ophiolite fragments, by metamorphosed volcano-sedimentary sequences, and by metamorphosed black shale. An additional component of this nappe, recognized earlier (Tucker, 1988; Gautneb and Roberts, 1989) but receiving special emphasis in this paper, is a variety of Middle to Late Ordovician medium- to coarse-grained calc-alkaline intrusive igneous rocks that were broadly contemporaneous with the extrusion of the arc volcanics. A common distinction between the lower and upper nappes is that the lower one contains medium- to high-grade rocks with coarse garnet, whereas the upper one contains low- to medium-grade rocks with no more than 2-3 mm garnets if any at all. For this paper we have adopted the name Seve for the lower nappe to emphasize its broad geotectonic affinities and high-grade metamorphism, and the name Støren for the upper nappe to emphasize its Ordovician igneous characteristics, its fossil affinities, and its general lower grade metamorphism.

Uppermost Allochthon

In Nordland and Troms, North Norway, the Köli Nappes are overlain by the Rödingsfjället and Helgeland Nappe Complexes and other nappes of the Uppermost Allochthon. These consist of Neoproterozoic to Early Paleozoic, metamorphosed sedimentary rocks including migmatitic paragneisses and thick marble units, as well as ophiolitic rocks with overlying cover sequences of Late Ordovician – Early Silurian age. There is evidence in southern Nordland for crust-derived Arenig to Llanvirn peraluminous intrusions at 477 to 466 Ma (Yoshinobu and others, 2002), and emplacement of Ashgill to Llandovery, calc-alkaline intrusive rocks at 448 to 430 Ma (Nordgulen and others, 1993, 2002; Eide and others, 2002). Recent structural, geochronological and stable isotope data from different parts of the Uppermost Allochthon support a Laurentian, or possibly a microcontinental origin for the rocks and have shown that west-directed contractional deformation and granitoid magmatism occurred during an Ordovician Taconic episode (Roberts and others, 2001, 2002a; Melezhik and others, 2002; Yoshinobu and others, 2002). Reconnaissance (Solli and Robinson, unpublished data, 1997) suggests strongly that the rocks exposed on the northern part of Hitra and on Frøya should be assigned to the Helgeland Nappe Complex. Immediately south of this exposure there is a narrow belt of strongly layered pink granitoid gneisses and amphibolites, closely resembling the Baltican basement of the Western Gneiss Region. However, both this basement and the adjacent inferred Helgeland Nappe rocks are dominated by steep linear fabrics and lack the dominant subhorizontal linear fabrics characteristic of adjacent parts of the Western Gneiss Region. For this reason, we suspect that all of these rocks may be on the upper side of the Høybakken extensional detachment associated with the Devonian basins, and have been extensionally transported from an original location far to the northeast. U-Pb studies of zircon and titanite in these rocks would show to what extent these rocks have a parallel metamorphic history to the basement of the Western Gneiss Region.

Late-orogenic Clastic Sediments

At the top of the tectonostratigraphic section, and indeed not really a part of it, are the moderately deformed and slightly metamorphosed conglomerates, sandstones, shales and rare limestones of the Devonian 'Old Red Sandstone' basins (Steel and others, 1985). They are exposed on Smøla, Edøya, Hitra, and Ørlandet and a large number of small nearby islands, and in four major basins in West Norway, from north to south Hornelen, Håsteinen, Kvamshesten, and Solund. The rocks on Hitra contain an eurypterid fauna that may be as old as Late Llandovery (Størmer, 1935; Bassett, 1985). The best palynological data from Tristein islet, north of Ørlandet (fig. 2) suggests a Late Emsian age of deposition (Allen, 1976), about 403 to 394 Ma based on the most recent Devonian time scale (Tucker and others, 1997b, 1998). Ar-Ar study of detrital K-feldspar from Asenøya, northeast of Ørlandet, suggests a Givetian age of deposition, 387 to 382 Ma, for part of the section there (Elizabeth Eide, personal communication, 2003). According to a structural study by Seranne (1992) (see fig. 2), and in agreement with studies of other Devonian basins in West Norway (Andersen and Jamtveit, 1990; Andersen, 1993), all of these strata lie on the upper plates of major top-to-west extensional detachment faults that carried both the Devonian strata and their immediately underlying igneous-metamorphic substrate for many kilometers southwestward or westward from their original sites of deposition. The rocks unconformably beneath the basins have escaped much of the deformation characteristic of the Western Gneiss Region and appear to belong to parts of the Caledonides normally exposed far to the east and also, in some of the West Norwegian examples, rather low in the regional nappe tectonostratigraphy.

The Devonian basin of Hitra rests with demonstrated unconformity on both the volcanic and the intrusive rocks of the Støren Nappe on the southern side of the island, but its relationship with the basement rocks and rocks of the Helgeland Nappe Complex of northern Hitra, also proposed to lie above the extensional detachment, are unknown. In the case of the basins near Trondheimsfjord, detailed studies (Séranne, 1992) suggest that movement on the detachment fault was west-southwestward, in essentially the same direction as the slightly earlier and more ductile folds and dominant lineations that pervade the region.

U-Pb DATING

Laboratory Methods

Samples analyzed in this study include metamorphosed felsic volcanic rocks, intrusive igneous gneisses, and weakly deformed, unmetamorphosed granitic pegmatites. Samples ranged in size from 0.5 to 20 kg from which heavy mineral concentrates were obtained by standard techniques of crushing, Wilfley table concentration, and separation by heavy liquid and magnetic susceptibility methods. Following separation of zircon, monazite, and titanite, individual grains or small fractions of these accessory minerals were picked, abraded, and cleaned. This procedure is standard treatment for isotope dilution analysis (see, Krogh, 1982).

Isotope dilution ages were measured in three laboratories over a period of ~15 years using slightly different analytical techniques and thermal ionization mass spectrometers. Samples A-G, J-L, and N-V were first analyzed at the Royal Ontario Museum over the period from 1985 to 1990 using the procedures outlined by Krogh (1973, 1982) with slight modifications described by Tucker and others (1990). Selected fractions of zircon and titanite from these rocks were also analyzed in the Geochronology Laboratory at Washington University over the period from 1992 to 2002. At the Royal Ontario Museum the mass spectrometry procedures were as follows: Lead fractions smaller than 1 ng and all uranium fractions were analyzed in a VG Sector 54 mass spectrometer using a single-collector procedure with a Daly-type photomultiplier detector operating in pulse-counting mode. Daly bias and nonlinearity were periodically monitored with NIST and CBNM isotopic reference materials, and correction factors for Daly gain were used in data reduction (table 1). Mass dependent fractionation of Pb and U was monitored regularly and a discrimination factor for Pb (0.094 ± 0.04 percent amu-1; 2s) and U (0.111 ± 0.04 percent amu-1; 2s) has been applied to the measured ratios. Analytical techniques at Washington University follow those described in Tucker and others (2001). Isotope ratio measurements at Washington University were performed on a VG Sector 54. Lead fractions smaller than 1 ng and all uranium fractions were analyzed as they were at the Royal Ontario Museum. Lead fractions larger than 1 ng were analyzed using a two-step, quasi-static procedure with a collector assembly of three Faraday cups and the Daly photomultiplier detector. The 204Pb was measured in the Daly channel only, whereas the 205Pb was measured in the H1 Faraday channel at position 1 and in the Daly channel at field position 2. Other lead isotopes were measured in Faraday channels H1 to H3. Isotope ratios involving 205Pb, 206Pb, 207Pb, and 208Pb were calculated using a static multicollector algorithm. This procedure allowed for internal gain calibration of the Daly channel relative to the H1 Faraday channel in each scan and eliminated biases related to Daly gain and ion beam instability.

Total-procedure blanks at both the Royal Ontario Museum and Washington University averaged between 10 to 2 pg for Pb and 2 to 0.5 pg for U; total common-Pb contents for each analysis are reported in tables 1 and 3. Common-Pb corrections were made by first correcting the measured ratio for mass-dependent fractionation and introduced spike, then subtracting Pb equal in amount and composition to the laboratory blank. Any remaining 204Pb is assumed to represent a model lead composition given by Stacey and Kramers (1975) at the estimated age of the rock. In nearly all cases involving zircon, the uncertainty in the amount and composition of common-Pb represents an insignificant contribution to the uncertainty of the isotopic ages (table 1). The titanite analyses, however, have relatively low measured 206Pb/204Pb ratios owing to their small size or copious initial-Pb contents; hence the uncertainty of their isotopic ages is rather large (see tables 1 and 3). Error propagation is similar to that

TABLE 1

U-Pb isotope dilution analyses, Outer Trondheimsfjord Region

FRACTIONS		CONCENTRATIONS					ATOMIC RATIOS							AGE [Ma]	
No.	Properties (1)	Wt. [μg] (2)	Pb rad [ppm] (2)	U [ppm] (2)	Pb com [pg] (3)	Th/U (4)	$^{206}Pb/^{204}Pb$ (5)	$^{207}Pb/^{206}Pb$ (6)	±	$^{206}Pb/^{238}U$ (6)	±	$^{207}Pb/^{235}U$ (6)	±	$^{207}Pb/^{206}Pb$ (6)	±
ORDOVICIAN INTRUSIVE IGNEOUS ROCKS															
A. RT-87-2 medium-grained granodiorite, Smøla [181/358]															
1	+200-100,cl,c,s	201	15.2	215	11	0.279	7,530	0.05589	4	0.07179	4	0.5533	33	448.1	1.6
2	-100+200,cl,f,pr	232	13.9	201	11	0.273	3,975	0.05585	4	0.07061	8	0.5438	37	446.6	1.6
3	-100+200,cl,c,n	420	26.9	396	40	0.231	13,265	0.05589	5	0.06978	17	0.5373	130	447.8	1.9
4	-100+200,cl,c,pr	25	13.2	185	3	0.352	6,661	0.05572	5	0.07101	10	0.5455	8	441.1	1.9
5	-100+200,cl,c,pr	6	10.7	158	1	0.155	2,564	0.05569	17	0.07096	11	0.5448	18	439.9	6.9
B. RT-86-63 Medium-grained granite Hitra [692/356]															
6	-100+200,c,cl,t-p	19	15.5	174	3	0.475	1,965	0.05578	9	0.07123	11	0.5478	10	443.7	3.4
7	-100+200,c,cl,t-p	9	12.3	171	2	0.382	3,443	0.05576	5	0.07053	9	0.5422	7	442.7	2.2
8	-100+200,cl,c,t-p	18	21.0	309	2	0.227	9,799	0.05577	4	0.06990	10	0.5375	8	443.0	1.8
C. RT-86-57 Hornblende diorite, Hitra [815/485]															
9	-100+200,cl,c,sh	29	18.9	253	2	0.520	13,461	0.05579	4	0.07124	11	0.5480	8	444.2	1.7
10	-100+200,cl,c,sh	20	38.9	531	2	0.424	23,559	0.05581	3	0.07120	9	0.5479	7	444.9	1.1
11	-100+200,cl,c,sh	24	21.8	293	2	0.482	13,658	0.05581	4	0.07124	8	0.5482	7	444.8	1.5
12	-100+200,pb,s	10	27.6	1,070	3	0.389	8,654	0.05580	4	0.07125	9	0.5482	8	444.4	1.7
D. RT-86-61 Hornblende diorite gneiss, Hitra [835/503]															
13	Tit,-100,ob	450	9.5	93.4	271	1.92	645	0.05571	6	0.07046	7	0.5412	8	440.7	1.8
E. RT-86-58 Fillan diorite porphyry, Hitra [986/533]															
14	Tit,-100,ob	287	17.5	164	201	2.09	910	0.05583	5	0.7182	9	0.5527	8	445.6	1.6
F. RT-86-82 Lerberen granite, Ørlandet [815/485]															
15	-100+200,cl,c,pr	152	21.5	225	24	0.418	4,009	0.05564	5	0.07074	18	0.5442	15	439.1	1.9
16	-100+200,cl,c,t-p	101	21.2	321	2	0.406	9,504	0.05574	5	0.07079	10	0.5441	8	442.0	1.9
17	-100+200,cl,c,eq,p	99	12.0	166	13	0.414	2,545	0.05577	3	0.07073	11	0.5439	10	443.1	1.2
18	-100+200,cl,c,pr	11	19.9	284	3	0.326	3,973	0.05565	7	0.07025	8	0.5389	9	438.3	2.7
G. RT-86-83 Uthaug gneiss, Ørlandet [292/672]															
19	Tit,+200,db,f	209	56.1	709	572	0.774	1,088	0.05570	3	0.07035	7	0.5404	6	440.4	1.4
H. Gjæsingen Quartz Monzonite															
20	-200,cl,c,pr	-	30.4	420	-	-	9,602	0.05553	7	0.06908	13	0.5289	16	433.6	4.0
21	-200,cl,c,pr	-	31.5	438	-	-	16,289	0.05578	7	0.06853	13	0.5270	16	443.4	4.0
22	-200,cl,c,pr	-	36.0	481	-	-	1,101	0.05562	7	0.06917	13	0.5305	16	437.2	4.0
23	-200,cl,c,pr	-	23.4	347	-	-	18,017	0.05605	7	0.06415	13	0.4958	16	454.4	4.0
J. RT-86-85 Kopparen diorite gneiss, Fosen [364/758]															
24	-200,cl,c,l-p	306	24.8	333	14	0.205	13,325	0.05665	5	0.07712	7	0.6024	7	477.9	1.5
25	-200,c,cl,l-p	335	21.9	295	2	0.185	23,410	0.05730	6	0.07728	8	0.6101	8	503.1	1.6
26	-200,c,cl,l-p	24	12.4	145	2	0.318	9,336	0.06226	6	0.08512	13	0.7307	12	682.9	2.1
27	-200,cl,c,l-p	352	29.6	278	31	0.479	10,732	0.07050	4	0.10538	2	1.0244	20	942.9	1.4
K. RT-86-40 Kjørsvika diorite gneiss [868/318]															
28	-100+200,cl,c,fr	8	13.0	167	1	0.519	3,364	0.05628	14	0.07398	13	0.5741	16	463.6	5.5
29	-100+200,cl,c,fr	25	11.9	153	2	0.514	8,782	0.05625	6	0.07400	15	0.5739	12	462.2	2.4
30	-100+200,cl,c,sp	48	10.3	134	4	0.527	7,535	0.05620	4	0.07315	9	0.5668	7	460.2	1.6
31	-100+200,cl,c,sp	21	8.4	108	1	0.524	7,143	0.05618	7	0.07388	9	0.5723	9	459.4	2.6
32	Tit,+200,cl,br	1.53	42.8	575	988	0.482	1,933	0.05607	6	0.07242	15	0.5599	15	455.2	2.3

TABLE 1
(continued)

FRACTIONS		CONCENTRATIONS					ATOMIC RATIOS							AGE [Ma]	
No.	Properties (1)	Wt. [µg] (2)	Pb rad [ppm] (2)	U [ppm] (2)	Pb com [pg] (3)	Th/U (4)	^{206}Pb/^{204}Pb (5)	^{207}Pb/^{206}Pb (6)	±	^{206}Pb/^{238}U (6)	±	^{207}Pb/^{235}U (6)	±	^{207}Pb/^{206}Pb (6)	±
L. TK-86-55 Lensvik granodiorite gneiss [415/455]															
33	-200,cl,c,l-p	563	20.2	266	10	0.443	15,835	0.05674	5	0.07632	10	0.5971	11	481.4	1.5
34	-200,cl,c,l-p	180	21.2	278	6	0.414	5,969	0.05671	6	0.07648	11	0.5981	11	480.5	1.6
L. TK-86-56 Lensvik granodiorite gneiss [415/455]															
35	-200,cl,c,l-p	676	33.8	447	823	0.368	1,579	0.05681	5	0.07633	10	0.5979	10	484.0	1.5
36	-200,cl,c,l-p	654	30.0	398	12	0.346	16,515	0.05674	6	0.07656	10	0.5990	8	481.4	1.6
M. TT89048 Foliated diorite, Simadalen															
37	NM (-1) AA	1.771	26.0	359	60	-	7,852	0.05581	3	0.07090	13	0.5456	8	444.9	1.3
38	NM (0)	5.028	23.6	327	100	-	9,557	0.05579	3	0.07066	13	0.5436	8	444.0	1.4
39	NM (+1)	2.647	24.5	338	71	-	9,900	0.05628	4	0.07086	13	0.5499	8	460.4	1.6
N. TT89021 Tonalite gneiss, Follafoss															
40	NM (-2) AA	2.32	18.9	249	-	-	14,945	0.05621	8	0.07182	13	0.5566	8	460.5	1.4
41	NM (-1)AA	5.13	25.8	338	-	-	25,634	0.05620	9	0.07243	13	0.5612	8	460.1	1.3
42	NM (0)	7.75	32.4	428	-	-	9,668	0.05617	8	0.07276	13	0.5635	8	459.2	2.2
43	NM (-1)	8.37	28.7	377	-	-	13,291	0.05610	9	0.07257	13	0.5613	8	456.2	1.3
EARLY-SCANDIAN PEGMATITES															
P. RT-86-5 Tråsåvika [481/247]															
44	-200,cl,c,pl	173	17.0	259	4	0.165	9,535	0.05544	9	0.06891	20	0.5268	13	429.9	2.5
45	-200,cl,c,pl	457	13.2	210	24	0.136	8,639	0.05547	10	0.06858	10	0.5246	8	431.4	2.6
46	-200,cl,c,pl	7	23.1	367	4	0.036	3,059	0.05553	8	0.06854	8	0.5248	9	433.8	3.4
47	-200,cl,c,pl	9	18.7	297	2	0.029	5,963	0.05542	9	0.06862	11	0.5244	11	429.3	3.7
Q. TK-84-48 Fannrem [381/113]															
48	-200,m,c,s-p	20	23.2	483	7	0.609	7,802	0.05567	15	0.06833	12	0.5246	10	439.5	2.8
49	-200,cl,cr,s-p	19	22.1	328	56	0.712	3,708	0.05703	16	0.07014	15	0.5515	11	445.9	2.9
50	-200,cl,cr,m-p	22	24.9	283	7	0.813	2,308	0.06583	19	0.08498	15	0.7714	12	801.2	2.9
METAGABBRO AND ECLOGITE															
R. Selnes coronitic metagabbro [162/263]															
51	-100+200,cl,c,cr,s	284	148.1	548	39	0.717	32,851	0.09085	3	0.23742	29	2.9739	37	1,443.4	0.7
52	-100+200,cl,c,br-s	257	158.3	589	20	0.714	45,047	0.09065	3	0.23564	23	2.9453	29	1,439.3	0.6
53	Badd,-200,b,pl,NA	125	88.3	380	69	0.011	7,240	0.09055	5	0.23288	8	2.9077	96	1,437.3	1.1
54	Badd,-200,b,pl,NA	20	50.5	235	27	0.014	1,857	0.09356	7	0.22905	2	2.8536	31	1,433.5	1.4
55	Zr+Badd,-100,t,gr	90	21.9	233	30	0.025	2,821	0.07627	7	0.10032	3	1.0046	31	1,003.6	1.8
56	Zr,-200,c,t,gr	112	13.0	215	23	0.022	2,938	0.05540	12	0.06525	13	0.4985	88	428.5	4.9
57	Zr,-200,cl,t,gr	674	13.3	220	104	0.025	4,355	0.05534	4	0.06497	6	0.4958	50	426.1	1.4
Hareidland eclogite															
58	-200,cl,c,eq,f	582	3.21	55.0	10	0.018	3,794	0.05471	4	0.06400	8	0.4828	6	400.5	1.6
59	-200,cl,c,eq,f	717	2.91	49.9	8	0.021	3,743	0.05478	4	0.06395	8	0.4830	6	403.2	1.7
60	-200,cl,c,eq,f	644	4.21	72.4	10	0.021	6,800	0.54852	5	0.06378	7	0.4820	9	400.2	1.5
61	-200,cl,c,eq,f	380	3.27	55.9	16	0.020	2,918	0.05476	3	0.06418	6	0.4850	7	402.6	1.3
LATE-SCANDIAN PEGMATITES															
S. RT-86-43 Nesvatn [004/247]															
62	-200,l,c,pl	481	102	1,761	140	0.003	21,423	0.05480	2	0.06420	1	0.4851	9	404.1	0.9
63	-200,cl,cr,fr	62	111	1,923	13	0.003	16,213	0.05476	2	0.06387	6	0.4823	5	402.6	0.7
64	-200,cl,c,fr	173	95.7	1,652	15	0.003	28,777	0.05478	2	0.06381	9	0.4820	7	403.3	0.7

TABLE 1

(continued)

FRACTIONS		CONCENTRATIONS					ATOMIC RATIOS							AGE [Ma]	
No.	Properties (1)	Wt. [μg] (2)	Pb rad [ppm] (2)	U [ppm] (2)	Pb com [pg] (3)	Th/U (4)	$^{206}Pb/^{204}Pb$ (5)	$^{207}Pb/^{206}Pb$ (6)	±	$^{206}Pb/^{238}U$ (6)	±	$^{207}Pb/^{235}U$ (6)	±	$^{207}Pb/^{206}Pb$ (6)	±
T. RT-86-81 Grønningen [384/505]															
65	+200,db,n,t-p	419	147	2,567	478	0.004	7,460	0.05479	2	0.06317	7	0.4773	6	403.9	0.8
66	+200,db,cl,t-p	596	150	2,660	528	0.001	4,334	0.05482	3	0.06216	5	0.4698	4	401.7	1.0
67	+200,db,cl,c,t-p	3	80.8	1,394	1	0.003	19,072	0.05478	3	0.06383	7	0.4816	6	403.3	1.0
68	-200,db,cl,t-p	3	113	1,952	1	0.005	3,993	0.05474	8	0.06372	13	0.4809	10	401.7	2.1
U. RT-86-7 Våvatnet [269/215]															
69	-200,cl,b,t-p	204	214	3,716	570	0.009	4,668	0.05463	4	0.06327	11	0.4771	8	399.5	1.5
70	+200,cl,c,p	9	205	3,578	13	0.008	9,739	0.05468	4	0.06315	11	0.4760	8	398.9	1.5
71	-200,b,t-p	11	208	3,661	13	0.010	12,902	0.05467	4	0.06263	28	0.4721	21	398.9	1.6
V. RT-86-18 Gagnåsvatn [376/167]															
72	+200,cl,cr,pr	550	55.9	958	37	0.008	3,952	0.05511	7	0.06414	17	0.4874	10	416.6	2.0
73	200,cl,cr,pr	210	19.3	312	44	0.003	4,583	0.05666	4	0.06792	11	0.5306	10	478.4	1.6
74	+200,cl,cr,pr	50	23.4	376	12	0.008	3,113	0.05667	18	0.06841	15	0.5346	20	478.8	4.5
75	+100,cl,c,eq,pr	190	19.9	297	63	0.007	2,718	0.05752	4	0.07061	10	0.5600	10	511.5	1.6
76	+200,cl,c,pl	167	17.6	286	70	0.006	2,221	0.05692	7	0.06757	17	0.5303	13	488.6	2.1

Notes:

(1) Unless otherwise indicated, all analyses are of zircon; Badd = baddeleyite, Tit = titanite; M = monazite. All mineral grains were selected from non-paramagnetic separates at 0° tilt at full magnetic field in Frantz magnetic Separator unless otherwise indicated: NM(0) = non-magnetic at o tilt; NM(-1) = non-magnetic at –1 tilt; +200 = size in mesh (>75 μm); +100 = size in mesh (~150 μm) a = anhedral; b = brown; c = colorless; cr = cracked; dbr = dark brown; eq = equant; eu = euhedral; f = faceted; fl = flat; fr = fragment; I = inclusion rich; l-p = long-prismatic; n = needles; m-p = middle parts of prisms; p = prismatic; pb = pale brown; s-p = short-prismatic; t = turbid; t-p = tips from prisms; vpb = very pale brown. All grains air-abraded following Krogh (1982) unless otherwise indicated (NA = not abraded). Samples H, L, and M analyzed at Syracuse University by M.E. Bickford. All other analyses were made at the Royal Ontario Museum or Washington University (St. Louis) by R.D. Tucker.

(2) Concentrations are known to ± 30% for sample weights of about 30 μg and ± 50% for samples < 3 μg.

(3) Corrected for 0.0125 mole fraction common-Pb in the ^{205}Pb - ^{235}U spike.

(4) Calculated Th/U ratio assuming that all ^{208}Pb in excess of blank, common-Pb, and spike is radiogenic ($\lambda\ ^{232}Th = 4.9475 \times 10^{-11}\ y^{-1}$). Th/U not available for samples L and M.

(5) Measured, uncorrected ratio.

(6) Ratio corrected for fractionation, spike, blank, and initial common-Pb (at the determined age from Stacey and Kramers, 1975). Pb fractionation correction = 0.094% / amu (± 0.025%, 1σ); U fractionation correction = 0.111% / amu (± 0.02% 1σ). U blank = 0.2 pg; Pb blank ≤ 10 pg. Absolute uncertainties (1σ) in the Pb/U and $^{207}Pb/^{206}Pb$ ratios calculated following Ludwig (1980). For titanite analyses (Tit) this column lists $^{206}Pb/^{238}U$ ages and errors; form monazite analyses (M) this column lists $^{207}Pb/^{235}U$ ages and errors. U and Pb half-lives and isotopic abundance ratios from Jaffey and others (1971).

described by Ludwig (1980), and analytical reproducibility of the mineral fractions confirms that the parameters used in data reduction and their errors have been evaluated correctly.

The U-Pb isotopic measurements from Localities H, M and N were made in the Isotope Geochemistry Laboratory at the University of Kansas, USA. Zircons were separated at the Geological Survey of Norway by standard methods of crushing, grinding, mechanical concentration, heavy liquid separation, and magnetic separation. At Kansas, the zircons were further purified by magnetic separation and hand picking to remove impurities. The purified zircons were fractionated on the basis of magnetic susceptibility. The least magnetic fraction was air-abraded (see, Krogh, 1982) to improve concordancy. Analysis for isotopic composition and concentration was done by standard methods of isotope dilution analysis and mass spectrometry, following, with minor modifications, the methods of Krogh (1973). Mass spectrometry was done with a VG sector multicollector instrument. During the period of this work analytical blanks were 250 pg 206Pb and less than 200 pg 238U. Analyses were corrected for blank Pb using the composition of Pb measured in the laboratory. Initial Pb was assumed to have the composition of mantle Pb of appropriate age, following the model of Stacey and Kramers (1975). All zircon fractions contained enough radiogenic Pb that a reasonable uncertainty in the composition of the non-radiogenic Pb component does not contribute significantly to the uncertainty in the calculated age. The decay constants used were 238U = 0.15513 × 109 yrs. −1 and 235U = 0.98485 × 109 yrs. −1 (Steiger and Jaeger, 1977). Uncertainties (1 sigma) in measured Pb ratios were typically about 0.05 percent or less for 207Pb/206Pb and 208Pb/206Pb and 1.0 percent or less for 204Pb/206Pb. The U-Pb ratios are considered accurate to ± 1.5 percent at 2 sigma.

Keys to U-Pb Geochronology

Analytical and age results are reported/summarized in tables 1, 2 and 3, and on concordia diagrams in figures 5-8, 10-11, 14-16, 19-20, 22, 23, 24 and 26. Two to five zircon fractions or single grains of zircon were analyzed for each igneous rock in tables 1 and 2, with the exception of samples E and G, both of which yielded abundant titanite, but little zircon. Data presented here in table 3 show the results of 56 analyses of titanite fractions or single grains and two fractions of monazite, from 37 gneissic rocks and one marble, scattered throughout this part of the Western Gneiss Region.

U-Pb ages were calculated in one of two ways: by the regression technique of Davis (1982) or by the weighted average of the 207Pb/206Pb ages (Ludwig, 1992). Because many of the analyses are concordant within error, the cited age for most rocks (15 in total) is the average 207Pb/206Pb age weighted according to the inverse variance of the individual analyses. The validity of the last approach is confirmed by the reproducibility of the 207Pb/206Pb ages, which is portrayed graphically in the concordia figures and quantified by the mean square of the weighted deviates (MSWD). In all cases, the MSWD is unity (or much less than one) indicating that errors assigned to individual 207Pb/206Pb ages (commonly less than ± 2 my) may be somewhat overestimated. For samples where all analyses (or a significant number of them) are discordant, the regression method of Davis (1982) is preferred because it can be reasonably inferred that discordance is attributable to the trace presence of inheritance or to secondary Pb-loss. In all cases, age uncertainties are quoted and shown in concordia figures, at 95 percent confidence limits.

Table 2 lists the age for each sample and provides clarifying remarks. Many of the zircon analyses are concordant and may be interpreted unambiguously as the age of crystallization; others exhibit slight discordance that, in most cases, may be attributed to the trace amounts of secondary Pb-loss. Notable exceptions include samples H (Gjæsingen quartz monzonite), Q (Fannrem pegmatite) and V (Gagnåsvatn pegmatite), all of which show signs of having inherited zircon in some analyses.

Table 2

Summary of U-Pb ages, Outer Trondheimsfjord

Sample	Age (Ma)	Comments
	ORDOVICIAN INTRUSIVE IGNEOUS ROCKS	
A. Smøla granodiorite	445.7 ± 3.8 [1]	Weighted average $^{207}Pb/^{206}Pb$ age of five zircon analyses, four of which are concordant.
B. Hitra granite	443.0 ± 2.5 [1]	Weighted average $^{207}Pb/^{206}Pb$ age of three zircon analyses, one of which is concordant.
C. Hitra hornblende diorite	444.7 ± 1.4 [1]	Weighted average $^{207}Pb/^{206}Pb$ age of four zircon analyses all of which are concordant.
D. Hitra diorite	440 ± 3	Single titanite analysis (analysis 13); minimum emplacement age.
E. Fillan diorite porphyry	446 ± 3	Single titanite analysis (analysis 14); minimum resetting age.
F. Lerberen granite	441.2 ± 2.9 [1]	Weighted average $^{207}Pb/^{206}Pb$ age of four zircon analyses, three of which are concordant.
G. Uthaug gneiss	441 ± 3	Single titanite analysis (analysis 19), possible resetting age.
H. Gjæsingen Quartz Monzonite	438 ± 4.5	Weighted average $^{207}Pb/^{206}Pb$ age of three discordant analyses(20-22). A fourth analysis is interpreted as having a trace amount of inherited zircon.
J. Kopparen diorite	476.6 +2.1/-2.2 [2]	Lower intercept of regression defined by four analyses (24-27). Upper-intercept (1599 +82/-77 Ma) is interpreted as the mean age of an inherited zircon component.
K. Kjørsvika diorite gneiss	460.7 ± 2.3 [1]	Weighted average $^{207}Pb/^{206}Pb$ age of four zircon analyses three of which are concordant. A single titanite analysis (32) defined an age of 455 ± 3 Ma interpreted as a time of partial resetting.
L. Lensvik gneisses	481.9 ± 1.5 [1]	Weighted average $^{207}Pb/^{206}Pb$ age of four zircon analyses.
M. Simadalen diorite	444 ± 3 [1]	Weighted average $^{207}Pb/^{206}Pb$ age of two zircon analyses (37,38) .
N. Follafoss tonalite gneiss	460 ± 3 [1]	Weighted average $^{207}Pb/^{206}Pb$ age of four zircon analyses (40-43)
	EARLY-SCANDIAN PEGMATITES	
P. Tråsåvika pegmatite	431.0 ± 2.9 [1]	Weighted average $^{207}Pb/^{206}Pb$ age of four zircon analyses (44-47) all of which are concordant.
Q. Fannrem pegmatite	422.7 ± 1.8 [2]	Lower intercept of regression defined by three zircon analyses (48-50). Upper intercept age of 1510 +24/-23 Ma is interpreted as the mean age of an inherited zircon component.
	METAGABBRO AND ECLOGITE	
R. Selnes metagabbro	1461 ± 2 [2] 401 ± 2 [2]	Upper intercept of regression defined by seven analyses of zircon and baddeleyite (51-57) interpreted as the age of gabbro emplacement. Lower intercept is interpreted as the time of new zircon growth, partial Pb-loss in igneous zircon and baddeleyite, and development of coronitic texture.
Hareidland eclogite	402 ± 2 [1]	Weighted average $^{207}Pb/^{206}Pb$ age of four zircon analyses (58-61) interpreted as the time of metamorphic zircon growth and eclogitization.
	LATE-SCANDIAN PEGMATITES	
S. Nesvatn pegmatite	403.3 ± 1.9 [1]	Weighted average $^{207}Pb/^{206}Pb$ age of three concordant zircon analyses (62-64).
T. Grønningen pegmatite	404.0 ± 2.1 [1]	Weighted average $^{207}Pb/^{206}Pb$ age of four zircon analyses (65-68).
U. Våvatnet pegmatite	399.1 ± 1.7 [1]	Weighted average $^{207}Pb/^{206}Pb$ age of three zircon analyses (69-71).
V. Gagnåsvatn pegmatite	391 +4/-5 [2]	Lower intercept of regression defined by five zircon analyses (72-76) interpreted as the time of pegmatite emplacement. Upper-intercept of regression (949 +54/-51 Ma) is interpreted as the mean age of inherited zircon components.

All ages reported at 95% confidence.

1) Weighted mean calculated with ISOPLOT algorithm of Ludwig (1992).

2) Regression age calculated using algorithm of Davis (1982).

TABLE 3

U-Pb titanite and monazite analyses, Western Gneiss Region, Norway

FRACTIONS		CONCENTRATIONS					ATOMIC RATIOS			AGE [Ma]	
No.	Properties (1)	Wt. [mg] (2)	Pb rad [ppm] (2)	U [ppm] (2)	Th/U (3)	$^{206}Pb/^{204}Pb$ (4)	$^{206}Pb/^{238}U$ (5)	$^{207}Pb/^{235}U$ (5)	$^{207}Pb/^{206}Pb$ (5)	$^{207}Pb/^{206}Pb$ (5)	% Discord-ance (6)
1a	Storvatn, 1.3.+150,a,b,rb,t 1.3,+1.5.a.b,rb,t,mc	1.412	41.8	74.7	3.81	778.7	0.28371 86	3.9570 133	0.10116 15	1645	5.1
1b	Storvatn, 1.3.+150,a,b,rb,t	0.421	43.1	78.1	3.69	851.6	0.28663 93	3.9991 141	0.10119 15	1646	5.1
2	Ingdal, 1.3+150,a,db,mc	0.815	44.6	90.2	2.99	740.9	0.27900 107	3.8851 158	0.10099 13	1642	6.1
3	Ingdal, 1.3,+150,a,db,mc,t	0.637	34.8	94.6	1.62	520.2	0.25731 67	3.5458 118	0.09995 19	1623	15.5
4a	Ingdal, 1.3,+150,db,a,t	2.503	20.1	69.8	1.12	287.6	0.21324 57	2.8472 124	0.09684 31	1564	34.7
4b	Ingdal, .3,+150,db,a,t	0.302	43.7	121	2.25	856.2	0.19997 115	2.6589 161	0.09644 20	1556	36.8
5	Ingdal,1.3,+150,br,mc,t	0.342	39.8	116	2.13	744.6	0.19123 58 ..	2.5024 120	0.09491 31	1526	39.8
6	Hundvatn, 1.3,+150,a,br,t 1.3,+150,br,mc,t 1.3,+150,br,mc,t	0.344	29.9	65.5	3.05	401.7	0.23773 71	3.2397 130	0.09884 22	1602	22.2
7a	Ruten, 1.3,+150,po,t,b	0.333	32.0	81.3	2.42	424.5	0.22071 122	2.9602 184	0.09727 24	1572	31.8
b	Ruten, 1.3,+150,br,t,mc,a	0.188	38.2	87.9	3.14	449.7	0.20565 72	2.7260 114	0.09614 24	1550	37.1
c	Ruten, 1.3,+150,br,t,mc,a	0.325	36.1	87.1	3.01	380.3	0.19483 71	2.5601 95	0.09530 14	1534	36.8
8a	Karøydal,1.3,+150,do,cl,s	1.926	33.6	63.1	4.11	426.2	0.23073 63	3.1245 103	0.09822 14	1591	27.5
b	Karøydal,1.3,+150,do,cl,s	0.322	38.9	77.7	3.61	511.0	0.23728 64	3.2233 97	0.09852 18	1596	25.1
c	Karøydal, 1.3,+150,do,cl,s	0.430	35.7	64.4	4.35	444.3	0.23495 77	3.1891 101	0.09844 19	1594	26.4
9	Sunndalsøra,1.3,+150,br,b,t	0.583	72.9	219	1.43	963.4	0.23715 103	3.2247 149	0.09862 21	1598	24.3
10	Hasselvika,1.0+150,db,cl.s	0.660	49.4	178	1.36	625.5	0.18539 107	2.3718 149	0.09279 21	1484	45.9
11	Arlottneset, 1.0+150, br,cl.i	0.193	35.9	110	1.77	348.1	0.20493 79	2.7206 118	0.09628 17	1553	37.6
12*	Hambortåa,1.0,+150,cl,f,pb	1.488	1.47	24.6	0.105	218.6	0.06387 17	0.4830 22	0.05485 17	406	99.5
13	Snilldal,1.3,+150,db,t,a,b	1.376	4.80	15.7	1.61	366.6	0.19487 113	2.5513 160	0.09496 28	1527	41.9
14a	U. Snilldal,1.3,+150,pb,t,a,mc	2.278	2.92	10.3	1.78	209.5	0.15741 47	1.9663 103	0.09060 35	1438	59.0
b	U. Snilldal,1.3,+150,pb,t,a,mc	0.640	22.1	88.5	1.25	329.1	0.16287 48	2.0499 75	0.09128 16	1453	57.1

TABLE 3

(continued)

FRACTIONS		CONCENTRATIONS					ATOMIC RATIOS			AGE [Ma]	
No.	Properties (1)	Wt. [mg] (2)	Pb rad [ppm] (2)	U [ppm] (2)	Th/U (3)	$^{206}Pb/^{204}Pb$ (4)	$^{206}Pb/^{238}U$ (5)	$^{207}Pb/^{235}U$ (5)	$^{207}Pb/^{206}Pb$ (5)	$^{207}Pb/^{206}Pb$ (5)	% Discord-ance (6)
15a	Våvatnet,1.3,+150,db,cl,s	0.298	94.2	267	1.95	1,288.	0.21618 83	2.8998 116	0.09729 9	1573	33.4
b	Våvatnet, 1.3,+150,db,t,mc,s	0.537	96.5	290	1.82	1,468.	0.20454 109	2.7188 162	0.09641 17	1555	34.9
c	Våvatnet, 1.3,+150,db,t,mc,s	0.378	99.9	298	1.79	1,590.	0.20883 104	2.7805 156	0.09657 17	1559	34.5
d	Våvatnet, 1.3,+150,2 gr,db,cl,s	0.055	91.7	309	1.64	1,379.	0.18290 86	2.3732 117	0.09411 18	1510	45.1
e	Våvatnet, 1.3,+150,1 gr,db,cl,s	0.021	88.7	284	1.78	1,098.	0.18794 73	2.4495 99	0.09453 27	1519	44.9
f	Våvatnet, 1.3,+150,1 gr,db,cl,s	0.044	119.	308	2.75	2,005.	0.23612 79	3.2143 109	0.09873 14	1600	24.0
16	Vutudal, 1.3,+150,pb,cl,a gr,db,cl,sh	0.709	32.7	122	1.46	534.8	0.16605 157	2.1092 201	0.09213 19	1470	55.0
17	Hemnesfjord, 1.3,+150,po,t,a gr,db,cl,sh	0.609	30.8	74.6	2.97	391.2	0.19674 60	2.5873 98	0.09538 20	1536	41.0
18	Smiset, 1.3,+150,br,t,i gr,db,cl,sh	0.777	33.9	71.4	3.44	622.2	0.22154 97	3.0082 145	0.09848 27	1596	31.1
19	Alvund,1.0,+150,cl,f,pb	1.496	25.2	72.9	2.24	437.8	0.18243 86	2.3575 123	0.09373 23	1503	48.1
20	Mulvikknuken, 1,+150,cl,f,pb	0.255	38.4	155	1.11	383.4	0.17178 103	2.1859 156	0.09229 41	1473	52.7
21	Meisingset,1.3,+150,br,t,mc	2.810	17.6	45.4	2.78	206.8	0.18501 60	2.4018 163	0.09416 52	1511	44.9
22	Verrafjord,1.0,+150,db,cl,s	0.269	59.9	237	1.28	1,136.	0.16417 40	2.0738 57	0.09162 9	1459	56.0
23*	Sagfjord,1.0,+150,py,f,cd	0.753	5.92	102	0.039	251.8	0.06322 17	0.4762 26	0.05463 24	397	99.8
24a	Åstfjord,1.3,+150,db,mc,t	1.753	19.8	89.1	1.28	313.2	0.13247 36	1.5782 99	0.08641 44	1347	70.1
b*	Åstfjord, 1.3,+150,db,t,b,i	1.587	2.85	45.2	0.042	587.9	0.06590 26	0.5195 25	0.05718 16	498	99.0
25	Hemnefjord,1.0,+75,po,cl,s	0.405	33.1	225	0.691	657.5	0.10168 27	1.0836 36	0.07729 12	1129	83.2
26	Dalem,1.3,+75,cl,br,f	0.569	24.8	115	1.19	461.8	0.13251 35	1.5734 50	0.08611 15	1341	70.0
27	Eidsfoss,1.0,+75,pb,cd,op	0.323	53.7	280	0.664	1,002.	0.15045 73	1.8610 92	0.08972 12	1419	62.0
28a*	Vinjefjord,1.7,+150,pb,cr,a	0.489	12.8	175	0.186	241.5	0.06448 42	0.5107 50	0.05745 41	509	98.5
b*	Vinjefjord, 1.7,+150,pb,cr,a	0.370	13.1	183	0.175	255.2	0.06397 48	0.4912 56	0.05569 50	440	99.1

TABLE 3
(continued)

FRACTIONS		CONCENTRATIONS					ATOMIC RATIOS			AGE [Ma]	
No.	Properties (1)	Wt. [mg] (2)	Pb rad [ppm] (2)	U [ppm] (2)	Th/U (3)	$^{206}Pb/^{204}Pb$ (4)	$^{206}Pb/^{238}U$ (5)	$^{207}Pb/^{235}U$ (5)	$^{207}Pb/^{206}Pb$ (5)	$^{207}Pb/^{206}Pb$ (5)	% Discord-ance (6)
29a	Tingvoll,1.2,+75,db,t,mc	0.757	30.9	133	1.42	469.1	0.13179 97	1.5833 121	0.08713 50	1363	67.1
b*	Tingvoll, 1.2,+75, pb,cl,f	0.984	3.49	56.4	0.036	151.4	0.06524 51	0.5070 130	0.05637 133	467	98.6
c	Tingvoll,1.3,+150,db,mc,t	4.328	29.8	113	1.77	456.3	0.13655 55	1.6491 78	0.08759 21	1374	67.0
d	Tingvoll, 1.3,+150,db,mc,t	0.897	29.6	118	1.62	445.5	0.13657 46	1.6519 70	0.08773 20	1377	66.5
e*	Tingvoll, 1.3,+150,pb,cl,f	0.809	3.74	59.4	0.169	193.9	0.06592 36	0.5223 81	0.05746 79	509	98.5
30a*	Nesvatnet, M,pr,cl	0.065	1100	2390	45.0	22,890	0.06399 35	0.4810 160	0.05456 5	394	100
b*	Nesvatnet, M,py,cl	0.246	1080	3590	13.0	22,400	0.06367 21	0.4790 157	0.05456 5	394	99.9
31a*	Gjela,1.7,+75,py,f,cd	0.086	23.4	404	0.080	437.1	0.06239 18	0.4695 23	0.05458 20	395	99.9
b*	Gjela, 1.7,+75,py,f,cd	0.972	22.8	387	0.082	703.3	0.06349 27	0.4775 24	0.05454 14	393	100
32*	Ertvåg, 1.7,+150,py,f,cd	0.346	13.4	228	0.094	403.8	0.06306 17	0.4762 24	0.05477 22	403	99.1
33*	Ertvåg, 1.7,+150,py,f,cd	1.218	21.5	365	0.040	671.2	0.06571 33	0.5159 28	0.05695 15	490	99.0
34	Vulvik, 1.7,+150,py,f,cd	1.272	21.4	188	2.76	345.7	0.07046 17	0.5928 30	0.06103 25	640	96.8
35*	Kvernberget, 1.3,+150,db	1.007	18.0	255	0.459	270.8	0.06653 19	0.5354 33	0.05836 30	543	97.9
36*	Kvernberget,1.3,+150, db	1.802	14.6	237	0.104	363.0	0.06574 21	0.5143 29	0.05674 24	481	98.8
37*	Frei Island, 1.3,+150, db,op	2.252	16.5	280	0.072	525.2	0.06352 17	0.4794 21	0.05474 17	402	99.8
38*	Kristiansund,1.7,+150,py,f,cl	0.813	5.09	81.6	0.251	552.6	0.06392 20	0.4876 22	0.05533 17	425	99.5

Notes:

(1) M = monazite (*e.g.* analyses 30a,b);all other analyses are titanite; 1.3 etc. = paramagntic at 1.3 amperes in Frantz Magnetic Separator at 10 degree tilt; +100, +75 = grain diameter greater than indicated mesh size (*i.e* +100 mesh); a = anhedral; b = blocky; br = brown; c = colorless; cd = clouded; cl= clear; cr = cracked; db = dark brown; do = dark orange; e = euhedral; f = faceted prismatic; gr = granular; i = contains inclusions; o = orange; mc = microcracks; op = outer portions contains clear faceted titanite; pb = pale brown;po = pale orange, py = pale yellow; rb = red brown, s = subhedral; sp = short-prismatic; t = turbid. All grains air abraded following Krogh (1982). Numbered analyses with an asterisk (*i.e.* 12*) are neocrystallized titanite.

(2) Concentrations are known to ± 5% for sample weights of ≥ 100 µg and ± 10% for samples ≤ 50 µg.

(3) Model Th/U ratio assuming that all ^{208}Pb in excess of blank, common-Pb, and spike is radiogenic and concordant at the 207/206 age given ($\lambda\ ^{232}Th = 4.9475 \times 10^{-11}\ y^{-1}$).

(4) Measured, uncorrected ratio.

(5) Ratio corrected for fractionation, spike, blank, and initial common-Pb (at the determined age from Stacey and Kramers (1975)). Pb and U fractionation correction = 0.1%/amu (± 0.07%); U blank = 1-5 pg, Pb blank ≤ 50 pg. Absolute uncertainties (1σ) in the Pb/U and $^{207}Pb/^{206}Pb$ ratios calculated following Ludwig (1980). U and Pb half-lives and isotopic abundance ratios from Jaffey and others (1971).

(6) Percent discordance between the intercepts of 1657 Ma and 395 Ma.

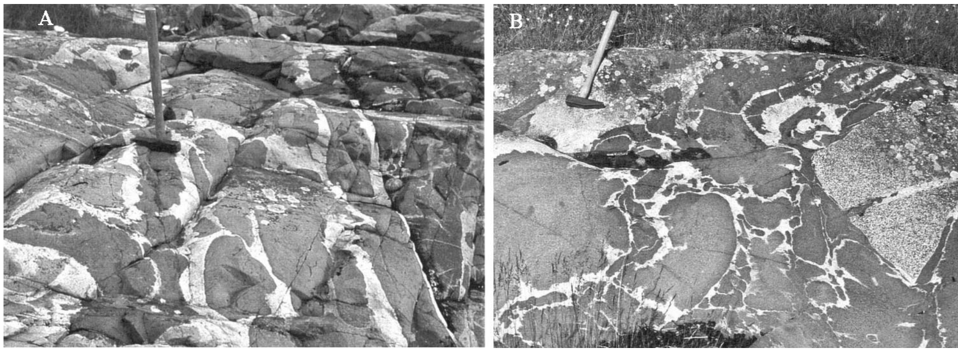

Fig. 4. Outcrops of undeformed diorite, granite, and tonalite from Smøla. Outcrops show both pillow-like injections and mafic xenoliths in more granitoid matrix, typical of many calc-alkaline arc magmas. Photographs by Håvard Gautneb (see Gautneb and Roberts, 1989).

Some of our titanite analyses, particularly those in Ordovician intrusions above the Høybakken and Agdenes detachments (table 1), are concordant but imprecise owing to a large component of initial-Pb in them. In the case of analyses 13, 14, 19, and 32 (table 1), the titanites are concordant at the same or nearly the same age as the zircon, thereby corroborating the fact that rocks above these detachments were not profoundly disturbed by Scandian effects that are recorded in rocks below the detachments. Below the Agdenes detachment, in late Paleoproterozoic gneisses throughout this part of the Western Gneiss Region, the titanites display a remarkable and variable degree of discordance from a common ~1650 Ma igneous or metamorphic closure age, in which combined effects of Pb-loss, reactions rims, and metamorphic recrystallization correlate with metamorphic grade. Least discordant titanites are from rocks of upper greenschist and low amphibolite facies, whereas moderate and severe discordance is observed in titanites from rocks of upper amphibolite facies. For details of titanite geochronology see the section "*Pb Loss and Neocrystallization of Titanite*".

NEW ISOTOPIC AGES OF INTRUSIVE IGNEOUS ROCKS

Distribution of Rocks

A major and essential point of this paper is that there is a large province of Ordovician and Early Silurian intrusive igneous rocks in the outer Trondheimsfjord region. These intrusive rocks are best known from Smøla, Hitra, Ørlandet, Frøya, and Froan (Gautneb and Roberts, 1989; Lindstrøm, ms, 1995; Nordgulen and others, 1995), above the Høybakken extensional detachment associated with outcrops of the Devonian basins. Smøla is dominated by a weakly deformed to undeformed complex of gabbros, diorites, tonalites and granites with complex primary igneous contact relationships (fig. 4) that are intrusive into a sequence of greenschist facies, weakly folded, Ordovician fossil-bearing sedimentary and volcanic rocks. The metamorphism and deformation have been considered to represent a Mid-Ordovician, Taconian equivalent event (Hall and Roberts, 1988). Like the Early Ordovician fossils in the Støren Nappe at Hølonda, the fossils on Smøla also have Laurentian faunal affinities (Bruton and Bockelie, 1979). The Arenig-Llanvirn fossils and field relationships show that these intrusions are Late Ordovician or younger, and preliminary Ordovician U-Pb zircon ages were reported previously (Tucker, 1988; Gautneb and Roberts, 1989). The following is the first complete report of these ages (table 1 and related concordia diagrams).

Ages Above the Høybakken Detachment

Sample localities A through H lie above the Høybakken detachment. Five zircon fractions from granodiorite at Locality A, including four that are concordant (fig. 5), give a weighted mean 207/206 age of 445.7 ± 3.8 Ma (Early Ashgill based on Tucker and McKerrow, 1995). Three zircon fractions from granite at locality B on Hitra, including one, which is concordant, give a weighted mean 207/206 age of 443.0 ± 2.5 Ma (Ashgill-Lllandovery). Four concordant zircon fractions from hornblende diorite at locality C (fig. 6) give a weighted mean 207/206 age of 444.7 ± 1.4 Ma (Ashgill). A single titanite analysis from gneissic diorite at Locality D gives a 207/206 minimum emplacement age of 440 Ma ± 3 (Early Llandovery). A single titanite analysis from diorite porphyry at Locality E near Fillan on Hitra gives a 207/206 minimum resetting age of 446 ± 3 Ma (Ashgill). Four zircon fractions from even-grained non-foliated leucogranite (fig. 7) near the quarry at Lerberen (Locality F), including three, which are concordant, give a weighted average age of 441.2 ± 2.9 Ma (Early Llandovery). A single titanite analysis from granitic gneiss at Uthaug (Locality G, fig. 7) gives a 207/206 minimum resetting age of 441 ± 3 Ma (Early Llandovery). Three zircon analyses from Gjæsingen quartz monzonite at Locality H (fig. 8) yield a weighted average age of 438 ± 5 Ma (Llandovery). The span of ages for dated rocks above the detachment is from 446 to 438 Ma.

Ages Below the Høybakken Detachment

In addition to the widespread occurrence of Ordovician – Early Silurian intrusive rocks above the detachment fault, recent reconnaissance, compilations, and radiometric age determinations indicate that the same or similar rocks are widespread below the

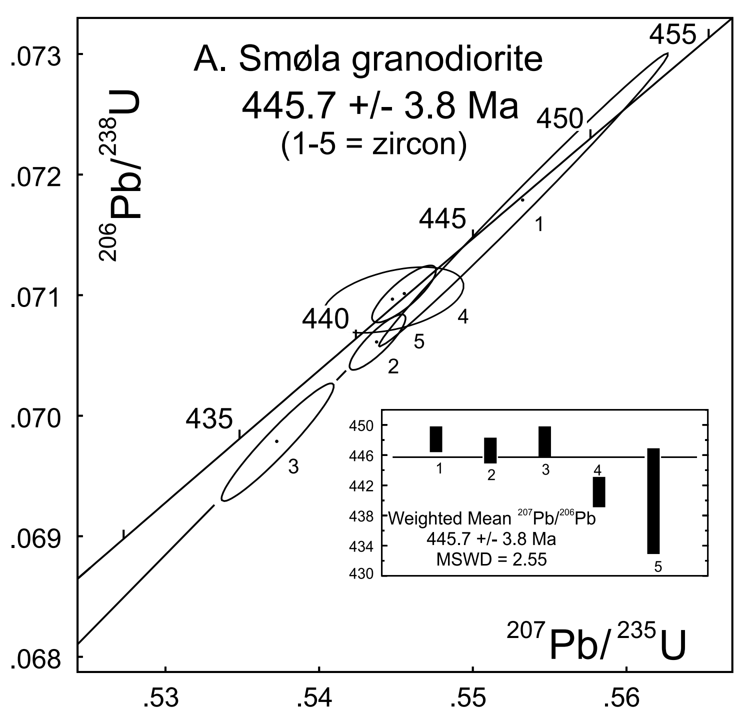

Fig. 5. Concordia diagram showing Late Ordovician U-Pb age of igneous zircon in granodiorite from Smøla (Locality A).

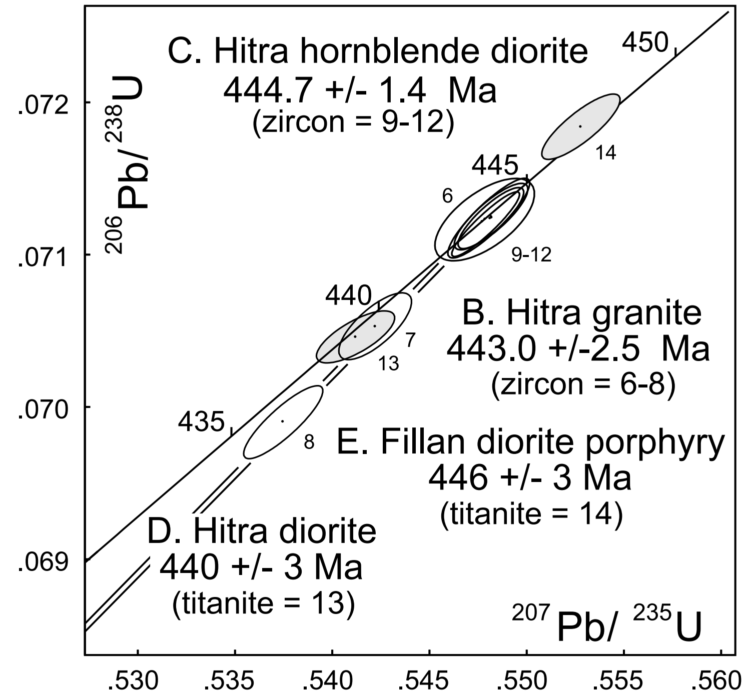

Fig. 6. Concordia diagram showing Late Ordovician and Early Silurian U-Pb ages of igneous zircon and titanite from granite, diorite, diorite gneiss, and diorite porphyry on Hitra (Localities B, C, D, E).

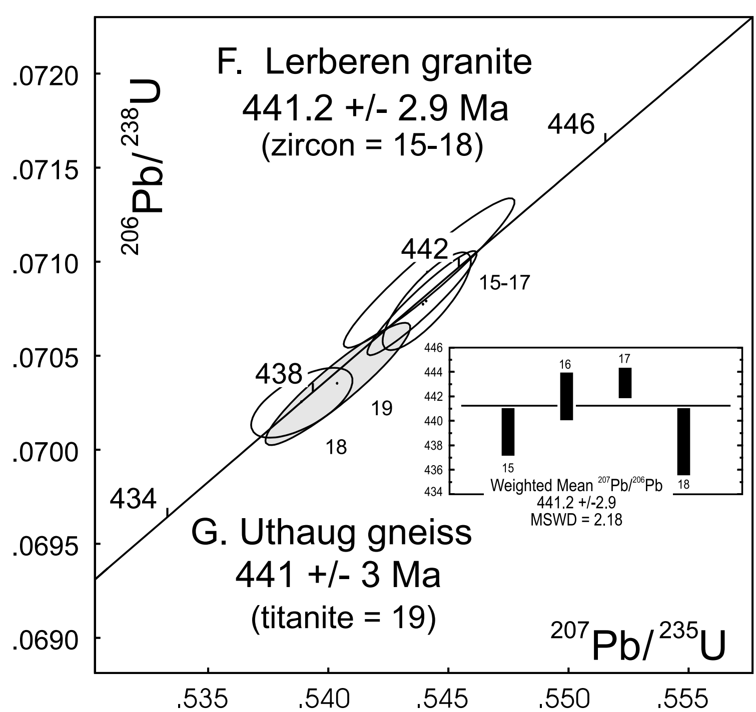

Fig. 7. Concordia diagram showing Early Silurian U-Pb age of igneous zircon from Lerberen Granite (Locality F) and igneous titanite from Uthaug Gneiss (Locality G).

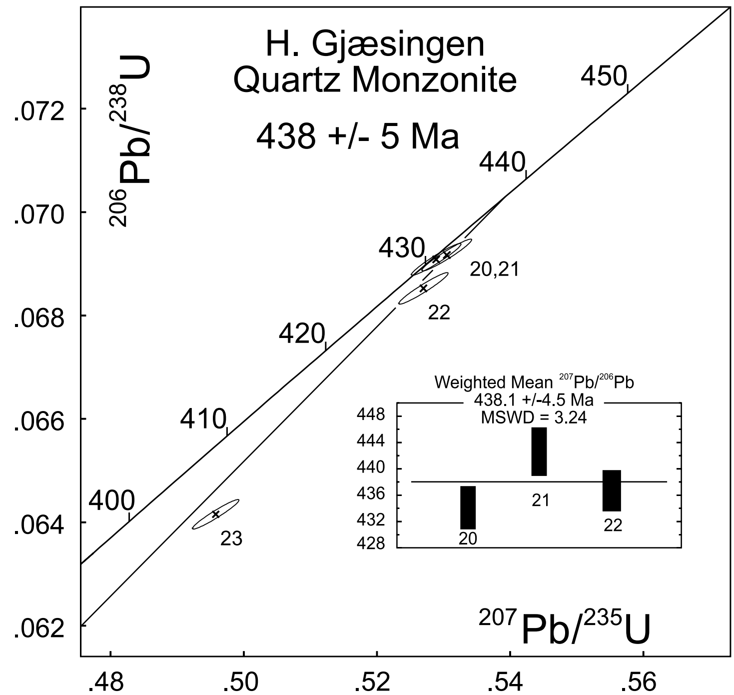

Fig. 8. Concordia diagram showing Mid Silurian U-Pb age of igneous zircon from Gjæsingen Quartz Monzonite (Locality H).

detachment. Here they occur as strongly foliated and lineated gneisses containing the same strong subhorizontal linear fabric found in the subjacent nappes and Baltican basement (fig. 9). Here we report U-Pb zircon ages from Localities J, K, L, M and N. Of four zircon fractions (fig. 10) from a granodiorite at Kopparen (Locality J) on Fosen Peninsula, two are concordant and two show substantial Proterozoic inheritance at 1599 +82/−77 Ma. Together, the four points yield a weighted mean 207/206 age of 476.6 +2.1/−2.2 Ma (Middle Arenig). Four zircon fractions (fig. 11) from locality K at Kjørsvika on the mainland south of Hitra, including three that are concordant, give a weighted mean 207/206 age of 460.7 ± 2.3 Ma (Late Llanvirn). A single titanite analysis at 455 ± 3 Ma may be the result of slow cooling or slight Caledonian resetting. The particular significance of this sample locality is that it lies just 2 km north from basement of the Western Gneiss Region in the area of 100 percent titanite resetting (see below) and contains the same strong, late-Scandian, subhorizontal, sinistral ductile shear fabric. Four zircon fractions (fig. 11) from felsic gneiss at Locality L in the Lensvik syncline give a weighted mean 207/206 age of 481 ± 1.5 Ma (latest Tremadoc).

On Fosen, northeastward from Locality J at Kopparen (fig. 2) to the vicinity of Follafoss there is an elongated massif, comprising tonalitic, granodioritic and granitic intrusive gneisses, which crops out over a distance of at least 70 km, and covers an area of approximately 400 km^2. This massif forms an enormous folded slab wrapping around a prominent late NE-plunging anticline having both limbs modified by faults of the Møre-Trøndelag Fault Complex, the Hitra-Snåsa Fault along the northwestern limb and the Verran Fault along the southeastern limb. Locality L at Lensvik, just described, lies in a complementary NE-plunging syncline. Over large areas, the massif is texturally and mineralogically rather homogeneous, though a varying degree of

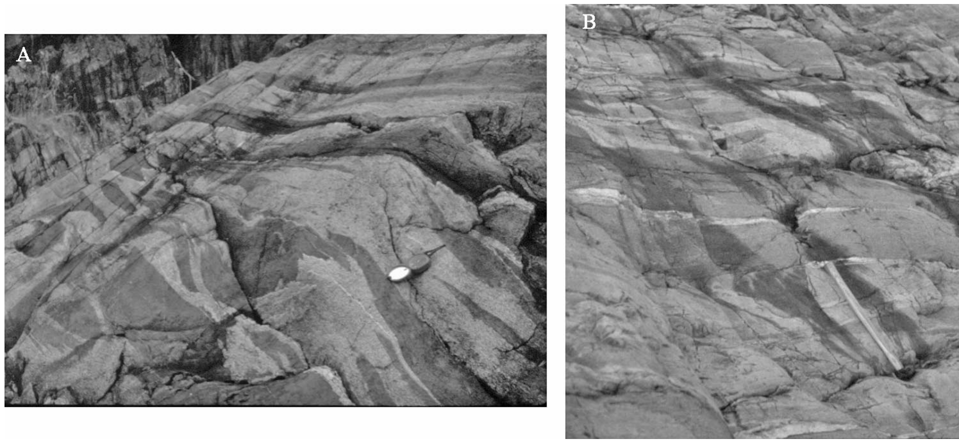

Fig. 9. Outrops of strongly foliated and lineated tonalite, granodiorite and granite from the Lensvik syncline (Locality L). Like the undeformed equivalents, these outcrops show evidence of complex coexistence of varied calc-alkaline arc magmas.

deformation related to the fault zones has given rise to mylonites and cataclasites. The core of the anticline is occupied by migmatitic granitic to tonalitic Paleoproterozoic basement gneisses complexly interfolded with supracrustal rocks such as amphibolite,

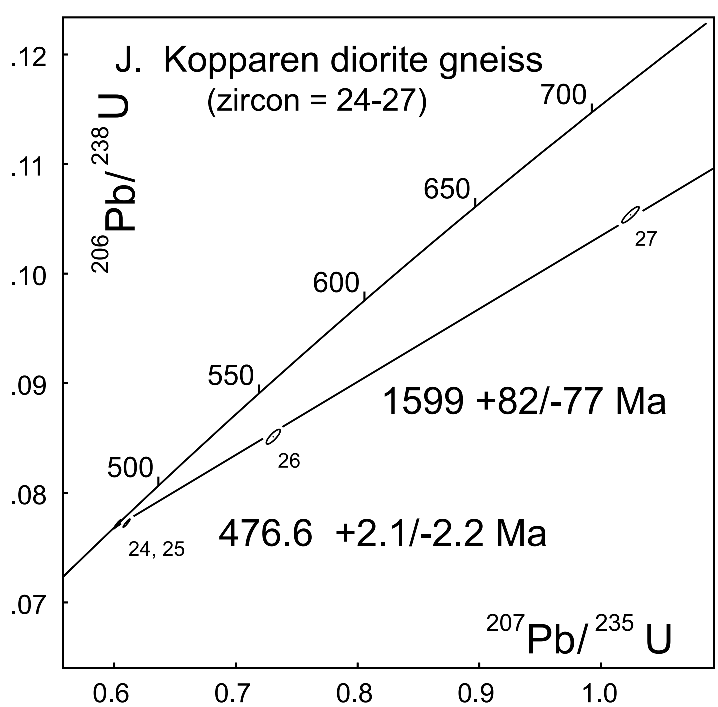

Fig. 10. Concordia diagram showing Mid Ordovician U-Pb ages of igneous zircon in granodiorite gneiss from Kopparen (Locality J). Two zircon fractions show Proterozoic inheritance.

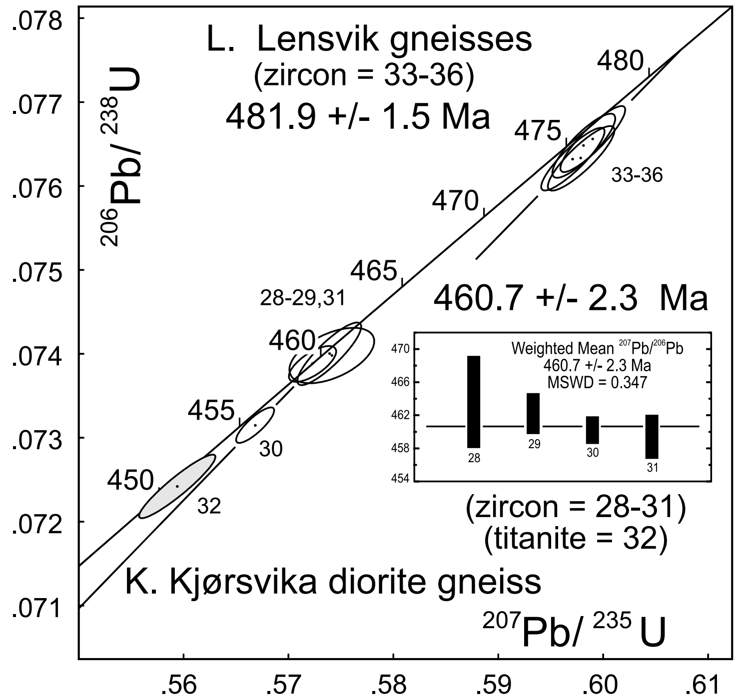

Fig. 11. Concordia diagram showing Ordovician U-Pb ages of igneous zircon from diorite gneiss at Kjørsvika (Locality K) and from granodiorite gneiss near Lensvik (Locality L).

marble and a dominant quartz-rich garnet-kyanite-mica gneiss (Thorsnes and Grønlie, 1990) here assigned to the Seve Nappe.

Where the top of the tonalitic gneisses crosses the crest of the anticline near Follafoss (fig. 12), the gneisses are unconformably overlain by a polymict conglomerate (Carstens, 1960; Thorsnes, 1989) (fig. 13), here named informally, the Almlia Conglomerate, and forming the basal formation of the Beitstad Group. The conglomerate is, in turn, overlain by metamorphosed well bedded volcanogenic sedimentary rocks of the Beitstad Group, which are assigned to the Støren Nappe (Tietzsch-Tyler and Roberts, 1990). The initial discovery of this conglomerate and overlying rocks, with obvious affinities to the Hovin Group succession of the Støren Nappe, resting unconformably on gneisses then interpreted to belong to the Proterozoic Baltica basement, produced reactions of disbelief. For this reason, we give some observations and descriptions of the setting of this locality in an Appendix to assist in interpretation of the zircon ages.

U-Pb zircon ages were obtained from specimens at Localities M and N. Locality M is a foliated diorite from north of the Hitra-Snåsa Fault and west of the area of figure 12. Of three zircon fractions (fig. 14), two are nearly concordant and give a mean age of 444 $\pm$ 3 Ma (Ashgill). Locality N is the foliated tonalite shown in figure 12 that is overlain by the Almlia Conglomerate. Four zircon fractions (fig. 14) regress to an age of 460 $\pm$ 3 Ma (Late Llanvirn). This age is consistent with the proposed correlation of the unconformably overlying Beitstad Group with the Late Ordovician Upper Hovin Group, requiring, however, relatively rapid uplift and erosion of the tonalite intrusion.

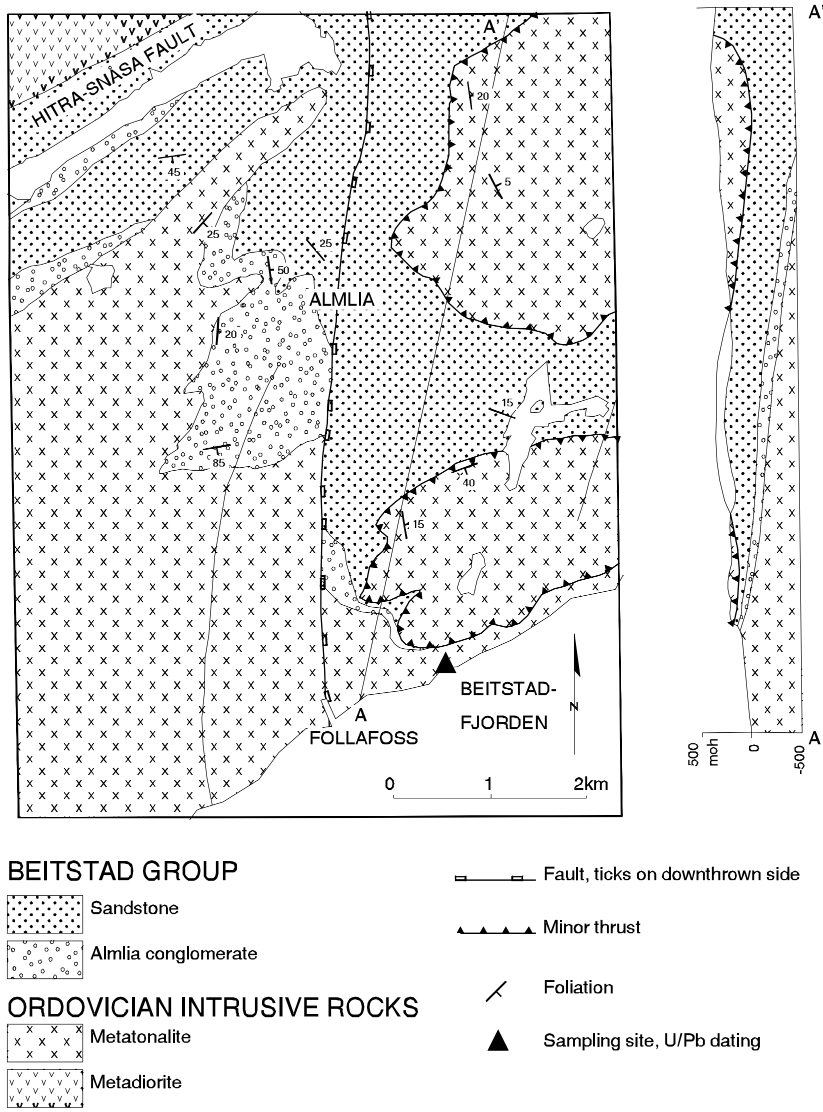

Fig. 12. Detailed bedrock and structural geologic map of the Follafoss area showing distribution of the Almlia Conglomerate and underlying tonalite gneiss (Locality N). From Thorsnes and others, unpublished manuscript.

Some Related Ordovician Intrusions

A pluton of particular interest to this paper lies about 100 km along strike northeast of Follafoss outside the area of figure 2, but indicated on figure 1. This pluton is the Møklevatn Granodiorite in the Gjersvik Nappe, one of the several Köli Nappes of the Upper Allochthon in Nord-Trøndelag. The granodiorite, dated by the U/Pb zircon method at 456 ± 2 Ma, has intruded a thick, bimodal sequence of Lower to Middle Ordovician volcanic rocks (Roberts and Tucker, 1991). Unconformably overlying the magmatic complex, there is a sequence of low-grade polymict

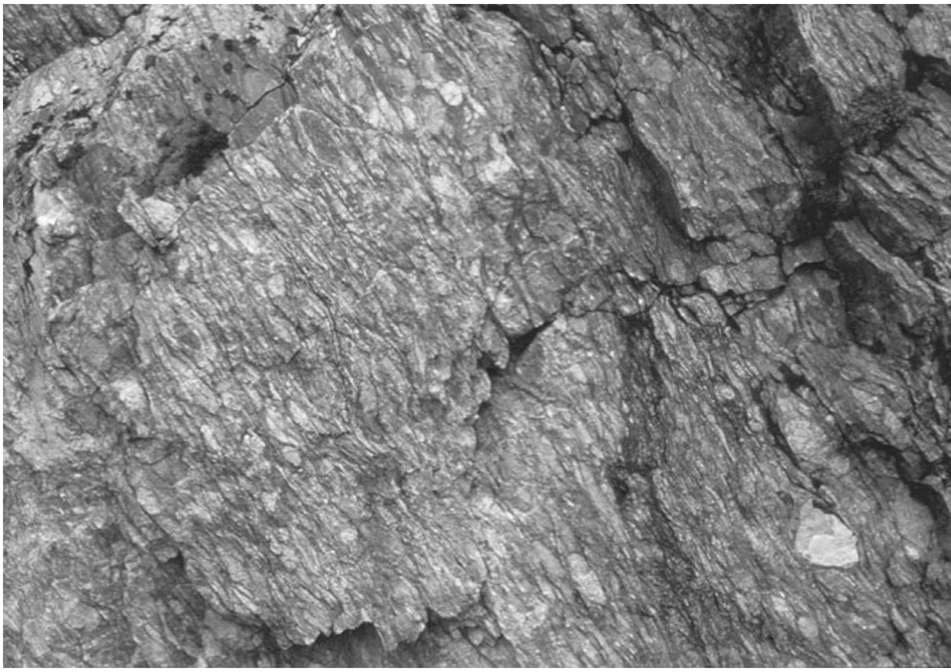

Fig. 13. Outcrop of Almlia Conglomerate at Follafoss that unconformably overlies Mid Ordovician tonalite gneiss with a U-Pb age of 460 Ma (Locality N). The clast population includes tonalite from the underlying substrate as well as a variety of metamorphosed volcanic rocks.

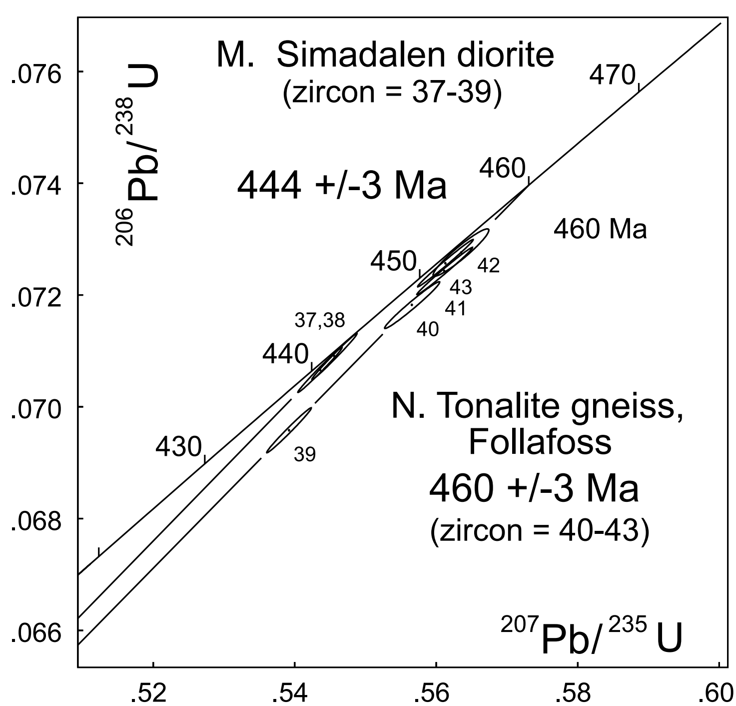

Fig. 14. Concordia diagram showing Ordovician U-Pb ages of igneous zircon from diorite at Simadalen (Locality M) and tonalite at Follafoss (Locality N).

conglomerates, calcareous sandstones, phyllites and thin volcanites, the Limingen Group, of assumed Late Ordovician age. The relationships are very similar to those near Follafoss. The nearby Nesåa Batholith, also in the Gjersvik Nappe, has recently been dated at 458 ± 3 Ma (Meyer and others, 2003).

Further Comments on Ordovician Intrusions

In evaluating the age range of the 13 zircon and titanite ages on intrusive rocks, note that the eight above the Høybakken detachment associated with Devonian basins are on average younger, 446, 446, 445, 443, 441, 441, 440, and 438, and the five below the detachment are older, 482, 477, 461, 460 and 444. Furthermore, the unconformity at Follafoss demonstrates that intrusive magmatic activity at that locality at 460 Ma had to have terminated and been followed by a significant erosional interval before deposition of the Almlia Conglomerate and overlying sediments. The younger intrusive activity shown by the rocks now mainly above the detachment presumably overlapped the time of sediment deposition of the Beitstad Group near Follafoss. It is perhaps tempting to imagine that the rocks above the detachment represent a higher and younger tectonic slice. However, it is well to remember that these igneous rocks represent parts of relatively large intrusions now preserved in a thrust nappe that is only a few kilometers thick, so that age variations within the nappe are much more likely to be related to original spatial distribution of plutons of different ages within a major magmatic province, rather than related to tectonic level.

EARLIEST AGES OF SCANDIAN METAMORPHISM

Firm evidence for the earliest high-grade Caledonian regional metamorphism in the area of figure 2 occurs in the Seve Nappe, parts of which contain coarse high-amphibolite-grade mineral assemblages, evidence for partial melting, and abundant pegmatites. In the area near Orkanger the pegmatites cut across an earlier strong tectonic-metamorphic foliation, but are themselves also foliated and lineated. Here, host rocks and pegmatites contain evidence of late sinistral shear (top-northeast) consistent with the position of this unit on the southeast, backfolded, upper limb of the older, originally southeast-facing recumbent Surnadal syncline. U-Pb zircon ages were obtained from two of these pegmatites (fig. 2), locality P at Tråsåvika, and locality Q on the Orkla River at Fannrem, southwest of Orkanger. At Tråsåvika (fig. 15), four concordant zircon fractions give a mean 207/206 age of 431.0 ± 2.9 Ma (Late Llandovery). At Fannrem (fig. 16), three zircon fractions contain varied degrees of Proterozoic inheritance, but regress to an age of 422.7 ±1.8 Ma (Wenlock-Ludlow) with an upper intercept age of 1510 +24/−23 Ma interpreted as a maximum age of an inherited zircon component. Together, these ages indicate that a high-grade regional metamorphism in the Seve Nappe in this region took place ~8-28 m. y. before the peak Scandian metamorphism of the underlying Proterozoic Baltica basement (see below). The high-grade metamorphic fabric cut by these pegmatites is still older and may not belong to the Scandian at all.

The problem of defining the setting and heat source for this early-Scandian metamorphism of the Seve Nappe in this area is common to the Seve and equivalent thrust nappes all along the orogen, and will not be addressed here. Very similar ages 437 to 427 Ma (Llandovery-Wenlock) were found by Gromet and others (1996) in the classic Seve Nappe in nearby Jämtland, Sweden. Similar ages of peak high-grade metamorphism of 432 Ma (Late Llandovery) were obtained by Northrup (1996) for the equivalent Narvik Nappe Complex in the lower part of the Upper Allochthon in North Norway (68 - 69° N). Northrup equated this age with the emplacement of the allochthon and beginning of cooling of the underlying Baltican basement. However, a short distance away in the Nasafjället Window (66.5° N), Essex and Gromet (1996, 2000) obtained geochronologic evidence that basement metamorphism only initiated about 415 Ma (Lochkovian), but metamorphic growth of titanite continued to about

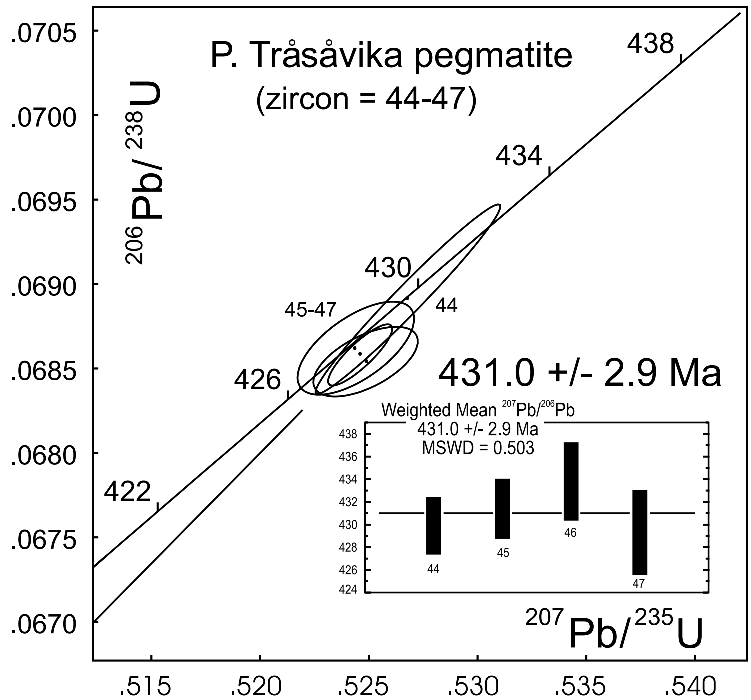

Fig. 15. Concordia diagram showing U-Pb ages of deformed early Scandian pegmatites in the Seve Nappe at Tråsåvika (Locality P).

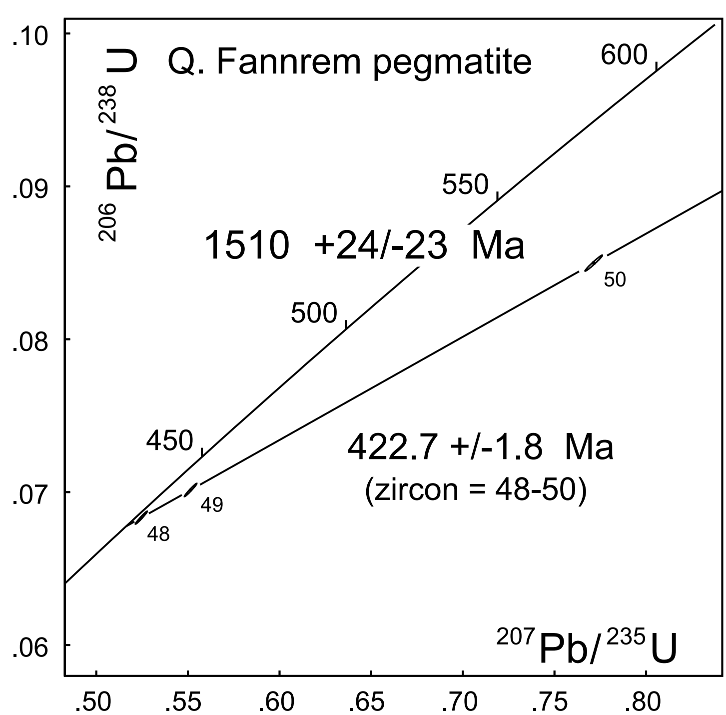

Fig. 16. Concordia diagram showing U-Pb ages of deformed early Scandian pegmatites in the Seve Nappe at Fannrem (Locality Q).

395 Ma (Late Emsian). This evidence was from within an upper basement thrust sheet, that itself tectonically overlies a lower basement of lower-grade granitic and mylonitic gneisses lacking metamorphic titanite. Essex and Gromet interpreted these results as showing that emplacement of the allochthonous thrust stack onto the Baltican craton could not have occurred before 415 Ma, that the metamorphism of the upper basement slice was younger than the metamorphism in higher thrust slices, and that this basement metamorphic age is comparable to metamorphic ages in the Proterozoic basement of the Western Gneiss Region. This interpretation is similar to the one we give below.

EFFECTS OF SCANDIAN DEFORMATION AND METAMORPHISM ON PROTEROZOIC BASEMENT AND ADJACENT NAPPES

Effects on Mafic Igneous Protoliths

In the immediate surroundings of the outer Trondheimsfjord, Scandian metamorphic overprinting of Proterozoic basement is intense, but apparently at slightly lower pressures than near Kristiansund to the southwest, as shown by the absence of eclogites. However, small bodies of gabbro with eclogitic rims are found about 30 km to the southwest.

At Selnes, on Snillfjord west of Orkanger (Locality R), a garnetiferous gabbro within gneissic amphibolite, has yielded four distinct populations of zircon and baddeleyite. These are illustrated in figures 17 and 18, and isotope ratio data from each population are given in table 1. The four populations include clear, broken fragments of skeletal zircon (#51, 52, table1), deep-brown broken blades of baddeleyite (#53, 54), turbid, granular grains of microcrystalline zircon (#56 - 57), and composite grains of baddeleyite and zircon in which brown baddeleyite is rimmed by microcrystalline zircon (#55, and fig. 18). U and Pb isotopic data obtained from fractions of each population are shown graphically in figure 19. Analyses of all fractions define a single discordia with intercept ages of 1461 ± 2 Ma and 401 ± 2 Ma, interpreted, respectively, as the age of initial gabbro emplacement and metamorphic conversion to garnet

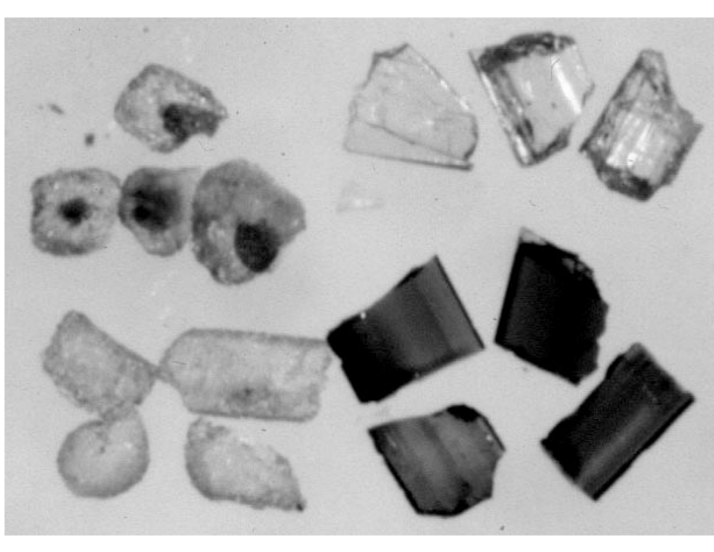

Fig. 17. Photomicrograph showing grains of Proterozoic igneous baddeleyite (dark), clear broken fragments of Proterozoic igneous zircon, microcrystalline Scandian metamorphic zircon, and composite grains of baddeleyite with zircon rims. From metamorphosed Mesoproterozoic gabbro at Selnes (Locality R).

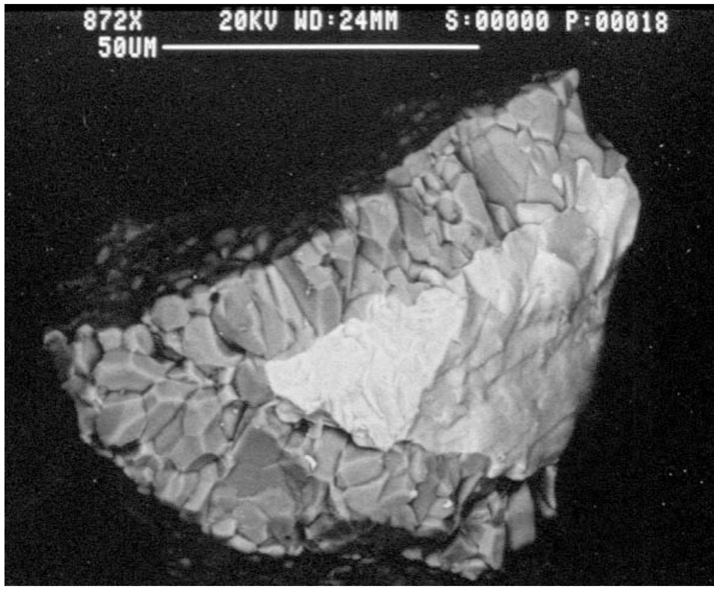

Fig. 18. Electron micrograph showing Mesoproterozoic igneous baddeleyite with rim of Scandian metamorphic zircon. From metamorphosed Proterozoic gabbro at Selnes (Locality R).

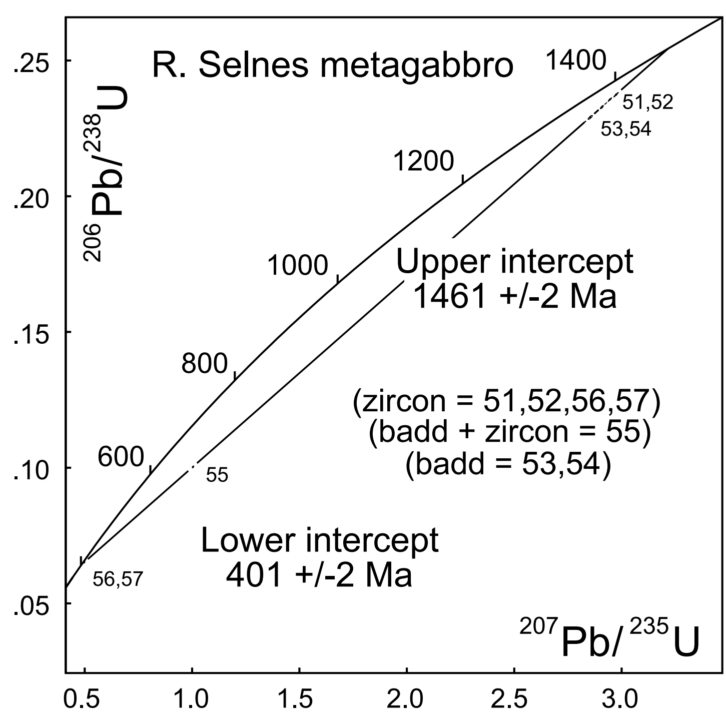

Fig. 19. Concordia diagram showing U-Pb ages of baddeleyite and zircon from metamorphosed Mesoproterozoic gabbro at Selnes (Locality R). The baddeleyite and clear skeletal zircon fragments give an original igneous age of 1461 ± 2 Ma. Microcrystalline metamorphic zircon gives an age of 401 ± 2 Ma, and composite grains lie on a chord between these.

metagabbro. Importantly, however, the different populations of U-bearing minerals plot at distinct positions on the discordia line. Deep-brown baddeleyite and clear skeletal zircon are the least discordant minerals plotting approximately 9 percent to 13 percent from the upper intercept age. Conversely, the populations of turbid microcrystalline zircon are the most discordant minerals that plot near the lower intercept age. In the clear case of mixed populations, the brown baddeleyite rimmed by microcrystalline zircon, analysis #55 plots between these two populations on the discordia at about 70 percent of the upper-intercept age. We interpret these data to mean that gabbro, which initially crystallized both brown baddeleyite and skeletal zircon, was emplaced into the Fennoscandian shield about 1461 m.y. ago. In the Devonian (Middle Emsian, ~401 Ma) this gabbro underwent subsolidus conversion to metagabbro at which time microcrystalline zircon formed at the partial or complete expense of baddeleyite. If these tiny microcrystalline zircons have lost lead, the age obtained would be a minimum age for the time of this reaction. Curiously, some grains of baddeleyite seem to have escaped reaction to microcrystalline zircon and they, like the grains of skeletal zircon, lost 9 to 13 percent of their radiogenic Pb during Scandian (Emsian) metamorphism.

A similar age of Scandian metamorphism was obtained from the eclogite (reportedly the world's largest) at Ulsteinvik, on Hareidlandet, 110 km southwest of the map area (Mysen and Heier, 1972). Based on four small zircon fractions (fig. 20), the weighted mean 207/206 age of growth of metamorphic zircon was at 402 ± 2 Ma (Middle Emsian). Although the Hareidland eclogite contains extensive secondary amphibole formation, the zircon fractions measured are believed to have come from

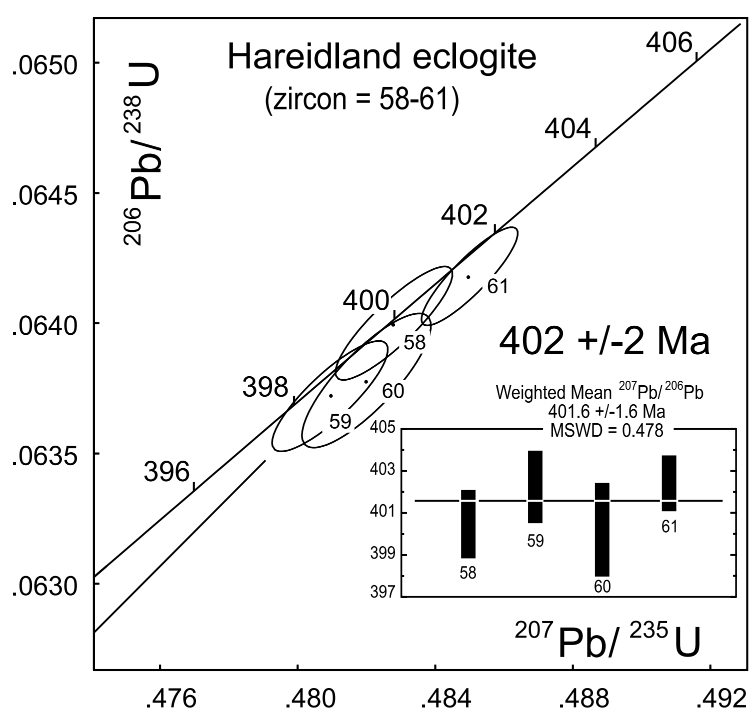

Fig. 20. Concordia diagram showing U-Pb ages of zircon from the eclogite at Ulsteinvik, Hareidlandet, southwest of the map area. The sample was provided by Bjørn Mysen (Mysen and Heier, 1972) from his Ph. D. thesis research. Based on four small zircon fractions, the weighted mean 207/206 age of growth of metamorphic zircon was at 402 ± 2 Ma.

some of the freshest eclogite, including cross-cutting omphacite-garnet veins. A dramatic recent development (Carswell and others, 2001, 2003) is the discovery of three grains of coesite, confirmed by Raman spectroscopy, included in some of the zircon separates originally prepared for dating by Krogh and Tucker. This discovery strongly reinforces the conclusion that eclogite formation took place in the Early Devonian. Tectonostratigraphic assignment of the Hareidland eclogite to Baltica basement is uncertain, because it appears to be encased in mica schist akin to lithologies in the Seve Nappe.

Additional evidence for Early Devonian (Emsian) eclogite-facies metamorphism of rocks correlated with those of the Seve Nappe comes from the work on metamorphic monazite from the microdiamond-bearing garnet-kyanite gneiss on Fjørtoft (Terry and others, 2000a) where monazite included in garnet has yielded 415 ± 6.8 Ma by ion probe and 408 ± 5.6 Ma by electron microprobe. These data have just been further supplemented by Tom Krogh, with three new U-Pb ages on metamorphic zircon in eclogites of Averøya and Nordøyane, west of Kristiansund, at 415 ± 2, 412, and 410 Ma (Robinson and others, 2003; Krogh and others, 2004).

Generation of Pegmatites

It is obvious that many of the Proterozoic rocks became hot enough to provide small amounts of partial melt that formed pegmatites. Commonly these pegmatites appear cross-cutting even in large outcrops, particularly of relatively massive host rocks, or where they appear in the neck lines of boudins of relatively massive rocks (fig. 21). Elsewhere, however, they show signs of strong deformation, and it is not easy to demonstrate their timing with respect to the widespread NE-SW-trending subhorizontal lineation and late-Scandian sinistral shear fabric. In outcrops containing eclogite southwest of the map area, it is obvious that the pegmatites post-date the peak

Fig. 21. Outcrop of Proterozoic basement gneiss in the map area showing Scandian melt segregation with ideomorphic poikilitic hornblende phenocrysts. These segregations have yielded approximately 400 Ma zircons.

eclogite-facies mineralogy and are commonly associated with prominent zones of development of secondary hornblende.

Three fractions of zircon from a pegmatite at Nesvatn (Locality S) are close to Concordia (fig. 22) and give a mean age of 403.3 ± 1.9 Ma. Four fractions from a pegmatite at Grønningen (Locality T), and three fractions from a pegmatite at Våvatnet (Locality U), lie along short chords close to Concordia and give mean ages of 404.0 ± 2.1 Ma, and 399.1 ± 1.7 Ma, respectively. Five fractions of zircon from a pegmatite cutting rocks of the Seve Nappe near Gagnåsvatenet (Locality U) regress (fig. 23) to a lower intercept age of 391 +4/−5 Ma (Late Emsian) with a mean upper intercept age of 949 +54/−51 Ma interpreted as a mean age of inherited zircon component. Given that analysis 72 has the highest U content, recent Pb loss is probable, making 391 a minimum age. This pegmatite is the youngest igneous rock we have dated in the region, but is the same, within error, as 395 Ma titanite ages and some other pegmatites. Krogh (personal communication, 1997; Krogh and others, 2003; Robinson and others, 2003; Krogh and others, 2004) has obtained multiple zircon fractions from a pegmatite cutting the 415 Ma eclogite at Averøya at the west edge of figure 2, southwest of Kristiansund. The coarser fractions show an inheritance extending toward 1570 Ma. Five single grains of small zircon, yield a mean age of 395.3 ± 1 Ma. This age is interpreted as a time of pegmatite crystallization, which is closely comparable to the date of titanite resetting reported below. Krogh has supplemented these zircon dates with three new dates on pegmatites in boudin neck lines of other eclogites, 395.6 Ma east of Averøya, 395 Ma on Flemsøya, and 394.5 on Fjørtoft (Krogh and others, 2003; Robinson and others, 2003; Krogh and others, 2004).

Most metamorphic zircon ages in eclogite and in gabbro, all located well southwest of Trondheimsfjord, are similar to the ages in pegmatites near Trondheimsfjord, centered around 402 to 400 Ma in the Middle Emsian. By contrast, the dated pegmatites near the dated eclogites are centered around 395 Ma, that is Late Emsian. Most pegmatites clearly crystallized in the amphibolite facies rather than the eclogite facies, possibly suggesting that the growth of metamorphic zircon in mafic rocks could have taken place mainly during amphibolite-facies hydration rather than during original eclogite-facies mineral growth. However, this suggestion is not supported by the discovery of coesite in the zircon fractions from the Hareid eclogite, nor by the descriptions of zircon development in the eclogite at Holsnøy in the Bergen area (Bingen and others, 2001). Ideally, one would hope to date eclogite zircon and pegmatite zircon from the same outcrop, to gain firm control on these relationships. This dating has now been accomplished by Krogh at Averøya (Krogh and others, 2003; Robinson and others, 2003; Krogh and others, 2004) showing about a 20 m. y. interval between zircon growth in eclogite and zircon crystallization from melt within an extensional boudin neck. It may be important to note that the cross-cutting pegmatites at Nesvatn and Grønningen, which are slightly older than the eclogite ages given here, are located well northeast of any eclogites, in a region that may never have reached eclogite conditions and reached partial melting earlier.

Pb Loss and Neocrystallization of Titanite

Results from an initial titanite traverse with 10 samples collected along a 25 km east-west section in the exposed Proterozoic basement, a few kilometers south of Trondheimfjord proved enigmatic (Tucker and others, 1987). All titanite data lay along a single discordia line between 1657 ± 3 ma and 395 ± 2 Ma, with the degree of discordance increasing from 6 to 100 percent with increasing metamorphic grade to the west. Here we present a compilation of data (table 3, fig. 24) for a much larger region including 36 basement titanite localities, one basement monazite locality (30) and one marble locality (12), representing perhaps more than 8,000 square kilometers of the northern part of the Western Gneiss Region that shares this enigmatic result (fig. 25). Now 56 analyses of titanite and two of monazite define intercepts of 1657 ± 3

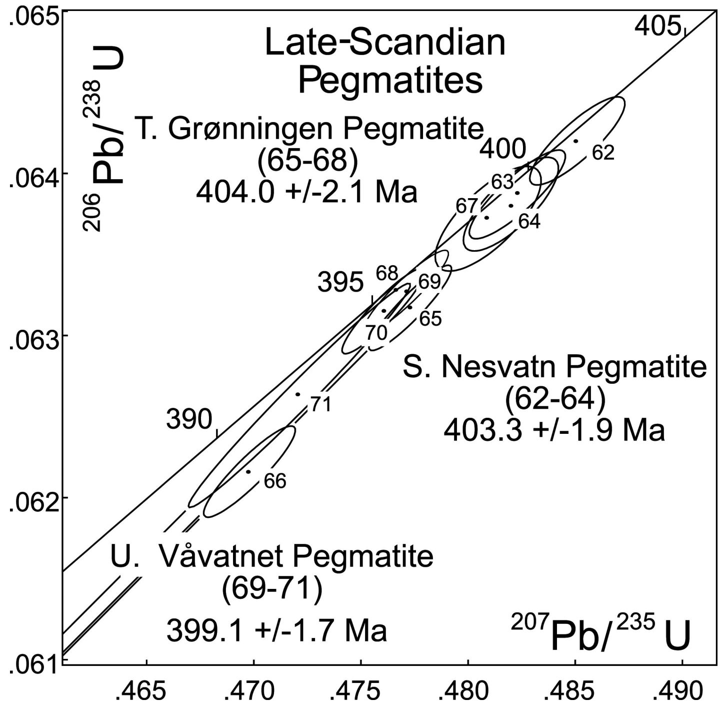

Fig. 22. Concordia diagram showing U-Pb ages of discordant pegmatites in Proterozoic gneisses of the Western Gneiss Region at Nesvatn (Locality S), Grønningen (Locality T) and Våvatnet (Locality U).

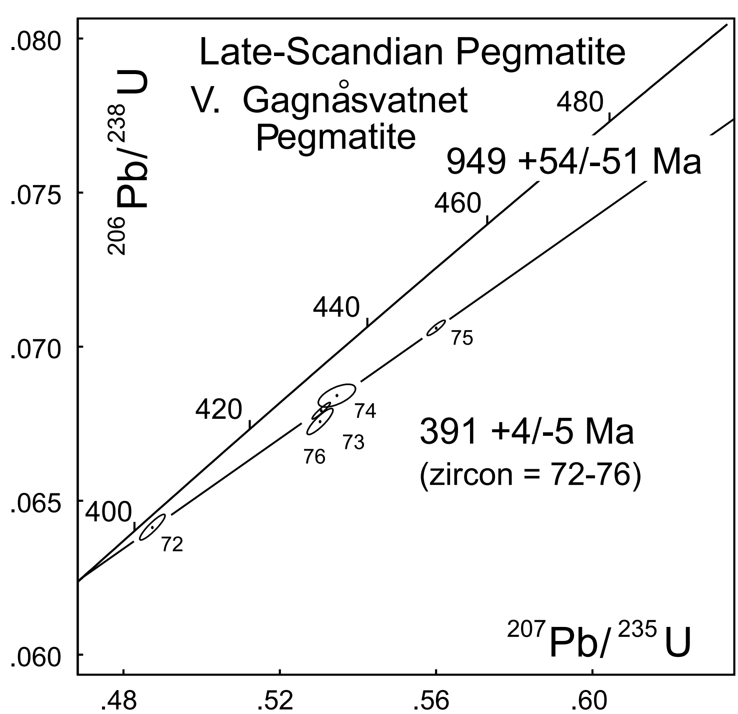

Fig. 23. Concordia diagram showing U-Pb age of discordant pegmatite in the Seve Nappe at Gagnåsvatnet (Locality V).

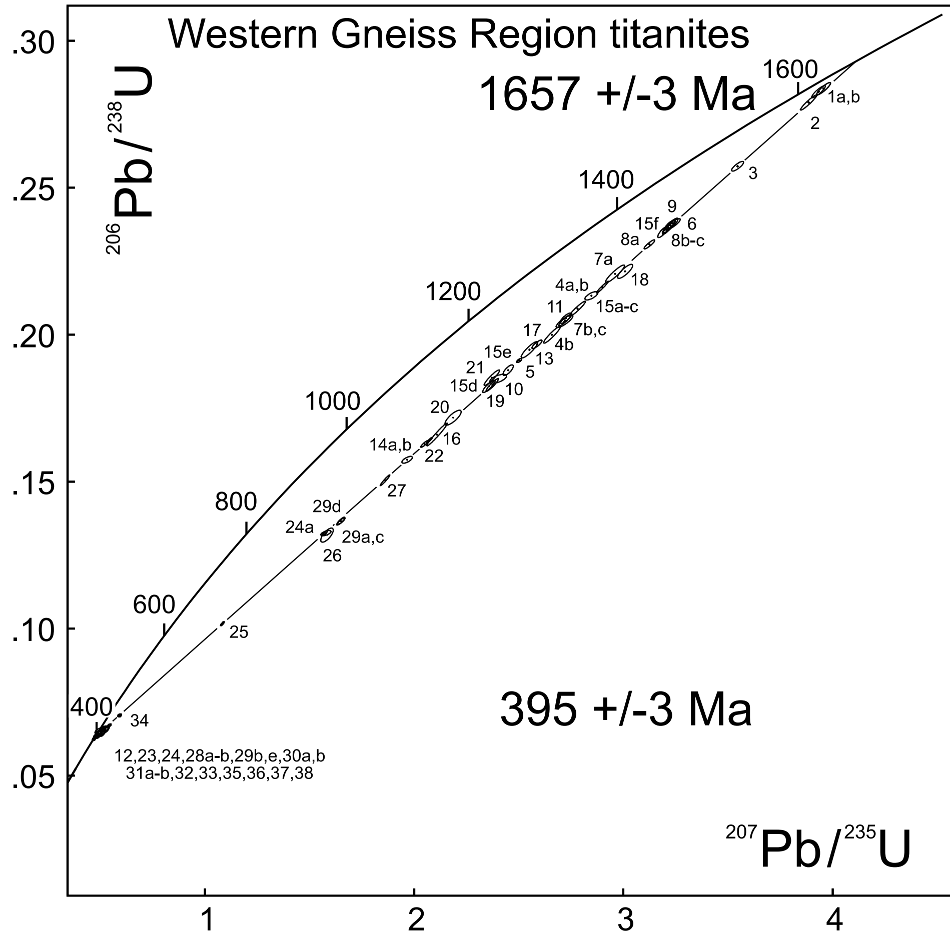

Fig. 24. Concordia diagram showing U-Pb ages of variably reset titanites from an extensive area of Paleoproterozoic granitoid gneiss of the Western Gneiss Region. Sample localities are shown on figure 25, which also shows the % resetting of Proterozoic titanite from very low values to 100%. The remarkable fact that all of the titanite analyses fall tightly on a chord between a Paleoproterozoic metamorphic age of 1657 ± 3 Ma and the end of Scandian Pb loss at 395 ± 3 Ma demonstrates two important features: 1) the lack of significant disturbing events between these times and 2) the brevity and temporal uniformity of the end of Scandian heating over a broad region.

and 395 ± 3. We then review critical observations that provide a basis for understanding the processes involved in creating the discordia and interpret these in terms of region–wide thermal events that must be considered as constraints on tectonic models.

In the 1987 study, data for one single sample was highly anomalous, but instructive. It was 90 percent discordant but located in an area where only a few percent discordance was expected. The material analyzed consisted of a sugary aggregate of low color microcrystalline titanite extracted from a highly strained granitic gneiss situated in the inverted region of an overturned dome (Tucker and others, 1987, p. 209.) Mechanically induced recrystallization is highly probable, hence in subsequent samples such material was avoided and only low-strain sites were collected. In a later study (Tucker and others, 1990) it was found that in many cases two types of titanite were present, and that these correlated directly with isotopic results. Large

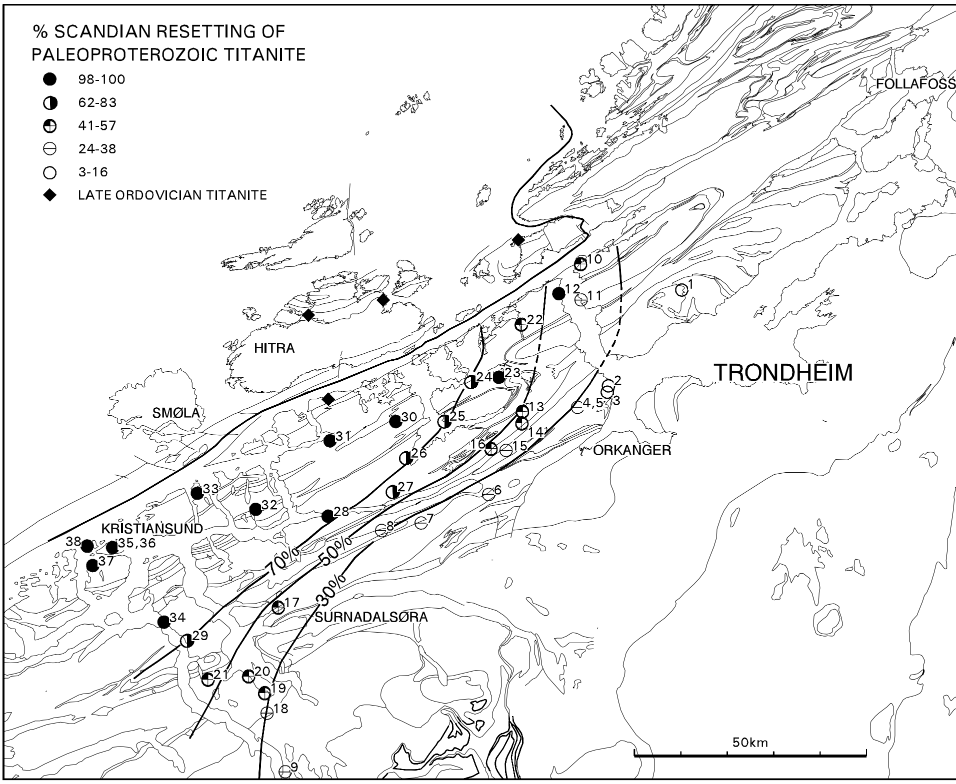

Fig. 25. Shows the results plotted in five classes along with average contours at 30, 50 and 70% resetting. At some localities, for example 29, two classes of grains were analyzed, reset Proterozoic grains that appear to have experienced Pb loss, and neocrystallized Devonian grains. Here neocrystallized grains were ignored in the contouring. The result from marble at locality 12, as well as gneisses at localities 23 and 28 containing only neocrystallized titanite, were also ignored in the contouring. The amount of resetting increases progressively from areas of little resetting to the east and southeast to large areas of 98–100% resetting to the northwest and west. Note that at Kvernberget (35, 36) and Frei Island (37) data for dark brown grains are 98, 99, and 100% respectively.

dark brown blocky grain fragments, that in some cases graded into granulated domains and appeared to be pre-metamorphic, gave data that plotted up the discordia line. Small euhedral pale yellow to pale brown grains and overgrowths, that appeared syn-metamorphic, gave data that plotted at the lower intercept. Ironically, in some cases incipient micro cracks were used to identify old grains.

Data for a single basement outcrop collected near Tingvoll (table 3, 29) are particularly revealing. Here both a biotite–hornblende tonalite and centimeter-scale plagioclase–quartz–hornblende melt pods were collected. Zircon overgrowths were present on the already oversized melt pod grains, as if Caledonian regrowth had occurred in circa 1650 melt rock (confirmed by dating), but, remarkably, the dark brown titanite in both rocks was not reset and both gave data that is 67 percent discordant (table 3, 29a and 29d respectively). Both rocks also contain small euhedral yellow to pale brown titanite (29b, 29e) and data for these are 99 percent discordant. Such a coincidence in the degree of discordance would be improbable if our discordia were a two-age-component mixture, so additional tests were carried out. Data for an oversize sample (4.32 mg. 29c) were compared to that for a previously published single grain (analysis 9b of Tucker and others, 1990) and each was again found to be 67 percent discordant. Replicate analyses in table 3 generally confirm this reproducibility in discordance within a few percent, hence the discordance is confirmed as a region–wide phenomenon (for example: 1 a, b at 5%; 4 a, b at 35 and 37%; 7 a , b, c at 32, 37 and 37%; 14 a, b at 59 and 57%; 15 a, b, c at 33, 35 and 35%.). Given the facts that: 1) second generation titanite has a much lighter color, reflecting different metamorphic conditions and was avoided during grain selection; 2) discordance increases with increasing metamorphic grade; and 3) replicate analyses with similar or vastly different sample size (for example 4.3 and 0.06 mg) give analytically identical discordance, we conclude that the discordia observed is primarily the result of thermally–induced diffusive lead loss. In some cases this could perhaps have been modified to a minor degree by mechanically induced recrystallization or inadvertent admixing of old or new components.

Figure 25 shows the results plotted in five classes along with average contours at 30, 50 and 70 percent resetting. At some localities (for example 29) two classes of grains were analyzed. These two classes were Proterozoic grains that appear to have experienced Pb loss, and neocrystallized Devonian grains. In this case neocrystallized grains were ignored in the contouring. The results from marble at locality 12, as well as gneisses at localities 23 and 28 containing only neocrystallized titanite, were also ignored in the contouring. The amount of resetting increases progressively from areas of little resetting to the east and southeast to large areas of 98 to 100 percent resetting to the northwest and west.

Region–wide titanite discordia of the type described here are extremely rare. Along and within the Grenville province boundary in Labrador, a section of exhumed overthrust basement records a 1650 to 995 Ma titanite discordia with new lower intercept zircon growth (Krogh, 1994). In this case, and elsewhere along the Grenville front, melt pod zircon has an age of 995 Ma that is identical to the closure age of titanite, as if rapid cooling followed uplift and/or tectonic unroofing. Although hardly comparable, but perhaps instructive, Hanson and others (1971) observed a similar discordia in a 7-km-long study of titanite from an Archean granite against the Duluth Gabbro, where heating on the order of 10's to 100's of thousands of years might be expected. How such a local resetting event can produce the same discordance as a region-wide tectonic process is particularly challenging.

In the Western Gneiss Region, total resetting of titanite and growth of new zircon was achieved to the south and west (Tucker and others, 1990) but to the east even where estimated temperatures approached 600°C (Griffin and others, 1985) titanite retained at least part of its radiogenic lead. More challenging is to explain the fact that titanite resetting occurred at the same time across a vast region, and that cooling followed immediately or within only a few million years across the same area. Perhaps the simplest explanation is best. Heating was initiated by pre 395 Ma tectonic loading/subduction that was greatest to the southwest and west. While local warming continued, the heating crust was thrust or buoyantly ejected from the subduction zone, initiating large-scale tectonic unroofing leading to coeval rapid cooling. Structural complexity was achieved either rapidly at 395 Ma or developed at lower temperatures that did not affect titanite, before this time. Implicit in the two-stage discordia observed is the fact that a circa 1650 metamorphism affected the basement gneisses, resetting all the titanite, and that no similar event preceded or followed the thermal overprint that partly or completely reset titanite at 395 Ma.

Figure 25 could be interpreted as an oblique crustal section wherein to the west, in deep structural levels, rocks were at amphibolite and locally eclogite grade, and to the east, in shallow structural levels, rocks were at upper greenschist to low amphibolite grade. We prefer to think of figure 25 as the pattern within a slab of Baltican crust that was variably subducted beneath Laurentia during the Scandian collision, then rapidly exhumed. The fact that titanites from all levels regress to a near-single discordia implies that Scandian high-grade metamorphism and ductile deformation, as recorded in various ways by titanite in basement gneisses, occurred at approximately the same time in this slab of crust. Where titanite discordance resulted from diffusion of Pb, then rocks in the eastern and central regions were not hot enough long enough for complete resetting, whereas rocks in western regions exceeded this temperature, but only for a few million years. Samples that are completely reset could have and probably did undergo metamorphism back to and even before eclogitization, but, oddly, they cooled below their blocking temperature at the same time that heating weakly changed the titanites to the east. Most neocrystallized titanite recorded an age of ~395, implying that reactions (amphibolite-facies hydration and perhaps decompression melting?) promoting this growth in the gneisses were particularly favored at about the same time as the cessation of Pb loss. However, new titanite in the marble of sample 12 suggests that titanite grew in this bulk composition earlier at 406 Ma, but this sample has relatively high common lead and is not 100 percent discordant, so further confirmation is required. The common 395 Ma age seems to correspond also to a range of pegmatite zircon U-Pb ages in the eclogite region to the southwest (Krogh and others, 2003; Robinson and others, 2003; Krogh and others, 2004), implying most titanite neocrystallization may have been coeval with the last phase of local partial melting, perhaps at a temperature around 650°C. The above features as well as ages recently reported for the eclogites, imply an interval of about 20 m.y. between eclogite metamorphism and late amphibolite-facies ductile deformation.

Broad implications of figures 24 and 25 concerning the evolution of this part of the Baltoscandian margin are as follows: 1) Baltican crust was subjected to progressively higher temperatures and pressures toward the west and northwest, probably as a result of subduction of Baltica beneath an overriding Laurentian plate. 2) When the process of subduction of this Baltoscandian segment of Baltica crust ceased, uplift and cooling was rapid so that most of the samples preserve the same resetting or neocrystallization age. These data, combined with the U-Pb minimum age of new metamorphic zircon in the Selnes gabbro at 401 ± 2 Ma, imply that many of these rocks were subducted, heated above 600°C, and then cooled below about 600°C, in a cycle lasting at least 6 m.y. The short period beginning with burial, followed by tectonic exhumation and ductile folding occurred while nappe translation and molasse sedimentation was taking place in foreland parts of the Scandinavian Caledonides, suggesting that exhumation of the Western Gneiss Region may have been assisted by tectonic as well as erosional unroofing. 3) The titanite data also imply that temperatures in this portion of the Western Gneiss Region did not exceed the resetting temperature of titanite at any other times than the Paleoproterozoic metamorphic age and the Scandian resetting age, thus not during the Sveconorwegian (1100 - 950 Ma) or Early Paleozoic Finnmarkian (530 - 485 Ma) orogenic episodes, nor at any time following the Early Devonian (~395 Ma) lower intercept event. 4) New time-scale data based on dating of tuffs in fossiliferous sections (Tucker and others, 1997b, 1998) indicate that the Devonian began at about 418 Ma; and thus that most of these Scandian events took place in Early Devonian rather than Silurian time, though some events (see below) appear to have lasted nearly to the end of the Devonian at 362 Ma.

Geochronology from Adjacent Areas

In the Roan area, northwestern Fosen (see fig. 2), Dallmeyer and others (1992) have interpreted a Sm-Nd isochron (opx-cpx-wr-gt) of 432 ± 6 Ma on a high-pressure granulite in basement to represent the peak of metamorphism. Thirteen Ar-Ar ages of hornblende both from basement and supracrustal rocks (interpreted by us as Seve Nappe) yield plateau ages ranging from 413 ± 3 Ma to 386 ± 6 Ma and represent the subsequent unroofing and cooling. Zircons from an undeformed granodioritic pegmatite give an age of 398 ± 3 Ma, which is a lower age limit for the deformation in that area. In the region from north of Roan to Vikna, Schouenborg (1988), and Schouenborg and others (1991) have dated 3 to 4 pegmatites with ages of ca. 403 to 400 Ma. These results from northwestern Fosen imply an earlier beginning to metamorphism than in the basement regions close to Trondheimsfjord. Although not obvious in the pegmatite results, the Ar-Ar ages imply an earlier end to metamorphism in northwestern Fosen than in the basement regions close to Trondheimsfjord.

Terry and others (2000a) completed *in-situ* U-Pb dating of monazite in the microdiamond-bearing garnet-kyanite gneiss at Fjørtoft and a derivative mylonite, 40 km northeast from Hareidlandet. The microdiamond-bearing gneiss is associated with a UHP eclogite containing polycrystalline quartz after coesite (Terry and others, 2000b). The rocks are tentatively assigned to the Seve Nappe in thrust contact above basement gneisses that only reached normal eclogite facies. Aside from presumed mid-to-late-Proterozoic detrital grains, the results, by ion probe and electron probe, yielded ages of 415 ± 6.8 (Lochkovian) and 408 ± 5.6 Ma (Early Emsian) for monazite included in large garnet in the gneiss, 394.8 ± 2.3 Ma (Late Emsian) for amphibolite-facies overgrowths in gneiss and mylonite, and 374.6 ± 2.7 Ma (Early Famennian) for small monazite porphyroclasts in the mylonite. These three ages were interpreted, parallel with present results, as 1) the time of peak eclogite-facies metamorphism, 2) the time of amphibolite-facies reequilibration during exhumation as shown by the titanite data given here and also the new pegmatite results by Krogh, and 3) the time of low-amphibolite facies mylonite formation that was possibly synchronous with final positioning of rocks of the Devonian clastic basins.

Important new U-Pb geochronology has recently been accomplished in the eclogites superimposed on Mesoproterozoic granulite-facies basement located in the Bergen Arcs (Bingen and others, 2001; Bingen and others, 2004). The finally revised age for the eclogite metamorphism is 423 ± 4 Ma. This age is entirely appropriate for early-Scandian subduction and exhumation of an extreme distal part of the Baltican crust.

EFFECTS OF SCANDIAN DEFORMATION AND METAMORPHISM ON ORDOVICIAN INTRUSIONS

The most crucial aspect of this paper concerns the contrast between titanite ages of Baltic basement and those obtained in the Ordovician intrusions of the Støren Nappe. Four titanite localities in Ordovician intrusions are shown in figure 25 and U-Pb ages are plotted in a Concordia diagram in figure 26. Three of the localities lie above the Høybakken detachment, and the titanite ages of 446, 440 and 440 Ma are within ±1 m.y. of the zircon ages of nearby intrusions of 446 to 441 Ma, believed to represent the times of Ashgill to Early Llandovery igneous crystallization. The fourth locality is from the strongly lineated dioritic gneiss at Kjørsvika that gave an igneous crystallization age of 460.7 ± 2.3 Ma (Late Llanvirn). This locality lies about 1 km north of a contact with Proterozoic basement in the extensive area of 100 percent titanite resetting. The titanite from this sample gives a U-Pb age of 455 Ma (Late Caradoc) that is ~6 m.y. younger than the igneous zircon age, which indicates either slow cooling or slight metamorphic resetting.

The belt of dioritic gneiss at Kjørsvika (figs. 1, 2 and 25), with its strong deformational fabric and evidence for only weak recrystallization, follows the northwestern contact of the area of 100 percent titanite recrystallization in basement for a distance of at least 75 km. A similar contact continues for another 125 km, in a sinuous pattern trending toward the NE, but here the basement is less recrystallized. The higher-level nappe of Ordovician intrusive rocks with relatively weak metamorphic recrystallization lies above and in direct contact with, or very

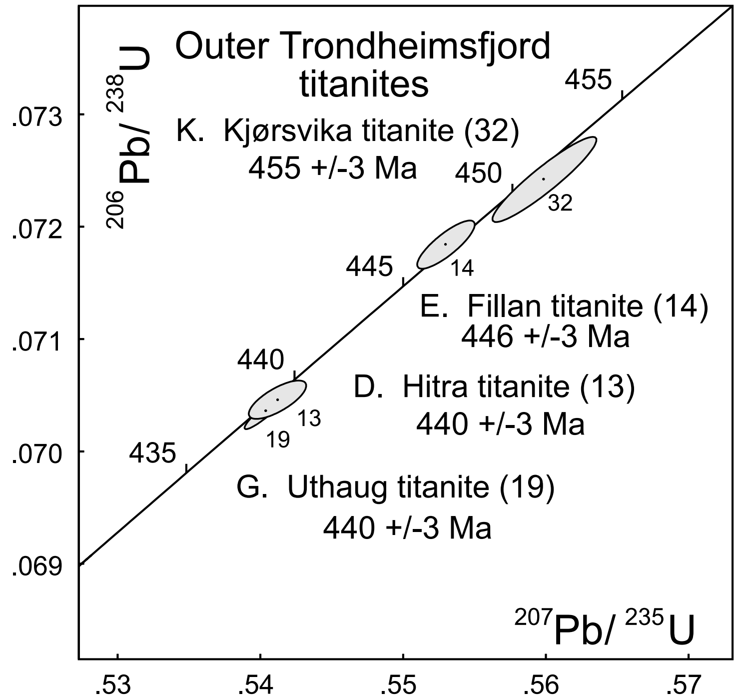

Fig. 26. Concordia diagram showing U-Pb ages of unreset or very weakly reset igneous titanite from four localities (see fig. 25) in Ordovician intrusive rocks of the Støren Nappe. The oldest age of 455 Ma is from the foliated and lineated diorite gneiss at Kjørsvika (Locality K), which lies only 1–2 km from basement gneiss with 100% resetting of Proterozoic titanite at 395 Ma. Our interpretation is that the contact between the unreset Ordovician tonalites and the completely reset Paleoproterozoic basement is a middle Scandian extensional fault of large magnitude. This fault brought relatively cool Ordovician rocks that had originally been thrust far toward the front of the orogen back into contact with Proterozoic basement that had earlier been far down the subduction zone. The fact that both the Ordovician and Proterozoic rocks now share that same strong NE-SW lineation and fold axes, indicates that major extensional faulting in the late middle Scandian slightly preceded the imposition of this regional fabric in the early late Scandian phase, which was in progress at the time the basement rocks passed approximately 600°C at 395 ± 3 Ma. This fabric was developed before the more brittle fabric found near extensional faults associated with the outcrop areas of the Devonian basins.

close to, Proterozoic basement that was at a much higher temperature and a higher degree of recrystallization. Nevertheless, rocks on both sides of this contact share the same late subhorizontal linear fabric and evidence for sinistral shear that has been related by Séranne (1992) to the deep-seated effects of top-west extensional deformation associated with emplacement of the Devonian basins on the Høybakken detachment. Our interpretation of this contact is that it represents an early thrust or thrusts, modified by major early extensional deformation. In effect, this contact is a tops-west detachment, now called Agdenes detachment (Robinson and others, 2004), in which cooler high-level rocks from nearer to the front of the orogen were extensionally emplaced against much deeper rocks that had attained much higher temperatures and pressures during the peak of Scandian continental subduction of Baltica. After extensional juxtaposition of these two blocks with very different metamorphic histories, they were deformed together in the later phases of extensional deformation and sinistral shear to produce their present common ductile fabric. This ductile fabric is itself distinct from the very weak ductile fabrics, or later brittle fabrics found in rocks immediately above the Høybakken detachment associated with the outcrop of the Devonian basins.

SCANDIAN STRUCTURAL DEVELOPMENT

Sequence and Timing

Throughout the mountain belt from Magerøya in the north at least to Jämtland and Trøndelag and probably the Bergen Arcs in the south, the Silurian successions provide evidence for the start of Scandian orogeny. Basin deepening occurs in the Mid-Late Llandovery and influx of turbidites (Gee, 1975; Bassett, 1985) followed rapidly thereafter. The evidence is to be found in the Jämtland Supergroup of the Lower Allochthon (Bassett and others, 1982), the Lower Köli Nappes (Kulling, 1933; Stephens and Gee, 1985) and the Middle Köli Nappes (Getz, 1890; Hardenby, 1983). Graptolites provide good control of the ages of the black shale facies, which gives way upwards transitionally into the turbidites; the latter coarsening upwards, in some areas dramatically (for example, in the Meråker Nappe in eastern Trøndelag and in the Støren Nappe northeast of Trondheim), with the influx of fanglomerates. The sediments were apparently derived from a hinterland source. Whereas the graptolitic facies in the Jämtland Supergroup (Bängäsen shales) is of Late Llandovery age (underlain by Middle and Lower Llandovery coral- and brachiopod-bearing limestone), and the overlying turbidites are at least partly Early Wenlock (Bassett, 1985), the evidence from the Köli Nappes is that the basin subsidence started somewhat earlier (Middle Llandovery). Thus, it seems probable that the passage from Early Silurian shallow-marine environments to basin deepening and influx of orogen-derived clastics was diachronous over an interval of a few millions of years and started in the west at ca. 435 Ma (accepting the time scale of Tucker and McKerrow, 1985). This extensive evidence of hinterland uplift in the mid-Llandovery is inferred to mark the onset of Scandian orogeny.

Silurian faunas have not been found in the Upper Köli Nappes and the Uppermost Allochthon of the central Scandes, but several localities are known in the north. For example, poorly preserved Late Ordovician – Early Silurian brachiopods and corals have been found in the Vaddas Nappe of the Upper Allochthon, east of Lyngen (Zwaan, 1988), graptolites of Early to Mid-Llandovery age occur at the very base of a 2.4 km thick formation in the Magerøy Nappe (Köli, Upper Allochthon) (Roberts and Andersen, 1983; Krill and others, 1988), and fossiliferous successions of Late Llandovery age are known in the Balfjord Group of the Lyngsfjell Nappe of the Uppermost Allochthon in Troms (Bjørlykke and Olaussen, 1981; Zwann and others, 1998).

The thrust complexes of the Køli contain ophiolites (for example, Støren, Bymarka, Vassfjellet, Løkken and Leka) that were inferred to have been thrust either onto the Laurentian margin or a microcontinent in Iapetus (Grenne and others, 1999; Roberts and others, 2002b) in the Early Ordovician, during development of an outboard Early-Ordovician magmatic arc. These rock complexes were probably involved in the early-Scandian (Mid Llandovery) loading of the outer margin of Baltoscandia prior to their emplacement onto the Middle Köli Nappes. Palinspastic reconstruction of the thrust sheets in the Lower and Middle Allochthon (Gee, 1978; Kumpulainen and Nystuen, 1985; Gayer and others, 1987) require that this early-Scandian orogenic activity, involving the Uppermost Allochthon and Köli Nappes, occurred at least a couple of hundred kilometers west of the presently exposed Western Gneiss Region. Thus, the Early Devonian record of basement shortening, upper crustal extension and uplift in central and western Norway is only the late phase of a 40 to 50 million year period of Scandian collisional orogeny, involving many hundreds of kilometers of crustal shortening and deep subduction of the outer Baltoscandian margin that had been much extended in the Late Neoproterozoic.

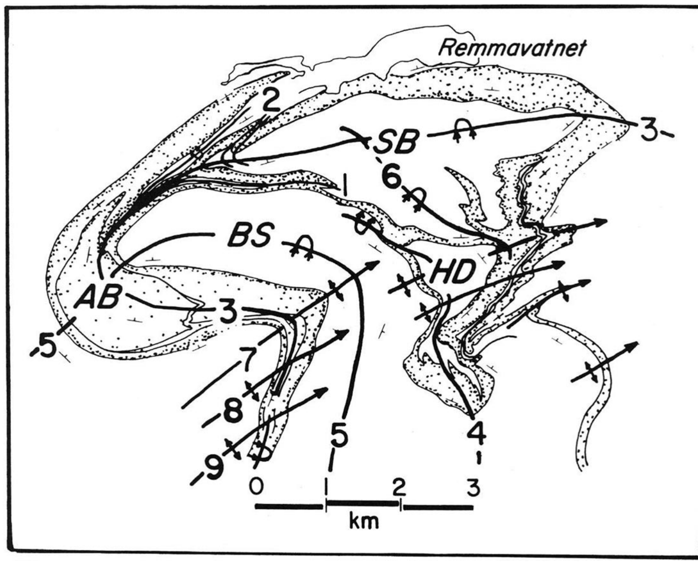

Fig. 27. Fold axial surface map of the Remmafjell structure, southwest of locality L of figure 2, showing major structural features and the traces of various Scandian surfaces; from Tucker (1986). Arrows denote the trend and plunge of map-scale folds. Stippled area is cover rocks. AB - Almfjell Basin; BS - Bergsvard synform; HD - Heklefjell dome; SB - Skropligdal basin. Numbers refer to structures described in the text.

Interestingly, the so-called 'post-orogenic molasse' in the westernmost hinterland of the Scandes on Hitra contains a eurypterid fauna that may be as old as Late Llandovery (Størmer, 1935; Bassett, 1985). This evidence is compatible with the conclusion above that the emplacement of the Uppermost Allochthon onto the upper Köli Nappes started in the Mid Llandovery and continued into the Wenlock. The Hitra molasse could, in part, represent the hinterland strata deposited during early-Scandian thrusting, at a time when turbidites were filling the foreland basin to the east. The Late Emsian palynoflora from Tristein demonstrates that this continental deposition continued at a high level when deeper rocks of the Baltoscandian margin were still at eclogite facies, or undergoing thrust-related exhumation in amphibolite facies.

The discussions of deformational events given above cannot bring the reader to a full appreciation of the complexity of the western part of the Western Gneiss Region, nor how strongly the Proterozoic basement was involved. Figure 27 from Tucker (1986), showing a small area that can be recognized on figure 2 not far southwest of Locality L, gives a greater appreciation. The oldest recorded deformation was the establishment of a series of thrust nappes involving transport of various terranes for hundreds of kilometers onto the Baltoscandian margin. Locally, some folds may have also formed during this deformation. This thrusting essentially established the sequence of rock units upon which maps are based. It was during this phase that Baltican basement reached its deepest location in the northwest-dipping subduction zone beneath overriding Laurentia. It has been argued above that this phase was followed by early extension, which brought some cooler high-level nappes into close or direct contact with cooling, high-T, high-P Baltican basement, while at the same time probably producing great thinning of some of the nappe units. This early extension and consequent cooling terminated Pb loss and neocrystallization in titanite of the Baltica basement at about 395 $\pm$ 3 Ma. After or even while the extension was proceeding, this thrust and extensionally juxtaposed column was subjected to several phases of ductile folding. In the area of figure 27, Tucker recognizes a phase of recumbent folding which he divides into three parts, Early (axial surfaces 1 and 2), Main (axial surface 3) and Late (axial surfaces 4, 5, and 6). All of these are then deformed in a phase of tight upright folding (axial surfaces 7, 8, 9 and others) associated with a strong generally NE-SW-trending subhorizontal stretching lineation in most outcrops. The latter is commonly believed to represent the early ductile phase of sinistral transtension that led up to the ductile-to-brittle detachments associated with the outcrop areas of the Devonian basins. A slight variant of this interpretation would have most or all of the folds formed during a single prolonged phase of sinistral transtension with continued folding about NE-plunging tubular axes (see Lutro and others, 1997; Terry and Robinson, 2003). This alternative in no way changes the sequence of major events, nor the obvious conclusion that in these circumstances basement and cover deformed together in an extremely ductile fashion.

Tectonic Reconstruction

Preparation of tectonic reconstructions of mountain belts such as the Scandinavian Caledonides is difficult. While the horizontal shortening distances were enormous, the vertical dimension was relatively small, and was made even more difficult by extreme tectonic thinning. For example, the Särv Nappe, which may be up to 2 km thick in Sweden, has been successfully mapped in parts of the Western Gneiss Region where it is only 10 meters down to 1 meter thick. To gain a clearer idea of process, it is commonly necessary to model tectonic features like a machinist dealing with homogeneous materials. This modeling makes possible a formalized sequence of development, illustrating various tendencies, without becoming embroiled in the details of individual rock masses, though, in fact, it is the exact array and behaviors of rock masses in the deforming zone that determine the true outcome. We have created a formalized geometric model (fig. 28) based on an expansion of a figure given by Terry and Robinson (2003).

Figure 28 shows the Baltoscandian margin of Baltica going down a subduction zone beneath Laurentia. There is no vertical exaggeration. No attempt is made to portray the main mass of Laurentia. A sharp bend is shown in Baltican crust where it passes beneath the main mass of Laurentia. The total convergence is 1400 km and is accomplished in 6 consecutive thrust imbrications, each peeling off a slice of upper Baltican crust or cover in a progressively more proximal position. Each slice is 233 km in lateral extent and each is about 5.5 km thick, probably a little too thick compared to the real situation, but about as thin as can be easily shown in a scale drawing. The geometry of imbrication of each slice is essentially identical. As each slice is activated, the thrust at the base of the antecedent slice is deactivated and the entire thrust pile is carried piggy-back style on the basal thrust.

No geometrical record is given here for several features, but that very lack emphasizes the importance of those features to overall evolution. 1) Isostatic loading of the continental margin by the increasing weight of the imbricated pile is not shown. Such loading would have an effect of providing a) depressions to be filled by sediments, in this case the Early to Mid Silurian and younger clastic sequences in the Lower Allochthon; b) inboard bulges possibly resulting in local erosion; and c) depression of the entire nappe pile to deeper levels (though not to higher pressures), thus also lowering the overall height of the imbricated pile and also probably moving the position of the bend in Baltican crust to a more inboard position. 2) The distance traveled down the subduction zone is determined by the position of the trailing edge of each imbrication with respect to the bent continental edge, in this case very shallow. Deeper trailing edges would result in thrusting of rocks from deeper levels. We postulate that deep trailing edges in outboard regions of very thinned continental crust would result in imbrication of slices of subcontinental mantle lithosphere, and

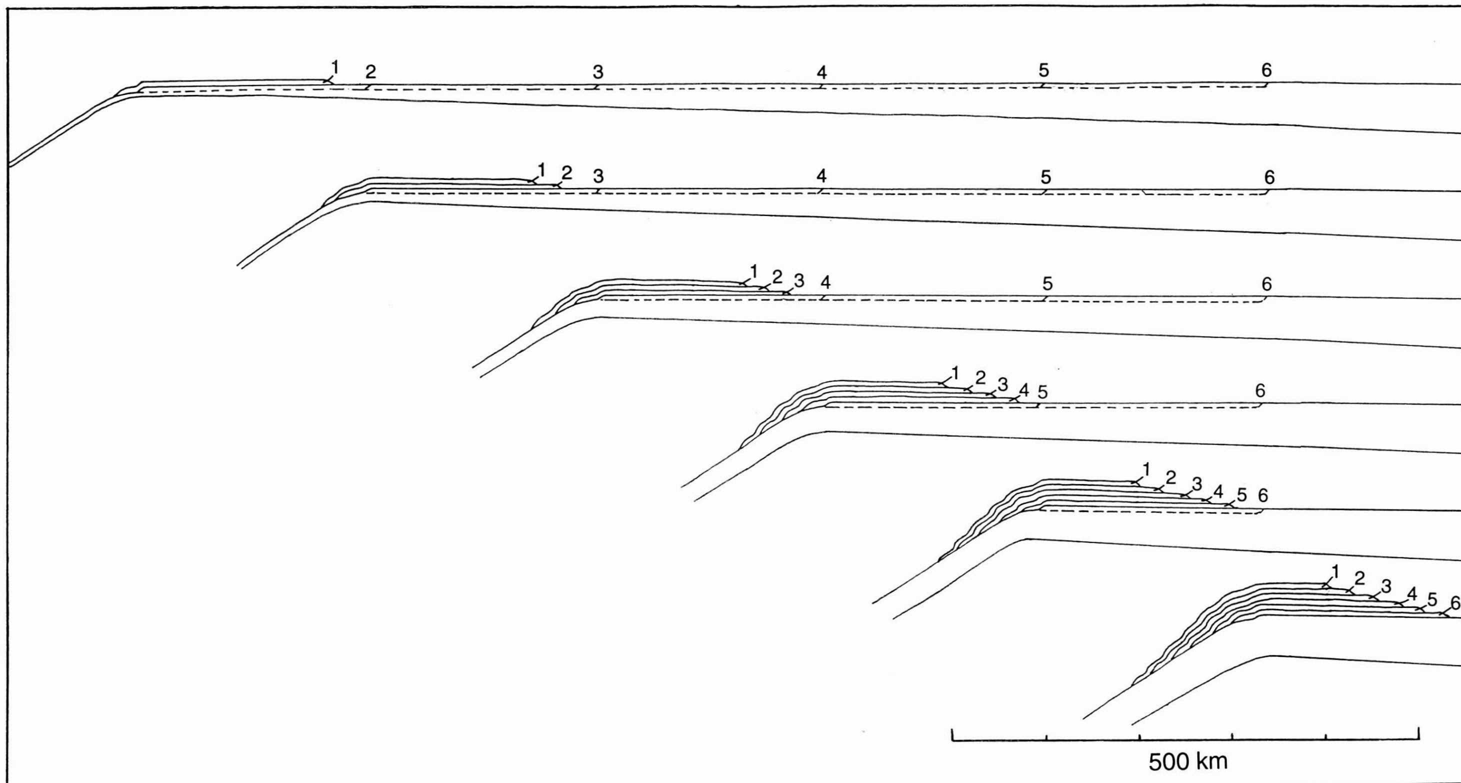

Fig. 28. Schematic mechanical scale drawing of Baltica being subducted beneath Laurentia. Scandian allochthons are represented by six imbricate thrust slices all of uniform extent and thickness. Baltica continental ± oceanic crust is shown as a uniformly thinning wedge from 55 km in the east (right) to 10 km in the west (left). See text.

could explain the common occurrence of garnet peridotite masses in higher-pressure parts of the Western Gneiss Region (Terry and Robinson, 1998; Robinson and Terry, 2001). 3) The imbricated thrust pile is allowed to thicken without either forward or backward extension under the influence of gravity, yielding a nappe stack 33 km thick after six imbrications. In reality, each imbrication would increase the gravitational potential for extension and erosion, the only two mechanisms by which exhumation can take place, and that potential would result in movements even during the early imbrications. The expected differential flattening, coeval extensional faulting, tectonic sliding *et cetera* would have prevented the theoretical 33 km thickness from ever having been achieved. Furthermore, this simple model, and also figure 29 illustrate simple, non-oblique convergence, rather than the generally accepted oblique continent-continent collision and sinistral shear regime that could have led to departures from the assumed thickness. In addition, because of the ordered geometry of the slices, with each imbrication there would be a progressive forward movement of the extensional flow divide (Terry and Robinson, 2003) leading to an increasing proportion of extension toward the hinterland such as that described in this paper.

Another key observation on this model is that no single thrust slice is thick enough mechanically to rise under its own buoyancy, with an active thrust at the base and an active normal fault at the top (Case A). Rather, as the basal fault on each slice is activated, the top fault is deactivated, but the thrusting builds the pile until higher-level surfaces become activated as normal faults. Thus, the end result is a slab with an old thrust fault at the base and a slightly younger low-angle normal fault at the top (Case B). So long as the imbrication process proceeds fairly rapidly, the mechanically implausible Case A may be geochronologically indistinguishable from the rational Case B.

The foregoing data and analysis are integrated into simplified two-dimensional graphic cartoons in figure 29 with major vertical exaggeration. Only a few of many probable active faults are shown. No attempt has been made to explain the intensity and age of metamorphism within nappes at intermediate levels between basement and the Støren Nappe, although we have given evidence for high-grade metamorphism, deformation and pegmatite intrusion at and before 430 to 423 Ma in the Seve Nappe.

Panel A shows the results of early-Scandian nappe stacking (430 - 410 Ma) in which the Helgeland Nappe Complex and Støren Nappe have been transported at a high level onto a cool upper surface of Baltica. At the same time the rocks of the extreme outer Baltican margin, including parts of the Seve Nappe, have traveled far down a subduction zone with the temperature and pressure locally reaching ecologite facies conditions. The most recent revised U-Pb age of eclogite in the Bergen Arcs (Bingen and others, 2004) may record this early distal subduction at around 420 Ma. Some high-level "post-orogenic" clastic basins were probably already initiated during this stage (see Roberts, 2003, fig. 7), also marked by widespread Late Llandovery-Wenlock clastic sediment loading on the distal part of the Baltoscandian foreland now represented in the Lower Allochthon.

Panel B shows the early Middle Scandian (410 - 406 Ma) situation. Continued deep-level thickening by imbrication is seen as providing the gravitational potential for foreland- and hinterland-directed extension at high-levels, and deposition in Devonian clastic basins.

Panel C shows late Middle Scandian (406 - 396 Ma) continued subduction and imbrication of a more proximal part of the Baltican margin, including Proterozoic basement, with its heating and HP and UHP metamorphism; its production of early, transverse, top-SE shear fabrics in basement (Terry, ms, 2000; Robinson and others, 2003); its new metamorphic zircon growth at 401 ± 2 Ma; its local partial melting to produce pegmatites; and its progressive Pb loss and neocrystallization in titanite.

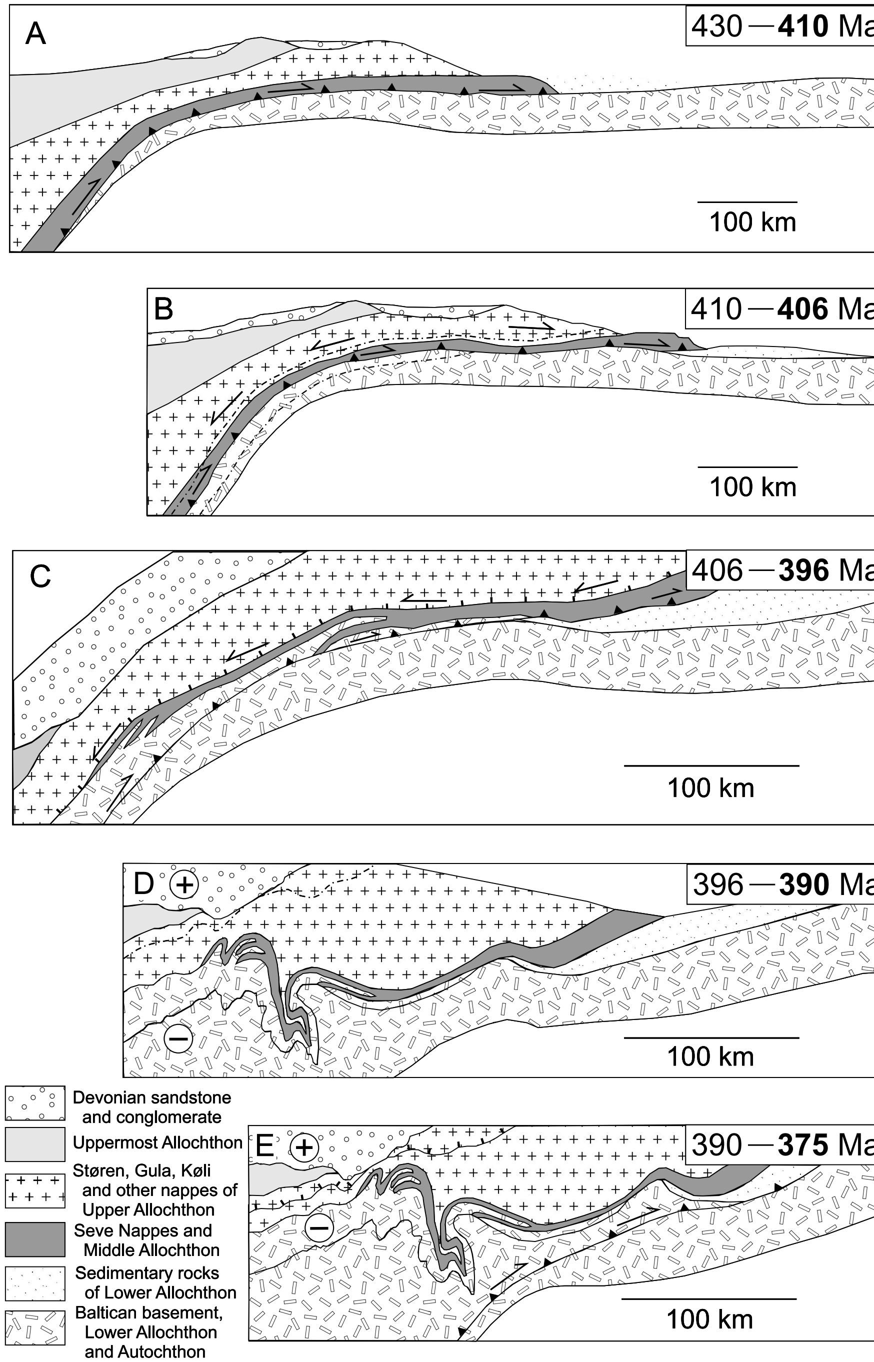

Fig. 29. Schematic cross-sections with exaggerated vertical and compressed horizontal scale illustrating the proposed sequence of Scandian events in the Trondheimsfjord region. Only selected thrusts (teeth) and normal faults (hachures) are shown during approximate time of activity. Also shown are some thrusts (dashed) and normal faults (dash-dot) just previous to activity. Sinistral and top-SW shear quasi-normal to the sections are shown by + (toward viewer) and - (away from viewer). See text. **A)** Early Scandian nappe stacking (430 - 410 Ma). **B)** Early Middle Scandian (410 - 406 Ma) continued subduction and imbrication, with foreland- and hinterland-directed extension. **C)** Late Middle Scandian (406 - 396 Ma) uplift of a subducted and heated proximal continental slab by thrusting and slightly later-low angle normal faulting, leading to exhumation and cooling of the slab. **D)** Early Late Scandian (396 - 390). Cooling of the slab in C leading to termination of Pb loss in basement titanite when passing approximately 600°C at 395 ± 3 Ma. Synchronously the rocks were undergoing top-west ductile extension progressing into a sinistral shear field producing a range of nearly orogen-parallel folds and lineations. **E)** Late Scandian (390 - 375 Ma) extension in a sinistral top-SW shear field of semi-brittle to brittle deformation.

Toward the end of this phase, thrusting of a subducted and heated proximal continental slab took place. This previously subducted, heated slab of Proterozoic basement was imbricated onto cooler basement and its Neoproterozoic cover toward the foreland. There is evidence at Storli, in Trollheimen (see fig. 2), for recumbent folding of the earlier assembled tectonostratigraphic section before this thrusting (called the Storli thrust by Robinson and others, 2004). This, or a later and deeper imbrication, induced slightly later backsliding at a higher level and initiated extensional emplacement of the cool high-level Støren Nappe against cooling basement along the Agdenes detachment. Major deposition in high-level Devonian clastic basins continued.

Panel D shows the inferred situation in early Late Scandian (396 - 390 Ma) time. Cooling of the basement slab in Panel C, first from below, along the Storli thrust, and then from above, along the Agdenes detachment, terminated the short period of Pb loss and neocrystallization in basement titanite at 395 ± 3 Ma, while igneous titanites in overlying Ordovician intrusions in the Støren Nappe were never warm enough to be reset substantially. During this period, conditions in the basement changed from upper amphibolite facies to low amphibolite facies, incidentally passing the conditions where titanite ceased neocrystallization and/or Pb loss at around 600°C. The rocks were simultaneously undergoing top-west ductile extension progressing into a sinistral shear field with + and - symbols showing toward and away movement quasi-normal to the section. Early in this extension in the SW, the deep-level rocks were still hot enough for pegmatites to form in neck lines adjacent to eclogite boudins. This extension appears to have involved much of a package previously assembled by thrusting and early extension under upper-amphibolite-facies conditions, but brought it against a higher level section that had never seen conditions above low-amphibolite facies. The earliest thrust-related tectonostratigraphy is thrown into major isoclinal to recumbent folds, that were then refolded about more open and upright folds, commonly overturned toward the northwest, with NE-SW-trending axes, a strong NE-SW trending lineation and top-W and sinistral shear fabrics. It is uncertain if these folds developed in distinctly separate episodes of recumbent and open folding, or whether all were integrated into a single episode of development of complex sheath-like and tubular folds within a broad sinistral, top-W strain field (Terry and Robinson, 2003).

Panel E shows Late Scandian (390 - 376 Ma) extension in a sinistral and top-SW shear field of semi-brittle to brittle deformation. In this, cool levels of the Støren Nappe with their unconformably overlying cover of Silurian to Devonian clastic basinal sediments, were extensionally emplaced along the Høybakken detachment against the more ductilely deformed substrate. This episode was probably a continuation, under relatively cooler conditions and in the same strain field, of the ductile deformation illustrated in Panel D. The rocks above the Høybakken detachment were emplaced not only from a higher level, but from a different geographic location, from at least 80 to 100 km to the northeast nearly along strike, parallel to the late Scandian extensional transport direction (Braathen and others, 2002).

Taking the time intervals from the end of each panel (number in bold) to the end of the next, and the amount of shortening from one panel to the next (admittedly subjective and minimal), we calculate transverse convergence rates. A to B: 410-406 = 4 m.y., 873-741 = 132 km, rate 3.30 mm/yr.; B to C 406-396 = 10 m.y., 741-497 = 244 km, rate 2.44 mm/yr.; C to D 396-390 = 6 m.y., 497-436 = 61 km, rate 1.02 mm/yr.; and D to E 390-375 = 15 m.y., 436-362 = 74 km, rate 0.49 mm/yr. These rough results are understandably on the low side of global plate convergence rates but consistent with a progressive reduction in plate motion normal to the plate boundary as Baltican continental crust was subducted, possibly with an increase parallel to the boundary.

A major conclusion of this paper is that a high proportion of the exhumation of the Proterozoic basement rocks that had been metamorphosed at high pressure took place during thrusting and consequent high-level extensional collapse (Panels B, C, early D) while convergence was still in progress at deeper levels. Similar relationships were envisioned by Roberts (2003, his fig. 7), and also by Steel and others (1985, fig. 14). Subsequent ductile deformation associated with sinistral transtension (late Panel D), as well as ductile to brittle detachments in the same strain field associated with outcrop areas of the Devonian basins (Panel E), played a subsidiary though still significant role in this exhumation.

SUMMARY

The Trondheimsfjord part of the Western Gneiss Region (fig. 2), like the part immediately to the southwest, is characterized by a series of complex NE-SW-trending synclines exposing Scandian thrust nappes between anticlinal regions exposing strongly deformed and metamorphosed Baltican basement. The lower-level nappes are less easily correlated than those farther southeast in the orogen. They are dominated by high-grade pelites, amphibolites, and marbles characteristic of the Blåhø-Surna and Seve Nappes, but locally there are interlayered quartzites and amphibolites characteristic of the Sætra and Särv Nappes, and laminated feldspathic quartzites characteristic of the Åmotsdal unit of Trollheimen. The Støren Nappe, with its mafic and felsic volcanics, conglomerates, volcanogenic sediments, and marbles, all in greenschist or lower amphibolite facies, is well represented in synclines in the southeastern part of the region, but gives way northwestward to a terrane dominated by highly deformed tonalitic intrusive igneous rocks. In terms of superimposed fabric, some of these plutons are easily confused with more massive parts of the underlying Baltica basement, except near the islands of Smøla, Hitra and Froan and the Ørlandet Peninsula above the Høybakken detachment fault associated with the Devonian basins. Mapping, plus a selection of concordant to nearly concordant igneous zircon ages in the range 481 to 438 Ma, indicates these intrusive rocks crystallized from the Early Ordovician through the earliest Silurian and appear to be remnants of a calc-alkaline intrusive suite similar in character and age to the Ordovician Bronson Hill - Shelburne Falls magmatic arc of the northern Appalachians (Tucker and Robinson, 1990; Robinson and others, 1998; Hollocher and others, 2002). Recognition that a significant proportion of the gneisses of the Trondheimsfjord region are made up of these Ordovician plutonic rocks, has major consequences for regional interpretation.

At Follafoss, some of the above plutonic rocks are overlain unconformably with a basal conglomerate by low- to middle-grade rocks characteristic of the Støren Nappe. Some prior assignments of the plutonic rocks below the unconformity to Baltican basement confounded rational regional tectonic interpretations. Alternatively, Wolff (1976) interpreted them as a basal gneissic part of the Gula Nappe Complex, and Carstens (1960) interpreted them as deformed-metamorphosed volcanics overlain by agglomerate. The conglomerate can now be visualized as resting on an Ordovician unconformity developed entirely in a stratigraphic setting that would later become incorporated in the Støren Nappe.

Below the Høybakken detachment, both the typical Støren rocks and the Ordovician intrusive rocks show evidence of intense Scandian ductile strain, particularly development of folds and extensional shear fabrics parallel to the NE-SW-trending anticlines and synclines. However, they do not show the intense metamorphism to high-amphibolite or even granulite facies, accompanied by partial melting, experienced by adjacent Baltican basement and lower nappes. This contrast alone requires either thrusting of lower-grade nappes on higher-grade rocks after the peak metamorphism, or extensional detachment to bring the low-grade nappes down against high-grade basement following earlier thrust emplacement. This problem is pinpointed acutely by recent U-Pb studies of the extent and age of titanite Pb loss and neocrystallization in the region. Throughout a large area, Proterozoic granitoid gneisses show 100 percent reworking of titanite to give a concordant age of 395 Ma, believed to be the time of cooling below about 600°C following the peak of Scandian metamorphism. On the other hand, the tonalitic gneiss from a 461 Ma Ordovician pluton in a nappe at Kjørsvika only a few hundred meters away from basement shows little adjustment of titanite, yielding an age of 455 Ma.

Based on current observations in the Trondheimsfjord part of the Western Gneiss Region, we view the Scandian tectonic history in three major phases. 1) Early southeastward emplacement of thrust nappes onto the Baltoscandian margin. During this phase intrusive and sedimentary rocks now constituting the Støren Nappe were transported to the southeast at a high level where they nearly completely escaped the intense peak-Scandian metamorphism enjoyed by the northwestward-subducted Baltican basement and nearby cover nappes. 2) Early extensional detachment or detachments bringing weakly metamorphosed cover nappes in direct contact with previously high-grade basement and lower nappes. Such detachments resulted in rapid cooling of the basement and probably set many basement titanite ages at 395 Ma. We believe it is possible, indeed probable, that this phase of high-level extension was contemporaneous with compressional deformation involving thrust imbrication of Baltica basement in the frontal parts of the orogen (see Roberts, 2003, fig. 7). 3) Once this extensionally attenuated tectonostratigraphy was established, or more probably while it was being established, it became involved in overturned to recumbent folds and later, open to tight, NE-SW -trending anticlines and synclines. The anticlines and synclines appear to be closely associated with and parallel to a pervasive stretching lineation and shear fabric indicating either top-W transport on flat limbs or sinistral shear on steep limbs. This fabric style is entirely consistent with that described by Séranne (1992) for the ductilely deformed rocks beneath the Høybakken detachment in Trøndelag as well as other detachment faults in southwest Norway, separating the Western Gneiss Region from the Devonian basins and their unconformably underlying low-grade metamorphic and igneous basement (Andersen and others, 1991; Andersen, 1993). This new interpretation illustrates the complex interplay of compression, extension, and regional metamorphism that took place in the Scandian hinterland and is illustrative of features known or yet to be discovered in the hinterlands of other thrust mountain belts.

ACKNOWLEDGMENTS

Tucker's early work in Norway beginning in 1980 was supervised by Professor John Rodgers of Yale University, and continued with support from the Geological Survey of Norway. This yielded an opportunity to begin and continue geochronological research with Krogh at the Royal Ontario Museum, Toronto, where most of the primary measurements in this paper were accomplished. Tucker's comments and questions about results and interpretation in 1994 led directly to the development of this paper. Robinson began field work in Norway in 1990 under the guidance of Professor A. G. Krill and under a NAVF Fellowship at the Norwegian Institute of Technology in Trondheim. This continued under a fellowship at Lund University, Sweden in 1993, including a University of Massachusetts Faculty Fellowship, and with support and eventually employment with the Geological Survey of Norway, Trondheim. Robinson's Ph. D. student, Michael P. Terry, was present during the initiating field excursions in 1995, and his research results on Nordøyane were influential in shaping some of the conclusions in this paper. Robinson and Terry were educated greatly concerning the tectonics of western Norway on a field trip in 1995 to the underpinnings of the Kvamhesten basin conducted by Torgeir Andersen of Oslo University. Final text preparation was done while Robinson was a visiting scientist at Australian Research Council Key Centre for Geochemical Evolution and Metallogeny of Continents (GEMOC), Department of Earth and Planetary Sciences, Macquarie University, New

South Wales, Australia. The work of Solli, Thorsnes, and Nordgulen was part of their employment with the Geological Survey, Trondheim, a key step being completion of a major compilation map in 1995 by Solli, which has been updated in recent years. The work of Gee, including cooperative field excursions in 1995, was supported by grants to Lund University. Bickford's cooperative research with Thorsnes and Nordgulen was funded by the Geological Survey of Norway. The manuscript benefitted greatly from careful reviews by David Roberts and Peter Gromet. To each of these persons and institutions we express our grateful acknowledgement.

Appendix

Geologic relationships near Follafoss

The sequence of strata of the Støren Nappe in the northeastern part of Fosen Peninsula includes the Snåsavatn Group and the Beitstad Group (Tietzsch-Tyler and Roberts, 1990). The Snåsavatn Group consists of metamorphosed volcanic and sedimentary rocks, including limestones of Mid Ordovician age (Roberts, 1982), and was considered by Roberts (1988) to form part of the elongate, orogen-internal, exotic "Smøla terrane", outcropping from Smøla in the southwest to Snåsa in the northeast. The main rock types of this group in the Follafoss region are greenschists and greenstones, felsic volcanites (keratophyres of rhyolitic composition), volcanoclastic sediments and minor amounts of marble. The presence of small anhedral garnets, blue-green hornblende, metamorphic plagioclase (An_{20}) and amphiboles with actinolitic cores and magnesio-hornblende rims indicates prograde metamorphism in the lower amphibolite facies during D1-deformation (Thorsnes, 1987). In Fosdalen, the Snåsavatn Group hosts major sedimentary-exhalative magnetite ore deposits (Carstens, 1955, 1960). The group is overlain by the Beitstad Group, dominated by low grade metamorphosed sandstones and conglomerates, with minor amounts of limestone (Tietzsch-Tyler, ms 1983, 1989). Pebbles of greenschist and rhyolite (keratophyre) found in the basal polymict Almlia Conglomerate of the Beitstad Group resemble rock types of the Snåsavatn Group. Together with low strains along the contact, this indicates a possible (tectonically modified) unconformable relationship between the Snåsavatn Group and Beitstad Group in this area (Thorsnes, 1989). The rocks of the Beitstad Group have been correlated with the Late Ordovician Upper Hovin Group (Vogt, 1945; Carstens, 1960; Tietzsch-Tyler, 1989).

Detailed relationships between the metamorphosed tonalite and strata of the Beitstad Group are shown in figure 12, which also shows a normal fault downthrown 500 to 1000 m on the east. West of the normal fault, strata of the Beitstad Group structurally overlie the tonalite and the contact is folded by a tight, major Z-fold with an overturned axial surface having a strike/dip of 060°/60° SE, and a fold axis plunging 5 to 30° northeast. In the short limb (fig. 12, loc. A), strains are comparatively low, and the sedimentary sequence fairly well preserved, consisting of a 0 - c. 500 m-thick, basal polymict conglomerate, and impure sandstones. Farther west, impure marbles are interbedded with the sandstones. On the east side of the fault the base of the conglomerate on the tonalite is shifted 1.5 km southward. However, two large slabs of foliated tonalite, probably once continuous above the present erosion surface, overlie the stratified rocks (note section in fig. 12). High strains in basal parts of the tonalite slabs, immediately above the sandstones, are recorded by protomylonitic to mylonitic textures in which the feldspars are reduced to augen. Furthermore, no 'basal' conglomerate is found along the contact between the sandstones and overlying tonalites, suggesting that the contact is a thrust fault of uncertain magnitude.

Contact relations between stratified rocks and tonalite have been mapped (Thorsnes, 1988) and studied in about 50 thin-sections (Thorsnes, 1989). The conglomerate (fig. 12) contains clasts of deformed igneous rocks comparable to the tonalite, also clasts of greenschist and rhyolite similar to the volcano-sedimentary Snåsavatn Group. The metamorphic grade of the pebbles does not exceed that of the matrix. None contain evidence for pre-pebble metamorphism, although an indistinct cleavage truncated by the margin has been observed in one pebble. The observations support the interpretation of Vogt (1945), Carstens (1960) and Tietzsch-Tyler (1989) that the contact in the short limb west of the normal fault (fig. 12, loc. A) is a primary unconformity modified by deformation.

References

Allen, K. C., 1976, Devonian spores from outer Trøndelag: Norsk Geologisk Tidsskrift, v. 56, p. 437–448.

Andersen, T. B., 1993, The role of extensional tectonics in the Caledonides of south Norway: Discussion: Journal of Structural Geology, v. 15, p. 1379–1380.

Andersen, T. B., and Jamtveit, B., 1990, Uplift of deep crust during orogenic extensional collapse: A model based on field studies in the Sogn-Sunnfjord region, W. Norway: Tectonics, v. 9, p. 1097–1111.

Andersen, T. B., Jamtveit, B., Dewey, J. F., and Swensson, E., 1991, Subduction and eduction of continental crust: major mechanisms during continent-continent collision and orogenic extensional collapse, a model based on the south Norwegian Caledonides: Terra Nova, v. 3, p. 303–310.

Austrheim, H., Corfu, F., Bryhni, I., and Andersen, T. B., 2003, The Proterozoic Hustad igneous complex: a low strain enclave with a key to the history of the Western Gneiss Region of Norway: Precambrian Research, v. 120, p. 149–175.

Bassett, M. G., 1985, Silurian stratigraphy and facies development in Scandinavia, *in* Gee, D. G., and Sturt, B. A., editors, The Caledonian Orogen – Scandinavia and Related Areas: Chichester, John Wiley and Sons, p. 283–292.

Bassett, M. G., Cherns, L., and Karis, L., 1982, The Röde Formation: an Old Red Sandstone facies in the Silurian of Jämtland, Sweden: Sveriges Geologiska Undersökning, v. C793, p. 1–24.

Bingen, B., Davis, W. J., and Austrheim, H., 2001, Zircon U-Pb geochronology in the Bergen arc eclogites and their Proterozoic protoliths, and implications for the pre-Scandian evolution of the Caledonides in western Norway: Geological Society of America Bulletin, v. 113, p. 640–649.

Bingen, B., Austrheim, H., Whitehouse, M., and Davis, W. J., 2004, Trace element signature and U-Pb geochronology of eclogite-facies zircon, Bergen Arcs, Caledonides of W. Norway: Contributions to Mineralogy and Petrology, DOI:10.1007/s00410–004–0585-z, v. 147, 671–683.

Bjørlykke, A., and Olaussen, S., 1981, Silurian sediments, volcanics and mineral deposits in the Sagelvvatn area, Troms, North Norway: Norges geologiske undersøkelse Bulletin, v. 365, p. 1–38.

Bøe, R., 1991, Structure and seismic stratigraphy of the innermost mid-Norwegian contiental shelf: an example from the Frohavet area: Marine and Petroleum Geology, v. 8, p. 140–151.

Bøe, R., and Bjerkli, K., 1988, Mesozoic sedimentary rocks in Edøyfjorden and Beitstadfjorden, central Norway: Implications for the structural history of the Møre-Trøndelag Fault Zone: Marine Geology, v. 87, p. 287–299.

Braathen, A., Osmundsen, P. T., Nordgulen, Ø., Roberts, D., and Meyer, G. B., 2002, Orogen-parallel extension of the Caledonides in northern Central Norway: an overview: Norwegian Journal of Geology, v. 82, p. 225–241.

Bruton, D. L., and Bockelie, J. F., 1979, The Ordovician sedimentary sequence in Smøla, west central Norway: Norges geologiske undersøkelse Bulletin, v. 348, p. 21–32.

Bryhni, I., and Andréasson, P. G., 1985, Metamorphism in the Scandinavian Caledonides, *in* Gee, D. G., and Sturt, B. A., editors, The Caledonide Orogen – Scandinavia and Related Areas: Chichester, John Wiley and Sons, p. 763–781.

Carstens, H., 1955, Jernmalmene: det vestlige Trondhjemsfelt og forholdet til kisforekomstene: Norsk Geologisk Tidsskrift, v. 35, p. 211–220.

——— 1960, Stratigraphy and volcanism of the Trondheimsfjord area, Norway, Guide to excursions no. 4 and no. C1: Norges geologiske undersøkelse Bulletin, v. 212b, p. 1–22.

Carswell, T., Cuthbert, S., O'Brien, P., and Tucker, R., 2001, Eclogite evolution and the timing of ultra-high pressure metamorphism in Western Norway: Journal of Conference Abstracts (Abstract EUG XI, 2001 Strasbourg), v. 6, p. 348.

Carswell, D. A., Tucker, R. D., O'Brien, P. J., and Krogh, T. E., 2003, Coesite micro-inclusions and the U/Pb age of zircons from the Hareidland Eclogite in the Western Gneiss Region of Norway: Lithos, v. 67, p. 181–190.

Dallmeyer, R. D., Johansson, L., and Möller, C., 1992, Chronology of Caledonian high-pressure granulite-facies metamorphism, uplift and deformatiom within northern parts of the Western Gneiss Region: Geological Society of America Bulletin, v. 104, p. 444–455.

Davis, D. W., 1982, Optimum linear regression and error estimation applied to U-Pb data: Canadian Journal of Earth Sciences, v. 19, p. 2141–2149.

Eide, E. A., Osmundsen, P. T., Meyer, G. B., Kendrick, M. A., and Corfu, F., 2002, The Nesna Shear Zone, north-central Norway: an $^{40}Ar/^{39}Ar$ record of Early Devonian - Early Carboniferous ductile extension and unroofing: Norwegian Journal of Geology, v. 82, p. 317–339.

Eskola, P., 1921, On the eclogites of Norway: Skrifter, Det Norske Videnskapsselskapet i Kristiania, I Matematisk-Naturvideskapelig Klasse, 8, 118 p.

Essex, R. M., and Gromet, L. P., 1996, Constraints on the timing of Caledonide thrust stack emplacement from U-Pb metamorphic ages of basement gneiss, Nasafjallet window (66.5 N, 15.5 E), Scandinavian Caledonides: Geological Society of America Abstracts with Programs, v. 28, p. 501.

——— 2000, U-Pb dating of prograde and retrograde titanite growth during the Scandian orogeny: Geology, v. 28, p. 419–422.

Gabrielsen, R. H., and Ramberg, I. B., 1979, Fracture patterns in Norway from Landsat images: results and potential use: Proceedings of the Norwegian Sea Symposium, Tromsø, Norwegian Petroleum Society NSP/ 1–28.

Gautneb, H., and Roberts, D., 1989, Geology and petrochemistry of the Smøla-Hitra batholith, Central Norway: Norges geologiske undersøkelse Bulletin, v. 416, p. 1–24.

Gayer, R. A., Rice, A. H. N., Roberts, D., Townsend, C., and Welbon, A., 1987, Restoration of the Caledonian Baltoscandian margin from balanced cross-sections; the problem of excess continental crust: Transactions of the Royal Society of Edinburgh: Earth Sciences, v. 78, p. 197–217.

Gee, D. G., 1974, Comments on the metamorphic allochthon on northern Trøndelag, central Scandinavian Caledonides: Norsk Geologisk Tidsskrift, v. 54, p. 435–440.

——— 1975, A tectonic model for the central part of the Scandinavian Caledonides: American Journal of Science, v. 275-A, p. 468–515.

——— 1977, Extension of the Offerdal and Särv nappes and Seve Supergroup into northern Trøndelag: Norsk Geologisk Tidsskrift, Supplement, v. 57, p. 163–170.

——— 1978, Nappe displacements in the Scandinavian Caledonides: Tectonophysics, v. 47, p. 393–419.

——— 1980, Basement-cover relationships in the central Scandinavian Caledonides: Geologiska Föreningens i Stockholm Förhandlingar, v. 102, p. 455–474.

Gee, D. G., and Sturt, B. A., 1985, editors, The Caledonide Orogen – Scandinavia and Related Areas: Chichester, John Wiley and Sons, 1266 p.

Getz, A., 1890. Graptolitførende skiferzone i det Trondhjemske: Nyt Magazin for Naturvidenskaberne, v. 31, p. 41–42.

Gilotti, J. A., and Hull, J. M., 1993, Kinematic stratification in the hinterland of the central Scandinavian Caledonides: Journal of Structural Geology, v. 15, p. 629–646.

Grenne, T., Ihlen, P. M., and Vokes, F. M., 1999, Scandinavian Caledonide metallogeny in a plate tectonic perspective: Mineralium Deposita, v. 34, p. 422–471.

Griffin, W. L., and Brueckner, H. K., 1980, Caledonian Sm-Nd ages and crustal origin for Norwegian eclogites: Nature, v. 285, p. 319–321.

Griffin, W. L., Austrheim, H., Brastad, K., Bryhni, I., Krill, A. G., Krogh, E. J., Mørk, M. B. E., Qvale, H., and Tørudbakken, B., 1985, High-pressure metamorphism in the Scandinavian Caledonides, *in* Gee, D. G., and Sturt, B. A., editors, The Caledonide Orogen – Scandinavia and Related Areas: Chichester, John Wiley and Sons, p. 783–801.

Gromet, L. P., Sjöstrom, H., Bergman, S., Claesson, S., Essex, R. M., Andréasson, P. G., and Albrecht, L., 1996, Contrasting ages of metamorphism in the Seve nappes: U-Pb results from the central and northern Swedish Caledonides (abstract): GFF, v. 118, p. A36-A37.

Hall, L. M., and Roberts, D., 1988, Timing of Ordovician deformation in the Caledonian-Appalachian orogen, *in* Harris, A. L., and Fettes, D. J., editors, The Caledonian-Appalachian Orogen: London, Geological Society Special Publication, n. 38, p. 291–309.

Handke, M. J., Tucker, R. D., and Robinson, P., 1995, Contrasting U-Pb Ages for the Risberget Augen Gneiss in the Norwegian Caledonides: Getting to the root of the problem: Geological Society of America Abstracts with Programs, v. 27, p. A-226.

Hanson, G. N., Catanzaro, E. J., and Anderson, D. H., 1971, U-Pb ages for sphene in a contact metamorphic zone: Earth and Planetary Science Letters, v. 12, p. 231–237.

Hardenby, C., 1983, Geology of the Kjølhaugen area, eastern Trøndelag, central Scandinavian Caledonides: Geologiska Föreningens i Stockholm Förhandlingar, v. 102, p. 475–492.

Hollocher, K., Bull, J., and Robinson, P., 2002, Geochemistry of the metamorphosed Ordovician Taconian Magmatic Arc, Bronson Hill anticlinorium, western New England: Physics and Chemistry of the Earth, v. 27, p. 5–45.

Hossack, J. R., 1984, The geometry of listric faults in the Devonian basins of Sunnfjord, W. Norway: London, Journal of the Geological Society, v. 141, p. 629–637.

Hurich, C. A., Palm, P., Dyrelius, D., Kristoffersen, Y., Wolff, F. C., and Roberts, D., 1988, Activation of Precambrian basement in the Scandinavian Caledonides: View from seismic reflection data: Norges geologiske undersøkelse Special Publication 3, p. 66–69.

Jaffey, A. H., Flynn, K. F., Glendenin, L. E., Bently, W. C., and Essling, A. M., 1971, Precision measurement of the half-lives and specific activities of U235 and U238: Physics Review, v. C4, p. 1889–1907.

Juhojunttii, N., Juhlin, C., and Dyrelius, D., 2001, Crustal reflectivity underneath the Central Scandinavian Caledonides: Tectonophysics, v. 334, p. 191–210.

Koistinen, T., Stephens, M. B., Bogatchev, V., Nordgulen, Ø., Wennerström, M., and Korhonen, J., 2001, Geological map of the Fennoscandian shield: Geological Surveys of Finland, Norway and Sweden and the North-West Department of Natural Resources of Russia, Scale 1:2000000.

Krabbendam, M., and Dewey, J. F., 1997, Exhumation of UHP rocks by transtension in the Western Gneiss Region, Scandinavian Caledonides: Special Publication of the Geological Society of London, v. 135, p. 159–181.

Krill, A. G., 1980, Tectonics of the Oppdal area, central Norway: Geologiska Föreningens i Stockholm Förhandlingar, v. 102, p. 523–530.

——— 1983, Rb-Sr study of rapakivi granite and augen gneiss of the Risberget Nappe, Oppdal, Norway: Norges geologiske undersøkelse Bulletin, v. 380, p. 51–65.

——— 1985, Relationship between the western gneiss region and the Trondheim region: Stockwerk-tectonics reconsidered, *in* Gee, D. G., and Sturt, B. A., editors, The Caledonide Orogen – Scandinavia and Related Areas: Chichester, John Wiley and Sons, p. 475–483.

——— 1987, Berggrunnskart STANGVIK 1420 4, 1:50,000, foreløpig utgave: Norges geologiske undersøkelse.

Krill, A. G., and Röshoff, K., 1981, Basement-cover relationships in the central Scandinavian Caledonides, Excursion B-5, Uppsala Caledonide Symposium.

Krill, A. G., Rodgers, J., and Sundvoll, B., 1988, Alternative to the Finnmarkian-Scandian interpretation on Magerøya, northern Norway: Norsk Geologisk Tidsskrift, v. 68, p. 171–185.

Krogh, T. E., 1973, A low contamination method for hydrothermal decomposition of zircon and extraction of U and Pb for isotopic age determinations: Geochimica et Cosmochimica Acta, v. 37, p. 485–494.

——— 1982, Improved accuracy of U-Pb zircon dating by the creation of more concordant systems using air abrasion technique: Geochimica et Cosmochimica Acta, v. 46, p. 637–649.

——— 1994, Precise U-Pb ages for Grenvillian and pre-Grenvillian thrusting of Proterozoic and Archean metamorphic assemblages in the Grenville Front tectonic zone, Canada: Tectonics, v. 13, p. 963–982.

Krogh, T. E., Mysen, B. O., and Davis, G. L., 1974, A Paleozoic age for the primary minerals of a Norwegian eclogite: Annual Report of the Geophysical Laboratory, Carnegie Institution, Washington, v. 73, p. 575–576.

Krogh, T. E., Robinson, P., and Terry, M. P., 2003, Precise U-Pb zircon ages define 18 and 19 m. y. subduction to uplift intervals in the Averøya-Nordøyane area, Western Gneiss Region: Alice Wain Memorial West Norway Eclogite Field Symposium, Selje, Norway, abstract volume, Norges geologiske undersøkelse Report 2003.055, 189 p.
Krogh, T. E., Kwok, Y., Robinson, P., and Terry, M., 2004, U-Pb age constraints on the subduction-extension interval in the Averøya-Nordøyane area, Western Gneiss Region, Norway: Copenhagen, Abstract Volume, Goldschmidt Conference, p. A611.
Kulling, O., 1933, Bergbyggnaden inom Björkvattnet–Virisen-området i Västerbottensfjällens centrala del: Geologiska Föreningens i Stockholm Förhandlingar, v. 55, p. 167–422.
Kumpulainen, R., and Nystuen, J. P., 1985, Late Proterozoic basin evolution and sedimentation in the westernmost part of Baltoscandia, *in* Gee, D. G., and Sturt, B. A., editors, The Caledonide Orogen – Scandinavia and related areas: Chichester, John Wiley and Sons, p. 213–232.
Lindstrøm, M., ms, 1995, Petrology of the Caledonian Hitra plutonic complex, central Norway: Dr. Ing. Thesis, University of Trondheim, Norway, 143 p.
Ludwig, K. R., 1980, Calculation of uncertainties of U-Pb isotope data: Earth and Planetary Science Letters, v. 46, p. 212–220.
——— 1992, ISOPLOT - a plotting and regression program for radiogenic-isotope data, version 2.57: United States Geological Survey Open-file Report 91–445, 40 p.
Lutro, O., Robinson, P., and Solli, A., 1997, Proterozoic geology and Scandian high-pressure overprinting in the Western Gneiss Region: Guidebook for Field Trip A-3 (August 14–17), COPENA Conference (Correlation of Proterozoic of Europe and the North Atlantic Region): Norges geologiske undersøkelse Report 97.132, 86 p.
Melezhik, V. M., Gorokhov, I. M., Fallick, A. E., Roberts, D., Kuznetzov, A. B., Zwaan, K. B., and Pokrovsky, B. G., 2002, Isotopic stratigraphy suggests Neoproterozoic ages and Laurentian ancestry for high-grade marbles from the North-Central Norwegian Caledonides: Geological Magazine, v. 139, p. 375–393.
Meyer, G. B., Grenne, T., and Pedersen, R. B., 2003, Age and tectonic setting of the Nesåa Batholith: implications for Ordovician arc development in the Caledonides of Central Norway: Geological Magazine, v. 140, p. 573–594.
Möller, C., 1988, Geology and metamorphic evolution of the Roan area, Vestranden, Western Gneiss Region, Central Norwegian Caledonides: Norges geologiske undersøkelse Bulletin, v. 413, p. 1–31.
Mysen, B. O., and Heier, K. S., 1972, Petrogenesis of eclogites in high grade metamorphic gneisses, exemplified by the Hareidlandet eclogite, western Norway: Contributions to Mineralogy and Petrology, v. 36, p. 73–94.
Nilsen, O., and Wolff, F. C., 1989, Geologisk kart over Norge, berggrunnskart RØROS og SVEG - 1:250 000: Norges geologiske undersøkelse.
Nordgulen, Ø., Bickford, M. E., Nissen, A. L., and Wortman, G. L., 1993, U-Pb zircon ages from the Bindal Batholith, and the tectonic history of the Helgeland Nappe Complex, Scandinavian Caledonides: London, Journal of the Geological Society, v. 150, p. 771–783.
Nordgulen, Ø., Solli, A., Bøe, R., and Sundvoll, B., 1995, Caledonian granitoids in the Frøya-Froan area, Central Norway: Norges geologiske undersøkelse Bulletin, v. 427, p. 48–51.
Nordgulen, Ø., Braathen, A., Corfu, F., Osmundsen, P. T., and Husmo, T., 2002, Polyphase kinematics and geochronology of the Kollstraumen detachment, central Norway: Norwegian Journal of Geology, v. 82, p. 299–316.
Northrup, C. J., 1996, U-Pb and 40Ar/39Ar constraints on the structural assembly, metamorphism, and cooling history of the Caledonian allochthon, Ofoten-Erfjorden, North Norway: Geological Society of America Abstracts with Programs, v. 28, p. 501.
Norton, M. G., 1987, The Nordfjord – Sogn Detachment, W. Norway: Norsk Geologisk Tidsskrift, v. 67, p. 93–106.
Palm, H., Gee, D. G., Dyrelius, D., and Björklund, L., 1991, A reflection seismic image of Caledonian structure in Central Sweden: Sveriges Geologiska Undersökning, Ca 75, 36 p.
Rickard, M. J., 1985, The Surnadal synform and basement gneisses in the Surnadal-Sunndal district of Norway, *in* Gee, D. G., and Sturt, B. A., editors, The Caledonide Orogen – Scandinavia and Related Areas: Chichester, John Wiley and Sons, p. 485–497.
Roberts, D., 1982, Disparate geochemical patterns from the Snåsavatn greenstone, Nord-Trøndelag, central Norway: Norges geologiske undersøkelse Bulletin, v. 373, p. 63–73.
——— 1988, The terrane concept and the Scandinavian Caledonides: Norges geologiske undersøkelse Bulletin, v. 413, p. 93–99.
——— 1997, Geologisk kart over Norge, berggrunnskart, GRONG; 1:250 000: Norges geologiske undersøkelse.
——— 2003, The Scandinavian Caledonides: event chronology, paleogeographic settings and likely modern analogues: Tectonophysics, v. 365, p. 283–299.
Roberts, D., and Andersen, T. B., 1983, Nordkapp Beskrivelse til det berggrunnsgeologiske kartbladet M 1:250 000 (Med fargetrykt kart) (with summary in English): Norges geologiske undersøkelse, 49 p.
Roberts, D., and Stephens, M., 2000, Caledonian Orogenic Belt, *in* Lundqvist, T., and Autio, S., editors, Description to the Bedrock Map of Central Fennoscandia (Mid-Norden): Geological Survey of Finland, Special Paper 28, p. 79–104.
Roberts, D., and Tucker, R. D., 1991, U/Pb zircon age of the Møklevatnet granodiorite, Gjersvik Nappe, Central Norwegian Caledonides: Norges geologiske undersøkelse Bulletin, v. 421, p. 33–38.
Roberts, D., and Wolff, F. C., 1981, Tectonostratigraphic development of the Trondheim region Caledonides, central Norway, *in* Dewey, J. F., Hancock, P. L., Mattauer, M., and Nicolas, A., editors, Tectonics: a selection of papers presented at the 26th IGC: Journal of Structural Geology, 3, p. 487–494.

Roberts, D., Heldal, T., and Melezhik, V., 2001, Tectonic structural features of the Fauske conglomerates in the Løvgavlen quarry, Nordland, Norwegian Caldedonides, and regional implications: Norsk Geologisk Tidsskrift, v. 81, p. 245–256.
Roberts, D., Melezhik, V. M., and Heldal, T., 2002a, Carbonate formations and early NW-directed thrusting in the highest allochthons of the Norwegian Caledonides: evidence of a Laurentian ancestry: London, Journal of the Geological Society, v. 159, p. 117–120.
Roberts, D., Walker, N., Slagstad, T., Solli, A., and Krill, A., 2002b, U-Pb zircon ages from the Bymarka ophiolite, near Trondheim, Central Norwegian Caledonides, and regional implications: Norsk Geologisk Tidsskrift, v. 82, p. 19–30.
Robinson, P., 1995, Extension of Trollheimen tectono-stratigraphic sequence in deep synclines near Molde and Brattvåg, Western Gneiss Region, southern Norway: Norsk Geologisk Tidsskrift, v. 75, p. 181–198.
——— 1997, Quartzite of Reksdalshesten, Moldefjorden, Western Gneiss Region: Another parallel with the tectonostratigraphy of Trollheimen (extended abstract): Norges geologiske undersøkelse Bulletin, v. 433, p. 15–16.
Robinson, P., and Krill, A. G., 1991, Definitive Trollheim tectono-stratigraphic sequence in deep synclines near Molde and Brattvåg, Western Gneiss Region (extended abstract): Geonytt (Norsk Geologisk Forening) v. 18, p. 46.
——— 1994, Sinistral ductile shear in the NE-SW trending coastal areas of the western gneiss region (abstract): Norsk Geologisk Tidsskrift, v. 74, p. 181.
Robinson, P., and Terry, M. P., 2001, Kinematics of HP and UHP metamorphism in the Western Gneiss Region, Møre og Romsdal, Norway: Journal of Conference Abstracts (Abstract EUG XI, 2001, Strasbourg), v. 6, p. 348.
Robinson, P., Tucker, R. D., Solli, A., Gee, D. G., and Thorsnes, T., 1996, Relationships between thrusting and extension in the Scandian hinterland, Norway: Interpretation based on a new tectono-stratigraphic compilation and new U-Pb ages on igneous zircon and metamorphic sphene: Geological Society of America Abstracts with Programs, v. 28, p. A501.
Robinson, P., Tucker, R. D., Solli, A., Gee, D. G., Thorsnes, T., and Terry, M. P., 1997, Re-interpretation of the Støren Nappe, Outer Trondheimsfjord, Norway: bearing on relationships between thrusting and extensional exhumation in the Scandian hinterland: Terra Nova, v. 9, Abstract Supplement n. 1, p. 330.
Robinson, P., Tucker, R. D., Bradley, D., Berry, IV, H. N., and Osberg, P. H., 1998, Paleozoic orogens in New England, U. S. A.: GFF (Geological Society of Sweden), v. 120, p. 119–148.
Robinson, P., Terry, M. P., Carswell, T., and van Roermund, H., 2003, Tectono-stratigraphic setting, structure and petrology of HP and UHP metamorphic rocks and garnet peridotites in the Western Gneiss Region, Møre og Romsdal, Norway: Guidebook for Post-Meeting Excursion, Alice Wain Memorial West Norway Eclogite Field Symposium, Selje, Norway, Norges geologiske undersøkelse Report 2003.057, 142 p.
Robinson, P., Tucker, R. D., Solli, A., Terry, M. P., Krogh, T. E., Gee, D. G., and Nordgulen, Ø., 2004, Scandian thrusting and extension in the Western Gneiss Region, Sør Trondelag and Møre og Romsdal, Norway: GFF (Geological Society of Sweden), v. 126, p. 84.
Schouenborg, B., 1988, U/Pb-zircon datings of Caledonian cover rocks and cover-basement contacts, northern Vestranden, central Norway: Norsk Geologisk Tidsskrift, v. 68, p. 75–87.
Schouenborg, B., Johansson, L., and Gorbatschev, R., 1991, U-Pb zircon ages of basement gneisses and discordant felsic dykes from Vestranden, westernmost Baltic shield and central Norwegian Caledonides: Geologische Rundschau, v. 80, p. 121–134.
Séranne, M., 1992, Late Paleozoic kinematics of the Møre-Trøndelag Fault Zone and adjacent areas, central Norway: Norsk Geologisk Tidsskrift, v. 72, p. 141–158.
Solli, A., 1995, Digitalt berggrunnskart over Nord-Trøndelag og Fosen: Norges geologiske undersøkelse.
Solli, A., Bugge, T., and Thorsnes, T., 1997, Geologisk kart over Norge, berggrunnskart NAMSOS 1:250000: Norges geologiske undersøkelse.
Sommaruga, A., and Bøe, R., 2002, Geometry and subcrop maps of shallow Jurassic basins along the Mid-Norway coast: Marine and Petroleum Geology, v. 19, p. 1029–1042.
Stacey, J. S., and Kramers, J. D., 1975, Approximation of terrestrial lead isotope evolution by a two-stage model: Earth and Planetary Science Letters, v. 26, p. 207–221.
Steel, R. J., Siedlecka, A., and Roberts, D., 1985, The Old Red Sandstone basins of Norway and their deformation: a review, *in* Gee, D. G. and Sturt, B. A., editors, The Caledonide Orogen – Scandinavia and Related Areas: Chichester, John Wiley and Sons, p. 293–315.
Steiger, R. H., and Jaeger, E., 1977, Subcommision on Geochronology: Convention on the use of decay constants in geo- and cosmochronology: Earth and Planetary Science Letters, v. 36, p. 359–362.
Stephens, M. B., 1988, The Scandinavian Caledonides: a complexity of collisions: Geology Today, v. 4, p. 20–26.
Stephens, M. B., and Gee, D. G., 1985, A tectonic model for the evolution of the eugeoclinal terranes in the central Scandinavian Caledonides, *in* Gee, D. G., and Sturt, B. A., editors, The Caledonide Orogen – Scandinavia and Related Areas: Chichester, John Wiley and Sons, p. 953–978.
Størmer, L., 1935, Dictycaris, Salter, a large crustacean from the upper Silurian and Downtownian: Norsk Geologisk Tidsskrift, v. 15, p. 267–298.
Terry, M. P., ms, 2000, Structural and thermal evolution of Baltica basement and infolded cover nappes on Nordøyane and their bearing on mechanisms for production and exhumation of high-pressure rocks, Western Gneiss Region, Norway: Ph. D. thesis, University of Massachusetts, Amherst, 200 p.
Terry, M. P., and Robinson, P., 1996, Caledonian structural fabrics related to subduction of continental crust, Western Gneiss Region, Norway: Geological Society of America Abstracts with Programs, v. 28, p. A501.

—— 1998, Eclogite-facies structural features and their bearing on mechanisms for production and exhumation of high-pressure rocks, Western Gneiss Region, Norway, including the mircrodiamond-bearing gneiss at Fjørtoft: International Workshop on Ultra-High-pressure Metamorphism and Exhumation, Stanford University, p. 74–78.
—— 2003, Evolution of amphibolite-facies structural features and boundary conditions for deformation during exhumation of HP and UHP rocks, Nordøyane, Western Gneiss Region, Norway: Tectonics, v. 22, p. 1036–58.
Terry, M. P., Robinson, P., Hamilton, M. A., and Jercinovic, M. J., 2000a, Monazite geochronology of UHP and HP metamorphism, deformation and exhumation, Nordøyane, Western Gneiss Region, Norway: American Mineralogist, v. 85, p. 1651–1664.
Terry, M. P., Robinson, P., and Ravna, E. J. K., 2000b, Kyanite eclogite thermobarometry and evidence for thrusting of UHP over HP metamorphic rocks, Nordøyane, Western Gneiss Region, Norway: American Mineralogist, v. 85, p. 1637–1650.
Thorsnes, T., 1987, Strukturgeologisk undersøkelse i Malm, Verran kommune, Nord-Trøndelag: Norges geologiske undersøkelse Report 87.070, 47 p.
—— 1988, HOLDEN 1623–2, berggrunnskart, M. 1:50 000, foreløpig utgave: Norges geologiske undersøkelse.
—— 1989, Fault-related sedimentation along the Hitra-Snåsa Fault, central Norwegian Caledonides: Geologiska Föreningens i Stockholm Förhandlingar, v. 111, p. 420–423.
Thorsnes, T., and Grønlie, A., 1990, ÅFJORD 1622–4, berggrunnskart, M. 1:50.000, foreløpig utgave: Norges geologiske undersøkelse.
Tietzsch-Tyler, D., ms, 1983, The Caledonian geology of the southwestern part of the Snåsa Synform in the central Norwegian Caledonides and its regional significance: Unpublished Ph. D. thesis, University of Wales, Cardiff, 417 p.
—— 1989, Evidence of intracratonic Finnmarkian orogeny in central Norway, *in* Gayer, R.A., editor, The Caledonide Geology of Scandinavia: Graham and Trotman, p. 47–62.
Tietzsch-Tyler, D., and Roberts, D., 1990, STEINKJER, Berggrunnskart, 1723–3; 1:50 000: Norges geologiske undersøkelse.
Tucker, R. D., 1986, Geology of the Hemnefjord-Orkanger area, south-central Norway: Norges geologiske undersøkelse Bulletin, v. 404, p. 1–24.
—— 1988, Contrasting crustal segments in the central Norwegian Caledonides: evidence from U-Pb dating of accessory minerals: Geological Association of Canada Program with Abstracts, p. A127.
Tucker, R. D., and Krogh, T. E., 1988, Geochronological investigation on the Ingdal granite gneiss and discordant pegmatites from the Western Gneiss Region, Norway: Norsk Geologisk Tidsskrift, v. 68, p. 201–210.
Tucker, R. D., and McKerrow, W. S., 1995, Early Paleozoic chronology: a review in light of new U-Pb zircon ages from Newfoundland and Britain: Canadian Journal of Earth Sciences, v. 32, p. 368–379.
Tucker, R. D., and Robinson, P., 1990, Age and setting of the Bronson Hill magmatic arc: A re-evaluation based on U-Pb zircon ages in southern New England: Geological Society of America Bulletin, v. 102, p. 1404–1419.
Tucker, R. D., Råheim, A., Krogh, T. E., and Corfu, F., 1987, Uranium-lead zircon and titanite ages from the northern portion of the Western Gneiss Region, south-central Norway: Earth and Planetary Science Letters, v. 81, p. 203–211.
Tucker, R. D., Krogh, T. E., and Råheim, A., 1990, Proterozoic evolution and age-province boundaries in the central part of the Western Gneiss Region, Norway: Results of U-Pb dating of accessory minerals from Trondheimsfjord to Geiranger, *in* Gower, C. F., Ryan, B., and Rivers, T., editors, Middle Proterozoic Geology of the Southern Margin of Proto Laurentia-Baltica: Geological Association of Canada Special Paper 38, p. 149–173.
Tucker, R. D., Robinson, P., Solli, A., Gee, D. G., and Thorsnes, T., 1997a, A re-interpretation of the Støren Nappe in the outer Trondheimsfjord region: its bearing on relationships between thrusting and extensional exhumation in the Scandian hinterland: Geonytt, v. 24, p. 94.
Tucker, R. D., Ver Straeten, C., Bradley, D. C., Harris, A. G., and Ebert, J., 1997b, Chronometric revision of the Devonian time-scale based on new U-Pb zircon ages from New York State, the central Appalachians, and New Brunswick, Canada: Geological Society of America Abstracts with Programs, v. 29, p. A116.
Tucker, R. D., Bradley, D. C., Ver Straeten, C., Harris, A. G., Ebert, J., and McCutcheon, S. R., 1998, New U-Pb zircon ages and the duration and division of Devonian time: Earth and Planetary Science Letters, v. 158, p. 175–186.
Tucker, R. D., Ashwal, L. D., and Torsvik, T. H., 2001, U-Pb geochronology of Seychelles granitoids: a Neoproterozoic continental arc fragment: Earth and Planetary Science Letters, v. 187, p. 27–38.
Tveten, E., Lutro, O., and Thorsnes, T., 1998, Geologisk kart over Norge, berggrunnskart ÅLESUND 1:250000: Norges geologiske undersøkelse.
Vogt, T., 1945, The geology of part of the Hølonda-Horg district, a type area in the Trondheim region: Norsk Geologisk Tidsskrift, v. 25, p. 449–534.
Wolff, F. C., 1976, Geologisk kart over Norge, berggrunnskart TRONDHEIM 1:250000: Norges geologiske undersøkelse.
Yoshinobu, A., Barnes, C. G., Nordgulen, Ø., Prestvik, T., Fanning, M., and Pedersen, R. B., 2002, Ordovician magmatism, deformation, and exhumation in the Caledonides of central Norway: An orphan of the Taconic orogeny: Geology, v. 30, p. 883–886.
Zwaan, K. B., 1988, Geologisk kart over Norge, berggrunnskart; NORDREISA. 1:250 000: Norges geologiske undersøkelse.
Zwaan, K. B., Fareth, E., and Grogan, P. W., 1998, Geologisk kart over Norge, berggrunnskart; TROMSØ 1:250 000: Norges geologiske undersøkelse.